Helsinki University of Technology Water Resources Publications

Teknillisen korkeakoulun vesitalouden ja vesirakennuksen julkaisuja

Espoo 2002 TKK-VTR-6

PROCESS-ORIENTED INVESTIGATION OF SNOW ACCUMULATION, SNOWMELT AND RUNOFF GENERATION IN FORESTED SITES IN FINLAND

Harri Koivusalo

Dissertation for the degree of Doctor of Science in Technology to be presented with due permission of the Department of Civil and Environmental Engineering for public examination and debate in Auditorium R1 at Helsinki University of Technology (Espoo, Finland) on the 10th of January, 2003, at 12 noon.

Helsinki University of Technology
Department of Civil and Environmental Engineering
Laboratory of Water Resources

Teknillinen korkeakoulu
Rakennus- ja ympäristötekniikan osasto
Vesitalouden ja vesirakennuksen laboratorio

Koivusalo, H., Process-oriented investigation of snow accumulation, snowmelt and runoff generation in forested sites in Finland, Helsinki University of Technology, Water Resources Publications, TKK-VTR-6, Espoo, 2002, 88 pp.

Distribution:
Helsinki University of Technology
Laboratory of Water Resources
P.O.Box 5300
FIN-02015 HUT
Tel. +358-9-451 3821
Fax. +358-9-451 3856
E-mail: contact@water.hut.fi

ISBN 951-22-6214-2
ISBN (pdf) 951-22-6237-1
ISSN 1456-2596

Otamedia OY
Espoo 2002

HELSINKI UNIVERSITY OF TECHNOLOGY P.O.Box 1000, FIN-02015 HUT, http://www.hut.fi	ABSTRACT OF DOCTORAL DISSERTATION

Author Harri Koivusalo

Name of the dissertation
Process-oriented investigation of snow accumulation, snowmelt and runoff generation in forested sites in Finland

Date of manuscript 14 June 2002	Date of dissertation 10 January 2003
☐ Monograph	☒ Article dissertation (summary + articles)

Department	Civil and Environmental Engineering
Laboratory	Water Resources
Field of research	Hydrology
Opponent	Professor Per-Erik Jansson (Royal Institute of Technology, Stockholm)
Supervisor	Professor Pertti Vakkilainen (HUT)
Instructor	Professor Tuomo Karvonen (HUT)

Abstract

This thesis summarises development and application of a hydrological model for simulating forest canopy processes, snow accumulation and melt, soil and ground water interactions, and streamflow routing. A motivation behind the model development is to outline a methodology for predicting the influence of land use changes on catchment hydrological processes. In addition, the development aims at providing linkages from the hydrological model to atmospheric models through implementation of surface energy balance and to water quality models through quantification of runoff components. The work started with comparison of two existing snow energy balance models using meteorological and snow data from Northern Finland. Based on the comparison the more simple of the tested snow parameterisations was modified to improve its performance in terms of snow heat balance simulation. The modified snow model was then coupled with a canopy scheme to account for the influence of forest on snow processes. The combined model was applied to clear-cut and coniferous forest sites in Southern Finland to identify the differences in snow mass and energy fluxes between open and forest. Finally, runoff generation in a forested catchment (Rudbäck, 0.18 km^2) was studied by using two different parameterisations. First, the catchment was parameterised as a three-dimensional domain, and secondly, as a vertical two-dimensional hillslope. The models produced similar results in terms of fit against measured daily streamflow, but the computed runoff components were different. Independent calibration of hydrological submodels yielded a more realistic partition of runoff into surface and subsurface components than did calibration merely against streamflow data. It is proposed that the hillslope model can be used to simulate runoff generation in each possibly non-contiguous area that is similar in terms of its land-use. A system where a set of such models is combined together can be used to quantify runoff contributions from pre-classified areas of different land-use, and constitutes a tool for studying hydrological impacts of land use changes.

Keywords	Hydrology, runoff, snow, forest, energy balance, mathematical models		
UDC	556.16:551.322:51.001.57:630*11	Number of pages	88
ISBN (printed)	951-22-6214-2	ISBN (pdf)	951-22-6237-1
ISBN (others)		ISSN	1456-2596
Publisher	HUT Laboratory of Water Resources		
Print distribution	Fax. +358 9 451 3856, E-mail contact@water.hut.fi		
☒ The dissertation can be read at http://lib.hut.fi/Diss/2003/isbn9512262371			

TEKNILLINEN KORKEAKOULU PL 1000, 02015 TKK, http://www.hut.fi	VÄITÖSKIRJAN TIIVISTELMÄ

Tekijä	Harri Koivusalo
Väitöskirjan nimi Lumen kertyminen, sulanta ja valunnan muodostuminen metsäisillä koealueilla Suomessa	
Käsikirjoituksen jättämispäivämäärä 14.6.2002	Väitöstilaisuuden ajankohta 10.1.2003
Osasto, laboratorio	Rakennus- ja ympäristötekniikka, Vesitalous ja vesirakennus
Tutkimusala	Hydrologia
Vastaväittäjä	Professori Per-Erik Jansson (Kungl Tekniska Högskolan, Tukholma)
Työn valvoja	Professori Pertti Vakkilainen (TKK)
Työn ohjaaja	Professori Tuomo Karvonen (TKK)

Tiivistelmä

Työssä käsitellään hydrologista mallijärjestelmää, jonka avulla voidaan laskea veden liikkeitä kasvustossa, lumipeitteessä, maaperässä ja valuma-alueen purku-uomassa. Järjestelmän kehittämisen taustalla on tavoite ihmistoimintojen hydrologisten vaikutusten ennustamisesta. Työ alkaa kahden eritasoisen lumen energiatasemallin vertailusta käyttäen Sodankylässä mitattuja lumi- ja säähavaintoja. Vertailun perusteella yksinkertaisempaa mallia lähdettiin muuttamaan mitatun ja lasketun lumen lämpötaseen yhteensopivuuden parantamiseksi. Lämpötaseen todenmukainen laskenta edellytti erityisesti lumen ja sen alapuolisen maakerroksen käsittelemistä erikseen. Uusi lumimalli liitettiin osaksi kasvustomallia, jotta lumen kertymistä ja sulantaa voitiin laskea fysikaalisesti perustellulla tavalla aukealla ja metsässä. Yhdistettyä laskentarutiinia käytettiin selvitettäessä metsän vaikutusta lumen sulantaan, kertymiseen ja lumipinnan energiavirtojen suuruuteen. Siuntiossa sijaitsevalla Rudbäckin valuma-alueella sademittareilla tehtyjen havaintojen perusteella kasvuston läpitullut sadanta oli kesäaikaan keskimäärin 29 % ja talviaikaan 26 % pienempi kuin hakkuuaukealla mitattu sadanta. Tästä seurasi pienempi lumen kertyminen metsässä aukeaan verrattuna. Toisaalta kasvusto hidasti lumen sulamista siinä määrin, että eteläsuomalaisen talven aikana lumen maksimivesiarvo saattoi useiden kertymis-sulamisjaksojen jälkeen saavuttaa talven suurimman arvonsa joko aukealla tai metsässä. Lopuksi valunnan syntymekanismeja Rudbäckin valuma-alueella tutkittiin kahden erityyppisen hydrologisen mallin avulla. Valuma-alueen maaperä diskretoitiin ensin kolmessa ulottuvuudessa, ja toiseksi alue yksinkertaistettiin tyypilliseksi kaltevaksi rinteeksi kahdessa ulottuvuudessa. Hajautettu kolmiulotteinen malli ja kaksiulotteinen tyyppiprofiilimalli tuottivat laskettujen kokonaisvaluntojen perusteella keskenään vertailukelpoiset tulokset, vaikka lasketut valunnan kulkeutumisreitit poikkesivat toisistaan. Hajautetussa mallissa maaperän kautta uomaan tulevan valunnan osuus oli ristiriidassa aikaisempien merkkiainekokeiden tulosten kanssa. Suoraan sadannasta tai lumen sulannasta muodostuvan valunnan osuus saatiin todenmukaisemmaksi tyyppiprofiilimallissa, jonka jokainen laskentarutiini oli kalibroitu ja validoitu itsenäisesti. Tulosten mukaan tyyppiprofiilimalli soveltuu kuvaamaan maankäytön suhteen yhdenmukaisen alueen hydrologisia prosesseja. Järjestelmää, jossa useita tyyppiprofiileja käytetään erityyppisten alueiden hydrologisen vasteen laskentaan, voidaan edelleen soveltaa maankäytön muutoksista aiheutuvien hydrologisten vaikutusten arvioimiseen.

Avainsanat	Hydrologia, valunta, lumi, metsä, energiatase, matemaattiset mallit		
UDK	556.16:551.322:51.001.57:630*11	Sivumäärä	88
ISBN (painettu)	951-22-6214-2	ISBN (pdf)	951-22-6237-1
ISBN (muut)		ISSN	1456-2596
Julkaisija	TKK Vesitalouden ja vesirakennuksen laboratorio		
Painetun väitöskirjan jakelu	Telefaksi +358 9 451 3856, Sähköposti contact@water.hut.fi		
☒ Luettavissa verkossa osoitteessa http://lib.hut.fi/Diss/2003/isbn9512262371			

LIST 0F APPENDED PAPERS

This dissertation is based on the following papers:

I: Koivusalo, H. and Heikinheimo, M. 1999. Surface energy exchange over a boreal snowpack: comparison of two snow energy balance models, Hydrological Processes, 13, 2395-2408.

II: Koivusalo, H., Heikinheimo, M. and Karvonen, T. 2001. Test of a simple two-layer parameterisation to simulate the energy balance and temperature of a snowpack, Theoretical and Applied Climatology, 70, 65-79.

III: Koivusalo, H. and Kokkonen, T. 2002. Snow processes in a forest clearing and in a coniferous forest, Journal of Hydrology, 262, 145-164.

IV: Koivusalo, H., Karvonen, T. and Lepistö, A. 2000. A quasi-three-dimensional model for predicting rainfall-runoff processes in a forested catchment in southern Finland, Hydrology and Earth System Sciences, 4, 65-78.

V: Koivusalo, H. and Kokkonen, T. Modelling runoff generation in a forested catchment in southern Finland, Hydrological Processes, in press.

The first author was responsible for the model applications in (I); writing and discussion of results were accomplished jointly with Dr. Martti Heikinheimo. Model development in (II) was conducted together with Prof. Tuomo Karvonen, and writing of the paper with Dr. Heikinheimo. The first author was responsible for the model development and computations in (III), and Mr. Teemu Kokkonen participated in the writing of the paper. The first author accomplished the model computations in (IV); the model was developed together with Prof. Karvonen and the paper was written together with Prof. Karvonen and Dr. Ahti Lepistö. The first author is responsible of the model computations in (V); model results were analysed and the paper was written together with Mr. Kokkonen.

Articles published or in press are reproduced by permission of the journals concerned*.

ACKNOWLEDGEMENTS - KIITOSSANAT

This thesis evolved from my earlier academic studies on surface runoff, erosion and hillslope hydrology at the Helsinki University of Technology (HUT), and snow modelling at the University of Washington (UW). I want to acknowledge professors Tuomo Karvonen (HUT), Pertti Vakkilainen (HUT) and Stephen Burges (UW) who sparked the start of my doctoral studies on hydrology. I am grateful for long-lasting support and supervision by Tuomo and Pertti through all phases of my studies at HUT.

The experimental work during four years in Siuntio was made possible by persistent help of Mr. Pertti Hyvönen from Pythagoras OY, Mr. Matti Keto from HUT and Mr. Noor Sepahi. I am also greatful to Margareta and Christer Segersven for their positive interest into the measurements on their land. I am indepted to Dr. Martti Heikinheimo from the Finnish Meteorological Institute and Dr. Ahti Lepistö from the Finnish Environment Institute for fruitful co-operation and data exchange. I owe special thanks to Mr. Teemu Kokkonen for friendship and long moments of brainstorming at the lab.

I am greatly indebted to all staff members and students at the Laboratory of Water Resources, where the friendly and inspiring atmosphere has given me strong support and motivation to work for my thesis. I warmly remember discussions and breaks with Dr. Ari Jolma, Ms. Maija Paasonen-Kivekäs, Mr. Mikko Jauhiainen, Mr. Tero Kärkkäinen, Ms. Terhi Helmiö, Ms. Irmeli Viitasaari, Ms. Erja Salermo, and many others.

I am thankful to Dr. Thomas Franti from the University of Nebraska for English language revisions.

This study was funded by the Academy of Finland project “Predicting impacts of land use changes on catchment hydrological processes.” Additional financial support was kindly provided by Maa- ja Vesitekniikan tuki ry. (the Land and Water Technology Foundation), the Finnish Cultural Foundation, the Sven Hallin Foundation, the Vilho, Yrjö and Kalle Väisälä Foundation and the Oskar Öfflund Foundation.

Tätä työtä valmisteltiin Otaniemessä verraten pitkän ajan vuodesta 1997 lähtien. Erityiset kiitokset haluan lausua kuluneista vuosista kotijoukoille, joiden myötämielinen tuki on kantanut minua työn eri vaiheissa. Pirjo, Anna, Olli ja Elina ovat pysyneet rinnallani ja opintojen vastapainona. Lopuksi haluan omistaa tämän työn vanhemmilleni, Maija-Liisalle ja Aarolle, joiden kannustamana olen saanut opin tietä käydä.

Espoo, 18.9.2002

Harri Koivusalo

TABLE OF CONTENTS

1 INTRODUCTION

1.1 Background

Variability in meteorological conditions between different years makes it difficult to distinguish the influence of other factors, such as human activities, on catchment hydrological response. Extreme flood events, for example, primarily result from extraordinary weather conditions and it is difficult to judge how much the flood is affected by past changes in land use, drainage conditions, channel geometry, etc. While the role of man-made alterations in the historical behaviour of catchment processes is hard to resolve, predicting the influence of future alterations is even more demanding. These challenges create the need to develop measures and tools that can aid in forecasting hydrological behaviour of a catchment. Such measures and tools are valuable for managing water resources, introducing protective measures against extreme hydrological events, and quantifying effects of land-use and climatic changes on hydrology. Hydrological models are regarded as indispensable tools for these purposes. For example, a precipitation-streamflow model is a necessary, if not sufficient, prerequisite for simulating leaching and transport of pollutants with runoff.

The broad objective of this thesis is to introduce methodology for predicting the influence of land use changes on catchment hydrological processes. The modelling aims at thorough quantification of hydrological sub-processes, and independently testing the sub-process computation schemes against measured hydrological state variables and fluxes. Physics-based process descriptions are selected in order to put together a system that is likely to be suitable for impact assessments.

The experimental and modelling work of this thesis has a special focus on wintertime processes. Finland is located at latitudes where accumulation and melt of seasonal snow cover has a prominent effect on catchment hydrology. About 30-50% of annual precipitation falls as snow, and about 15-30% of precipitation is stored in the snowpack at the time of maximum snow water equivalent. Spring snowmelt typically leads to the largest seasonal runoff volumes, giving rise to risk of flooding.

Predicting catchment hydrological processes in its entirety is a vast, multidisciplinary task extending to a range of spatial and temporal scales. The following subsections attempt to identify particular research needs in hydrological modelling and lead the reader to the specific scope and aims of this thesis.

1.2 Precipitation-streamflow modelling

This subchapter gives a brief literature review on precipitation-streamflow modelling and provides general background to relate the case studies of this thesis to a broader context. Runoff generation mechanisms are discussed first, following with a classification of hydrological models, and a list of hydrological modelling goals of this work.

1.2.1 Runoff generation mechanisms

Runoff in this thesis refers to water input from land areas and soils into a channel network, and streamflow refers to flow within the channel network. Runoff generation mechanisms describe different processes leading to water entering the channel network in response to rainfall, snowmelt and soil and ground water movement. Runoff generation processes within the catchment are essentially three-dimensional and a key feature of the processes is the spatial variability of areas producing runoff (e.g. Hewlett and Hibbert, 1967; Sivapalan et al., 1987). One approach for simplifying the distributed spatial description of the catchment is to characterise the three-dimensional catchment domain as a set of two-dimensional profiles around the stream network. The profiles can be determined following topographically driven flowpaths from a water divide down to the nearest stream segment. Such vertical two-dimensional sloping sections form hillslopes where a range of runoff generation processes can be described through concepts of hillslope hydrology as reviewed in Kirkby (1985; 1988) and Bronstert (1999).

Runoff from hillslopes to rivers and lakes has traditionally been partitioned into overland and subsurface flow. Overland flow may occur as infiltration-excess (Hortonian) overland flow, saturation excess overland flow, or return flow. Infiltration-excess overland flow as first introduced by Horton (1933) is generated over areas where rainfall or snowmelt intensity exceeds the infiltration capacity of soil surface layers. Saturation-excess overland flow may occur over areas where the soil water storage is filled up to capacity and rainfall or snowmelt cannot infiltrate into soils (Dunne and Black, 1970). Return flow is produced in locations where ground water flow leads to exfiltration from saturated soil to the soil surface (Dunne, 1983; Kirkby, 1988; Bonell, 1993). Infiltration-excess overland flow plays often an important role during high rainfall intensities and in arid areas or degraded land (Kirkby, 1985), whereas its contribution is of minor importance in natural land areas with permeable soils and with humid temperate climate (e.g. Bonell, 1993; Lepistö, 1994). Dunne (1983) suggested that the saturation-excess overland flow becomes important in thickly vegetated areas with thin soils, high water tables and long, gentle concave hillslopes.

The base flow component of the stream hydrograph is normally produced by subsurface flow. Environmental tracer studies carried out in headwater catchments have suggested that subsurface flow may dominate even peak streamflow during storm events (e.g. Sklash and Farvolden, 1979; Pearce et al., 1986; Rodhe, 1987). The importance of subsurface flow has been explained with different mechanisms of rapid runoff response via subsurface pathways. Bonell (1993) provides a review of runoff processes in forest areas, where generation of subsurface flow can be attributed to several possible mechanisms, such as macropore or preferential flow, subsurface stormflow, saturated wedge throughflow, ground water ridging and transmissivity feedback.

Kendall et al. (1995) note that hydrologic pathways are often incorrectly represented in the rainfall-runoff models. For example, when chemical data are coupled to the models, they rarely reflect the stream water chemistry accurately. Such shortcomings easily question the validity of the assumed runoff generation mechanisms. Progress in tracer techniques provides clues about hydrological pathways and residence times within a catchment. Information from a set of two- and three-component tracer analyses can lead to plausible conceptualisations of precipitation-runoff mechanisms (Rice and Hornberger, 1998; Brown et al., 1999; Sueker et al., 2000), which may be exploited in development of precipitation-streamflow models.

1.2.2 Historical perspective on hydrological modelling

The first attempt to relate maximum runoff to rainfall in mathematical terms was the introduction of the rational method by a group of Irish engineers in 1840s' (Dooge, 1957). Mathematical theories characterising the transformation of rainfall into runoff on a continuous time basis emerged during the first half of the 20th century. Later modelling activities were boosted with the increasing performance of digital computers.

In early studies, hydrographs of Hortonian surface runoff (flood runoff) and base flow were separated using simple methods, such as graphical separation. Then the aim was to identify the share of precipitation (excess rainfall) that becomes flood runoff, and estimate the delay between excess rainfall and flood runoff. The simplest way to estimate excess rainfall was to subtract infiltration losses from rainfall using available theories (e.g. Green and Ampt, 1911; Horton, 1940). Sherman (1932) determined the conversion from excess rainfall to streamflow at the outlet of a catchment by means of a unit hydrograph concept, and Zoch (1934) and Nash (1957, 1959) introduced the use of linear storages as delay functions.

Hydrological simulation techniques running on computers were developed in 1960s'. In the first simulation models (e.g. Linsley and Crawford, 1960) hydrological subprocesses were characterised as simplified conceptualisations, which lead to a system of interconnected linear and non-

linear storages. The Stanford Watershed Model (Crawford and Linsley, 1966), the Sacramento model (Burnash et al., 1973), and the HBV-model (Bergström and Forsman, 1973) are examples of such conceptual models. Later the concepts of classical continuum mechanics were utilised for better consideration of physical processes behind rainfall-streamflow conversion. The start of distributed hydrological modelling traces back to the blueprint of Freeze and Harlan (1969). Literature up to the present shows an excessive number of mathematical simulation models developed for predicting precipitation-streamflow processes. According to a categorisation presented in Refsgaard (1997) the models can be classified on the basis of their process description or on the basis of their spatial description.

1.2.3 Model classification based on process description

Hydrological processes that are commonly quantified in precipitation-streamflow modelling include precipitation, interception, evaporation, transpiration, snow accumulation and melt, soil and ground water movement, overland flow, and channel flow. The importance of each process depends on the catchment and climatic characteristics, as well as on the modelling objectives. Individual processes are always more or less simplified, and they may be ignored or embedded with others. These choices lead to models that are different in their process description. Precipitation-streamflow models can be loosely classified according to their process description as metric, conceptual, or physics-based.

Metric models are data-oriented and merely seek relationship between streamflow and excess rainfall without concern for the physical processes behind the measured series. The transfer function model, which was first popularised by Box and Jenkins (1976), is an example of a systems approach (e.g. Wood and O'Connell, 1985), and can be considered as a metric precipitation-streamflow model. Conceptual models mentioned above have remained in use because of their straightforward implementation and linkage with optimisation routines for model calibration. Comparative analyses of conceptual models are presented in Franchini and Pacciani (1991) and Ye et al. (1997).

The idea behind physics-based models has been an attempt to find a direct linkage between model parameters and field measurements. Such a linkage would enhance use of a model for predicting hydrological processes in ungauged catchments and simulating hydrological effects of land-use or climatic changes. One of the most rigorous physics-based hydrological models is the SHE model (Système Hydrologique Européen, Abbott et al., 1986; Bathurst, 1986), where soil and ground water movement, snow accumulation and melt, and channel flow routing are characterised in terms of partial differential equations. Examples of other models falling into the

same category are the IHDM (e.g. Calver, 1988), TOPOG (Vertessy et al., 1993), and KINEROS2 (Smith et al., 1995).

1.2.4 Model classification based on spatial description

The spatial description of precipitation-streamflow models can be regarded as lumped, distributed or semi-distributed. A model is lumped when state variables and fluxes characterise average behaviour within the catchment and spatial variability of hydrological processes is ignored. Distributed models account for spatial variability of hydrological state variables and fluxes, and are predominantly physics-based. Spatial variability can be described in distributed models within the resolution of a finite grid, where the relevant parameter values must be given for all grid cells. Such an extensive parameterisation over a catchment is demanding in terms of computational burden and data acquisition (Beven, 1989; Grayson et al., 1992; Woolhiser, 1996). The model parameters and state variables may depend on the grid resolution, and consequently, it may be difficult to relate point measurements to grid-scale effective model parameters.

Semi-distributed modelling approaches and subgrid-scale variability schemes have been introduced to alleviate the above-mentioned problems. All semi-distributed models share the assumption that spatial variability in key hydrologic properties can be described in a condensed form. In TOPMODEL topographic variability is presented as the topographic index curve, which can be used to determine the spatial extent of saturated areas at a given time (Beven and Kirkby, 1979). Becker (1992) and Becker and Braun (1999) aggregate areas of similar hydrological properties into a patch or a 'hydrotope', and Flügel (1995) subdivide the catchment into hydrological response units. Tao and Kouwen (1989) and Kite and Kouwen (1992) present a hydrological modelling system using land classification into areas regarded as hydrologically homogeneous. In this kind of framework, each of the identified units is assigned a water balance model. The model can be based on either conceptual or physics-based process description. When a conceptual model is selected, within the scope of the unit, the spatial description is of the lumped kind. And when a physics-based model is adopted, a simplified description of spatial dimensions within a unit is required. The simplified description retains the benefits of a semi-distributed approach.

Another approach to facilitate the application of distributed models in low-resolution grids is inclusion of subgrid-scale variability schemes. Subgrid-scale variability may be treated by means of distribution functions determining variability of model parameters in spatial scales smaller than the grid size. One of the early examples is the representation of non-uniformity of soil moisture storage distribution in Xinanjiang model (Zhao et al., 1980). Wood et al. (1992) and Liang et al. (1994) further extend this idea in VIC

model and Todini (1996) in ARNO model. Review of parameter scaling and subgrid scale processes is presented in Blöschl and Sivapalan (1995).

1.2.5 Why physics-based modelling?

In terms of streamflow reproduction it is hard to make general discrimination between performances of different hydrological models. Several studies suggest that both conceptual and physics-based models need calibration to some extent and can lead to comparable goodness of fit between measured and calculated streamflow (Ye et al., 1997; Refsgaard, 1997; Bergström and Graham, 1998; Beven, 2001). Ye et al. (1997) regard the use of distributed physics-based models disadvantageous, when increase in computational burden does not improve streamflow simulation. The justification of distributed hydrological modelling therefore requires more than producing merely streamflow.

Impact studies call for hydrological models which can separate processes and differentiate areas affected and unaffected by changing conditions. Simulations of hydrological effects of land-use or climate changes are examples of impact studies. Land-use types typically form a mosaic landscape structure, and changes in land-use are spatially variable impeding application of lumped precipitation-streamflow models. Distributed or semi-distributed models are set up with separate modelling components for areas affected and unaffected by a land-use change. When hydrological data from changed and unchanged land-use conditions are available, impact simulations may be conducted within the range of measured conditions using a conceptual or physics-based model that is calibrated against measured data. Such data are often unattainable, and then physics-based models remain as the best available tools for simulating effects of land-use changes. Physics-based models with detailed process description should be capable of simulating how land-use changes influence each hydrological process. Refsgaard (1997) emphasises that reliable extrapolation of simulation results has so far proven unattainable and calibration against measured data is required practically for each variable for which predictions are made. Ewen and Parkin (1996) call for generally applicable methods for validating catchment models that are aimed at predicting the impacts of changes in land-use and climate. A need for the development and testing of physics-based models for impact assessment is eminent.

Studying effects of climate change may necessitate coupling of hydrological models with atmospheric circulation models, which require surface temperature and albedo as part of their boundary condition (Marshall et al., 1999). Surface temperature and energy exchanges can be simulated by means of a land-surface-vegetation-atmosphere transfer (SVAT) scheme, which is an essential component of a physics-based hydrological model. Wigmosta et al. (1994), Nijssen et al. (1997), and Jansson (1998)

present examples of physics-based models capable of simulating surface energy exchanges.

1.2.6 Hydrological modelling in this work

Earlier studies suggest that the computational burden and overwhelming data requirements of physics-based models are major obstructions for their applications (Beven, 1989; Grayson et al., 1992; Woolhiser, 1996). This leads to questions of 1) how to decrease the computational burden of physics-based models, and 2) how to restrict data requirements for model implementation without losing the benefits that come with distributed predictions of hydrological state variables and fluxes? Much of the computational burden comes through coupling of vertical and lateral water flow models in a distributed setting. Simplification for coupling unsaturated and saturated flow in three-dimensional domain provides one avenue for reducing the burden. In this thesis a one-dimensional model that simulates vertical soil water dynamics in the unsaturated zone is coupled with a two-dimensional ground water model in order to develop a computationally efficient three-dimensional scheme for simulating soil and ground water interactions and runoff generation within a catchment. The unsaturated zone routine is based on DRAINMOD, which was originally introduced by Skaggs (1980) for simulating hydrology of drained agricultural fields. DRAINMOD has been shown to simulate unsaturated zone processes comparably to the results of more complex models that are based on Richards equation (Karvonen and Skaggs, 1993). The present study is a first attempt to extend the DRAINMOD approach to three-dimensional computation domain.

In addition to problems arising from vast data requirements, lack of functional linkage between grid-scale effective model parameters and point-scale field measurements impedes application of distributed models. This issue is a subject of ongoing research on subgrid-scale variability and scaling. Methodologies are needed for restricting spatial dimensions of distributed physics-based models in order to reduce data requirements. These methodologies should identify a modelling domain that can aid in establishing a meaningful linkage between model parameterisation and field measurements. Development of hydrological modelling in this thesis leads to a methodology that uses a vertical two-dimensional hillslope as a basic modelling unit. As stated earlier, a range of runoff generation processes can be identified experimentally and mathematically at the hillslope scale. The basic idea is that the part of a catchment that possesses homogeneous behaviour with respect to dominating hydrological processes is considered as a hydrologically similar area (e.g. Becker 1992; Schultz, 1993). Typical hillslopes are then identified for such areas, and a water balance model is implemented in each hillslope domain.

Many earlier studies suggest that use of physics-based models is not well justified when the objective is merely streamflow reproduction. Comparison of the model results against an aggregate variable, such as streamflow, does not validate any of the submodels included in a physics-based modelling system. Submodels of different hydrological processes must therefore be calibrated and validated separately against measured state variables or fluxes from each process. The current work presents new measurements from forested sites in northern and southern Finland for calibration and validation of hydrological process models. Snow mass, snow temperature, and surface energy flux data from Sodankylä are used to compare snow energy balance models and develop a new energy balance scheme for the current modelling system. Another set of hydrometeorological data from Siuntio is used to calibrate and validate models of interception, snow accumulation and melt, soil and ground water interaction, and streamflow routing separately against measured throughfall, snow water equivalent, ground water levels, and streamflow, respectively.

Inclusion of tracer study results into precipitation-streamflow modelling is increasingly receiving attention as a promising way to identify more realistic process representations. Such efforts are not expected to bring about any advances in prediction of calculated total streamflow volumes, but rather they can provide some basis to validate the assumed runoff generation mechanisms (Becker et al., 1999). Uhlenbrook and Leibundgut (1999, 2002) introduced a tracer aided catchment model where conceptualisations of runoff generation mechanisms were incorporated into the structure of a semi-distributed conceptual model. An interesting question is to what extent tracer results support assumptions behind physics-based models? In this thesis, development of the hydrological model aims at separation of overland and subsurface flow pathways in simulating runoff generation. The applications involve calibration and validation of a physics-based precipitation-streamflow model against hydrometric data, and assessment of the model generated runoff against fractions of isotopically traced event and pre-event water. This thesis is partially motivated by the fact that few studies have compared partitioning of runoff as computed in physics-based rainfall-runoff models against tracer results.

1.3 Snow accumulation and melt

Snow accumulation and melt have a significant influence on precipitation-streamflow processes in high latitudes. In the boreal region a large fraction of the area is covered with forests where the influence of the canopy on snow processes is significant. In the following subsections development and challenges of snow modelling are outlined.

1.3.1 Progress in snow modelling

Much early modelling work on snow processes is summarised in U.S. Army Corps of Engineers (1956). Extensive field data from the western United States were exploited to investigate physical processes of snow and develop methods for solving snow hydrology problems, such as forecasting snowmelt-induced runoff. In these investigations use of meteorological variables as snowmelt indices was analysed. Air temperature was found to be the best single index of snowmelt in forest, and net radiation in the open. These findings have been utilised in many modelling case studies where snowmelt is computed as a function of an energy-index, such as models based on daily mean, minimum, or maximum air temperature, or radiation intensity.

In a degree-day model snowmelt intensity is directly proportional to mean daily air temperature and only precipitation and air temperature are needed as model input data. Wide availability of such data has lead to popularity of degree-day (temperature-index) models especially in operational streamflow forecasting (e.g. Bergström, 1976; Kuusisto, 1984; WMO 1986; Vehviläinen, 1992; Bergström and Graham, 1998). Degree-day models can be complicated by inclusion of radiation as an additional snowmelt-index. Examples of combined radiation and temperature index models are presented in Rango and Martinec (1995) and Cazorzi and Fontana (1996).

Physics-based snow models use the energy balance approach, which permits computation of the heat available to change snow temperature or to melt snow. In addition to air temperature and precipitation data, energy balance models require short- and long-wave radiation, relative humidity, and wind speed as input data. The concepts of snow surface energy balance have already been presented by the U.S. Army Corps of Engineers (1956) and reviewed later in Anderson (1968) and Male and Granger (1981). Energy balance snow models may be further classified according to snowpack discretisation schemes. Simple one-dimensional models treat the snowpack as one or two horizontal layers, whereas more complete models subdivide the snowpack into several layers, whose total number, depth, and density change with time. Energy balance models are not superior to empirical approaches in predicting average snow water equivalent or snowmelt runoff (e.g. WMO 1986, Vehviläinen, 1992). The energy balance approach becomes necessary when separation of snow surface energy fluxes and prediction of the snow surface temperature are important. This is the case in the context of coupled land-surface-atmosphere models, when hydrological models are linked with climate models (e.g. Marshall et al., 1999; Gustafsson, 2002), and in the context of assessing hydrological effects of land-use changes, such as logging (Lundberg, 1996). Physics-based snow models are also useful in simulating small-scale processes of snow metamorphosis, melt, and thermal state, or for predicting spatially distributed

snow water equivalent and short-term extreme snowmelt conditions (Blöschl et al., 1991; Gray and Prowse, 1992).

In Finland, experimental studies of snow accumulation and melt have a long tradition (e.g. Korhonen, 1915; 1923) and emerged much earlier than snow modelling activities in the late 1970s'. Renqvist et al. (1939) remark that the Central Meteorological Institute and Geographical Society of Finland started regular snow depth measurements in the country in 1890. More extensive and systematic snow measurements were deemed necessary after occurrence of great floods in the end of 19th century. The Hydrographic Office set up their measurements in 1909, and later the Hydrological Office established a snow course network in 1935. The Agricultural Board operated additional snow course measurements in selected research basins starting from 1933 (Kaitera, 1939). In 1957, the research basins and snow course measurements were rearranged to distribute them all over the country (Mustonen, 1965).

Extensive records of Finnish snow course data have been exploited in snowmelt modelling by Gürer (1975) and Kaila (1977), who carried out long-term snowmelt simulations based on regression techniques. Kuusisto (1980), Hiitiö (1982), and Vakkilainen and Karvonen (1982) applied the degree-day approach in producing daily estimates of snowmelt. Statistical analysis of Finnish snow course measurements and testing of energy index snowmelt models are presented in Kuusisto (1984). Vehviläinen (1992) continued his work by incorporating different snowmelt routines into an operational streamflow forecasting model. According to Kuusisto (1984) and Vehviläinen (1992), the temperature index models are most suitable for computing snowmelt in operational hydrological models implemented at the Finnish Environment Institute.

1.3.2 Energy balance snow models

The energy balance approach in snow modelling became widely used in the middle of 1970s' when both one-layer and multi-layer snow models were introduced. Price and Dunne (1976) developed an energy balance model, which considered snowpack as one homogeneous layer. Anderson (1976) was among the first to introduce a multi-layer approach for modelling mass and heat balance of a seasonal snow cover. The one-dimensional model of Anderson (1976) discretised a snowpack vertically into homogeneous layers, whose number was allowed to change with time. In each layer the model simulates snow temperature, mass fluxes due to phase changes of water, liquid water transmission, and the snow density changes. Anderson (1976) introduced a number of empirical equations describing snow processes and properties, such as snow compaction and settling, density of precipitated snow, snow grain diameter, snow albedo, and effective thermal conductivity of snow.

Morris (1983) developed a physics-based snowmelt model, which was used as a subroutine in the SHE model (Abbott et al., 1986). In a vertical one-dimensional representation snow was considered as a mixture of three water phases and dry air. Jordan (1991) combined the mixture theory (e.g. Morris, 1983; Kelly et al., 1986) and the point model of Anderson (1976) into a snow temperature model, which she called SNTHERM. The model has been continuously refined and modified to take into account detailed processes affecting snowpack energy and mass balance (Jordan, 1992; Jordan et al., 1999). The model partitions a snowpack into horizontal layers in a similar fashion to the approach used by Anderson (1976), and simulates snow temperature, density, effective thermal conductivity and specific heat profiles under a variety of winter conditions. In addition to snow properties, the model simulates soil temperatures. The model is intended primarily for simulation of snow processes; water movement in soil is disregarded, and snowmelt outflow is drained artificially at the snow-soil interface. Other examples of multi-layer snow models are reported in Illangasekare et al. (1990), Brun et al. (1989; 1992), and Tuteja and Cunnane (1997).

Beside multi-layer point snowmelt models, a number of simple energy balance models treating snowpack as one or two layers have been introduced (Marks, 1988; Ohta, 1994; Wigmosta et al., 1994; Tarboton et al., 1995; Stähli and Jansson, 1998). These models are computationally simpler than the multi-layer algorithms and are typically intended for modelling spatially variable snow processes. Some of the simple models produce separate estimates of snow cover and snow surface temperatures (e.g. Tarboton et al., 1995), whereas others simulate only bulk heat content and temperature of the snowpack (e.g. Wigmosta et al., 1994).

The long list of different energy balance models calls for a comparative study to find out the degree of complexity in parameterisation needed to reproduce snow mass and heat balance. Such a comparison should not only focus on average mass and heat balance simulations of the snowpack, but also on surface energy exchange and snow surface temperature simulation, which are important links to atmospheric processes.

1.3.3 Modelling the effect of forest on snow processes

Snow energy balance models have typically been designed to operate in open areas where no canopy is present. Unforested areas exhibit energy exchange with the atmosphere that is radically different from the continuous forested areas (Harding and Pomeroy, 1996). Therefore the application of these models in forested areas requires the influence of the canopy on the energy flux components to be taken into account. In several studies conducted in boreal regions net radiation has been found to increase in importance with respect to turbulent fluxes when a forest canopy is present (Price and Dunne, 1976; Pomeroy and Dion, 1996; Vehviläinen, 1992; Link

and Marks, 1999; Woo and Giesbrecht, 2000). Incident solar radiation is decreased because of shading by the trees, but emission of downward long-wave radiation from trees increases the net radiation beneath the canopy. Turbulent fluxes are suppressed by the low wind speeds close to snow cover on the ground.

Hardy et al. (1997) and Davis et al. (1997) used a multi-layer snow energy balance model (SNTHERM) to assess snowmelt dynamics below a coniferous forest stand. The snow model was coupled with a radiation transfer model, which estimated the shading effect of the canopy. Woo and Giesbrecht (2000) and Giesbrecht and Woo (2000) considered spring snowmelt in a subarctic site in Yukon Territory, Canada, and accounted for the effect of canopy both at single tree and forest scales. All these studies have in common the fact that they concentrate on periods of little or no precipitation in the spring melt season and thus avoid the need to consider the effects of interception. Interception and sublimation of snow have been reported to result in substantial decrease in net precipitation in dense forests (Lundberg, 1993; Lundberg et al., 1998; Nakai et al., 1999; Pomeroy et al., 1998) and they have to be taken into account when snow processes are described over the entire winter season.

In the western United States Storck (2000) studied removal of intercepted snow by sublimation, melt-water drip and mass release, and implemented a physics-based model to simulate the influence of canopy on snow processes on the ground. Storck (2000) found that the interception process is strongly controlled by micrometeorological conditions, and that results of snow interception studies may not be extrapolated to areas with different climatic conditions. Detailed studies of snow processes in forests should therefore be extended to cover a range of climatic conditions in the boreal region.

1.3.4 Snow modelling in this work

Vehviläinen (1992) presented a comparison of two snow energy balance models, which treated the snowpack as one layer and had similar procedures for estimating the surface fluxes, but different representation of snow cover properties. Both models were calibrated against observed snow water equivalent and runoff. The meteorological data in Vehviläinen (1992) were daily time series and did not support comparison between the models at time scales less than a day. The snow studies in this thesis continue the examination of snow energy balance in Finnish climatic conditions, and extent the modelling efforts to hourly time scales. The objective is to test more rigorous energy balance schemes than those used in earlier model comparisons (e.g. Vehviläinen, 1992). The tested models are 1) UEB (Tarboton et al., 1995), which treats snowpack as one lumped layer, 2) SNTHERM (Jordan, 1991), which includes a complex multi-layer parameterisation of snow cover, and 3) a new snow energy balance scheme,

which subdivides the snowpack into two layers. Since the models can be regarded as physics-based, they are not calibrated against measured snow data. The model comparison is conducted not only in terms of snow water equivalent, but also in terms of snow surface temperature, snow heat content, surface energy fluxes, and liquid water content of snow.

The effect of different terrain types on snowmelt in Finland has received attention in many earlier studies exploiting data from the snow course networks (Kaitera, 1939; Mustonen, 1965; Kuusisto, 1984). Kaitera (1939) related ground measurements of snow water equivalent to canopy closure in mixed and coniferous forests, and noted that prior to spring melt snow water equivalent decreases when moving from sparse forests to open fields, and from fields to dense forests. Based on ground measurements Seppänen (1961) studied differences in snow water equivalent between open and pine-dominated forests. The results point out that interception of snow in the conifer tree canopy may have a major role in the water balance of dense forests. The earlier measurements, however, do not support detailed examination of the canopy and snow processes, or testing models at time scales less than one day. This thesis presents recent micrometeorological and snow measurements from a mature coniferous forest in southern Finland. These data provide the necessary basis for calibration and validation of process models characterising canopy interception, and snow accumulation and melt on the ground. Climatic conditions in the experimental site are more temperate than those in North American and Siberian regions having as northerly a location. Due to the effects of the Gulf Stream in the Atlantic Ocean, winters are relatively mild and snowmelt may occur in mid-winder conditions when intensity of the solar radiation is insignificant. The role of different energy sources giving rise to snowmelt in such conditions has not adequately been addressed. This study attempts to add to this knowledge.

1.4 Scope and objectives

The broad objective in the present model development is to formulate a system suitable for simulating the effects of land use changes on catchment hydrological response. Such a goal calls for implementation of physics-based models for each hydrological process separately. The case studies of this thesis show how each model is calibrated and validated against hydrological state variables or fluxes.

The modelling efforts are concentrated on conditions varying from open to forest. Testing of the models uses field data from a sparsely forested site in northern Finland and from a catchment covered by mature coniferous stand in southern Finland. Special focus is directed on winter and springtime processes.

Specific objectives of snow applications are to

1) test two snow models (UEB and SNTHERM) of different complexity in simulating snow surface energy exchange and snow mass balance, and identify the major differences in structures and performances of the studied models (I),

2) develop a new snow energy balance scheme, which can act as a subroutine in a physics-based hydrological model and which yields successful simulation results of snow mass and heat balance (II),

3) collect snow and micrometeorological data for testing the snow energy balance model over several winter seasons in open and forested sites (III)

4) introduce a canopy process scheme, couple it with the new snow model, and simulate snow processes in the absence and presence of a coniferous forest canopy (III)

5) identify energy fluxes contributing to snowmelt in the open and in the forest in mid-winter and spring conditions (III).

Runoff generation studies of this thesis aim at

6) collecting hourly runoff and meteorological data from a forested catchment for testing hydrological models (V),

7) developing physics-based runoff generation schemes in different spatial descriptions (IV, V),

8) simplifying the coupling of soil and ground water computation procedures by means of a DRAINMOD-type (Skaggs, 1980) approximation to one-dimensional Richards equation (IV, V), and

9) assessing the simulation results against hydrometric and tracer data from a small forested catchment (IV, V).

Two hydrological models with different spatial descriptions were developed. One is a distributed, quasi-three-dimensional model. The other is a semi-distributed model simulating catchment response from a single hillslope.

2 DATASETS

2.1 Outline

One dataset from Sodankylä, northern Finland, and two from Siuntio, southern Finland, were used in the case studies. The Sodankylä data were provided by the Finnish Meteorological Institute and included micrometeorological, snow and turbulence data for snow modelling case studies (I, II). The hydrometeorological and tracer data from Siuntio were available from the Finnish Environment Institute and were utilised in precipitation-streamflow modelling (IV, V). The third set of data was gathered in Siuntio by the Helsinki University of Technology for development and testing of canopy and snow modelling schemes (III) and for modelling runoff generation (V). The objective of these measurements was to gather a data set that is more extensive and more suitable for modelling purposes compared with the earlier measurements in Finland.

2.2 Sodankylä 1997 data

Sodankylä was the northern site for the WINTEX (winter experiment) field campaign, which concentrated on the land-surface-atmosphere interactions in a wintertime boreal forest (Heikinheimo and Halldin, 1996; Harding et al., 2001). WINTEX was a continuation of the NOPEX (northern hemisphere climate processes field experiment), which studied land-surface processes at a regional scale for a mixed land cover dominated by boreal forest (e.g. Halldin et al., 1998; 1999).

Sodankylä is located about 100 km north of the Arctic Circle (Figure 1); the climate there is subarctic and characterized by long and cold continental-type winters and relatively warm but short summers. During 1931-60 the average annual precipitation was 507 mm and the mean annual temperature –0.5 ºC.

The meteorological data from Sodankylä Observatory covered the period from 12 March to 30 May 1997. The data included downward short-wave radiation at a height of 16.8 m, reflected short-wave radiation at 2 m, net radiation at 2 m, both air temperature and relative humidity at 2 m, wind speed at 22 m, cloud cover observations, precipitation and form of precipitation. Radiation measurements were taken at one-hour and the other meteorological data were gathered at 3-hour intervals. Measurements of

turbulent energy exchange were made over a two-week period in March using the eddy correlation technique. For the purposes of this study, an estimate of the sensible heat flux was derived at the height of 3 m, and an estimate of latent heat flux at the height of 18 m.

Vertical profiles of snow density and temperature were measured in an opening within a sparse coniferous forest stand. Hourly variations of snow (or air) temperature were measured at 9 locations between heights from 0.1 to 0.9 m above the ground surface. In addition, two infrared sensors were pointed downward to measure the snow surface temperature once every hour. Snow depth, snow water equivalent and vertical snow density profile were measured at least once a week depending on the occurrence of precipitation and snowmelt.

2.3 Siuntio 1991-1996 data

Hydrometeorological and tracer measurements from a forested catchment (Rudbäck, 0.18 km^2, Figure 1) in southern Finland were provided by the Finnish Environment Institute. The elevation in the area ranges from 34 m to 65 m with exposed bedrock on top of the hills. The catchment has shallow depths of mineral soils underlined by impermeable bedrock. Soils are mainly composed of silty and sandy moraines, but layers of clay soils also occur. The catchment is covered by a mature forest stand dominated by Norway Spruce. More details on the site information are published in Lepistö (1996) and Lepistö and Kivinen (1997).

The climate in Siuntio is temperate with cold, wet winters, having several cycles of snow accumulation and melt. Mean annual precipitation (uncorrected) during 1991-96 was 700 mm, which includes 15-25 % of snowfall. Mean annual air temperature is about 5 °C. Daily discharge values at the outlet of a stream draining the catchment were available from the period 1991-96.

Precipitation was measured daily 2 km from the site and other meteorological data were available from stations operated by the Finnish Meteorological Institute. Mean, minimum, and maximum air temperature and relative humidity were measured in Vihti, which is located approximately 30 km from the catchment. Daily means of global radiation were available from the Helsinki-Vantaa airport, located 44 km from Rudbäck.

Lepistö (1994) measured oxygen isotope concentrations in precipitation and in stream water to determine monthly fractions of event and pre-event water for a period from 1991 to 1992. The tracer data of Lepistö (1994) was used in this thesis to assess model performance.

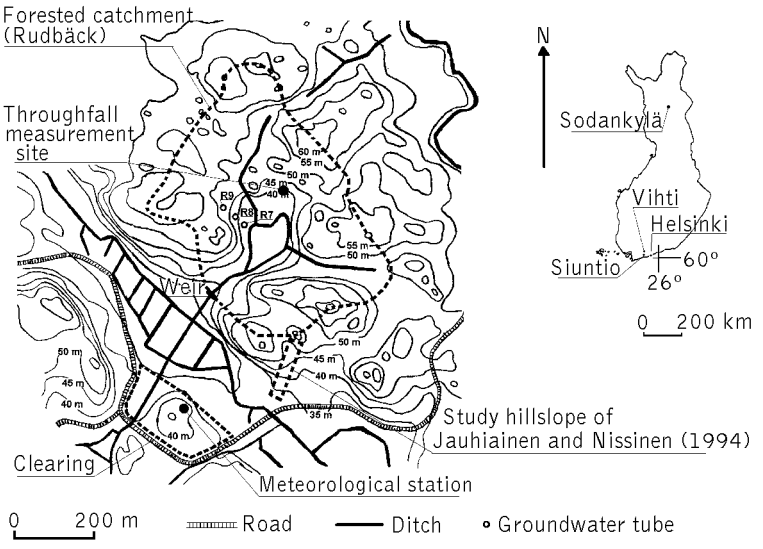

Figure 1. Locations of Sodankylä Observatory, study catchment (Rudbäck) in Siuntio and the meteorological stations in Vihti and Helsinki/Vantaa airport. Catchment layout shows the locations of the streamflow measurement weir, the meteorological station at site, and the ground water tubes (R7, R8, R9).

2.4 Siuntio 1996-2000 data

At the end of 1996, the site in Siuntio was supplemented with automated and manual hydrometeorological measurements. Snow depth was measured manually at 22 points in the forested catchment, and at 12 points in an adjacent clearing (about 0.03 km^2, see Figure 1). Water equivalent of snow was measured at three points in both forested and open sites by weighing cylindrical snow samples. Accumulated precipitation in the clearing was measured at one point using a shielded gauge and throughfall in the forest was measured in six unshielded gauges. Measurements were taken once or twice per week depending on the occurrence of snowfalls and snowmelt.

Starting from the end of November 1996, micrometeorological variables at a height of 2 m above the ground were recorded half-hourly in the clearing and in the forest beneath the canopy. The variables at both sites included air temperature, relative humidity, wind speed, downward short-wave radiation and reflected short-wave radiation. Downward long-wave radiation was measured in the open starting from January 1997, and the sensor was moved to the forest in January 1999 where it resided until the meteorological station was shut down in October 1999. Precipitation in the form of rain or snowfall was measured in the clearing, where the weight of a wind-shielded container (0.44×0.44 m^2) gave accumulated precipitation. Additional temperature measurements were recorded at a distance of 0.3 m

and 0.1 m below the soil surface, and at the heights of 0.1 m and 0.3 m above the ground in the open. Similarly, in the forest temperature measurements were recorded at 0.2 m intervals above and below the soil surface (from -0.5 m to +0.5 m). The meteorological station in the clearing continued to operate until the end of the study period in April 2000.

Precipitation in the open was corrected using the procedure recommended for the Finnish H&H-90 gauge in Førland et al. (1996). Six manually operated precipitation gauges in the forest accumulated throughfall between the field visits. The average of the six gauge readings was assumed to represent the cumulative net precipitation in the forest. Stemflow was assumed negligible.

Using a v-notch weir, discharge in the stream draining the catchment was determined every half-hour from February 1998 to April 2000. Wintertime freezing of water hampered the operation of the weir. During weekly field visits ice cover at the weir, if present, was broken and removed.

Table 1 presents accuracies of hydrometeorological instruments according to their technical specifications. The actual measurement errors, however, were likely to be larger than the ranges shown in Table 1. Especially during the wintertime the operation of instruments was hampered by cold temperature and snowfalls. For example, radiation sensors were occasionally covered with snow, precipitation container had a gauging error during snowfalls, cup anemometers became loaded with frost, etc. Checking and modification procedures were introduced to remove the influence of these error sources as explained more detailed in (III).

Table 1. Accuracy of automated measurements in clear-cut and forested sites.

Clear-cut site	Instrument	Accuracy
Datalogger	Campbell CR10	
Air temperature	Vaisala HMP35D	± 0.2 ºC
Relative humidity	Vaisala HMP35D	± 3 %
Wind speed	Vaisala WAA 15	± 0.1 m s^{-1}
Short-wave radiation	Skye pyranometer SKS1110	± 5 %
Long-wave radiation	Kipp&Zonen pyrgeometer CG1	± 10 %
Precipitation weigh module	Tedea 1250-E-100	± 0.03 %
Forest		
Datalogger	Campbell CR10	
Air temperature	Vaisala HMP 131 Y	± 0.2 ºC
Relative humidity	Vaisala HMP 131 Y	± 3 %
Wind speed	Vaisala WAA 15 A	± 0.1 m s^{-1}
Short-wave radiation (downward)	Kipp&Zonen pyranometer CM3	± 2.5 %
Short-wave radiation (reflected)	Li-Cor Inc. LI 200SZ	± 5 %
Water level at v-notched weir	Jensen PSL 0.2 LN2V/2	± 0.2 %

3 METHODS

3.1 Outline

The hydrological modelling system shown schematically in Figure 2 is developed step by step in each case study. (I) and (II) concentrate on testing and development of snow energy balance schemes, and (III) couples a canopy model component with a snow scheme. Study (IV) presents application of a hydrological modelling system that is driven by daily precipitation and air temperature data. Finally (V) shows application of a complete hydrological model using hourly input data.

This section presents the main model components that include the snow routine developed in (II), canopy model from (III), and models of soil and ground water interaction and streamflow delay functions used in (IV) and (V).

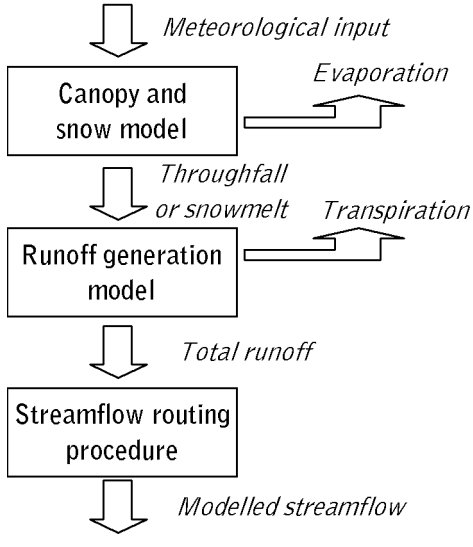

Figure 2. Schematic representation of the hydrological model.

3.2 Snow models

3.2.1 Development steps (I, IV)

When daily precipitation and air temperature data are available the temperature-index approach is selected to simulate snow accumulation and melt. In case study (IV) a degree-day snowmelt model is used to produce melt water input for a quasi-three-dimensional runoff generation scheme. The other snow modelling applications of this thesis are based on the energy balance approach and utilise three-hourly or hourly meteorological data including air temperature, relative humidity, wind speed, precipitation, and downward short- and long-wave radiation components.

The development of a new snow energy balance scheme rests on a comparison of two existing models UEB (Tarboton et al., 1995) and SNTHERM (Jordan, 1991), which are briefly described in (I). The developed snow energy balance scheme (II) is presented in the next subsections.

3.2.2 Two-layer snow model – energy balance computation (II)

The new energy balance snow routine is referred to as *two-layer snow model* indicating the number of modelled snow layers. As the heat exchange within a snowpack is extremely non-linear, a two-layer snow scheme is adopted to restrict the heat exchange with the atmosphere only to part of the snowpack. The water equivalent of snow in the snow layers and the heat content of all three layers (two snow layers and one soil layer) are updated at each computation time step. The water equivalent of the top snow layer is restricted to a maximum value, which is a model parameter. When the total water equivalent is less than this value the snowpack is modelled as one layer.

The energy balance equation for the snow layers and a soil layer reads

$$\frac{dU_j}{dt} = Q_{j-1} - Q_j + M_{j-1} - M_j \,,\; j = 1, 2 \qquad (1)$$

$$\frac{dU_g}{dt} = Q_2 - Q_g \,, \qquad (2)$$

where U_j is the heat content of the snow layer j, U_g is the heat content of the soil layer, Q_j is the heat conduction between layers j and $j+1$, Q_g is the assumed constant ground heat flux at the bottom of the soil layer, and M_j is the energy advected with liquid water percolation from layer j to $j+1$. In this section the subindex $j = 0$ refers to the snow surface and $j = 1, 2$ to the snow layers.

The boundary condition for the energy balance at the snow-air interface is formulated as

$$M_0 = R_{ns} + H + \lambda E + Q_P - Q_0, \tag{3}$$

where M_0 is the energy available to melt snow, R_{ns} is the net radiation on the snow surface, H is the sensible heat flux, λE is the latent heat flux, Q_p is the advective heat flux from precipitation, and Q_0 is the heat conduction to the top snow layer. Positive energy flux is directed towards snow. In freezing conditions (M_0 = 0) the snow surface temperature is iterated by balancing the atmospheric energy fluxes with the heat conduction into snow. When the snow surface temperature becomes 0 °C, the net energy input M_0 is used to melt snow in the top snow layer.

The heat conduction between the layers is calculated from

$$Q_j = -\overline{k_T}\left(\frac{T_{j+1} - T_j}{\Delta z_{j,j+1}}\right), \tag{4}$$

where Q_j is the heat conduction from layer j to layer $j+1$, $\overline{k_T}$ is the thermal conductivity between layers j and $j+1$, and $\Delta z_{j,j+1}$ is the distance between the center points of layers j and $j+1$. The thermal conductivity of snow was calculated as a function of density following Anderson (1976). The density of snow varies with time because of snow compaction and metamorphism, which were calculated using the equations given in Anderson (1976) and Jordan (1991). In the case study (II), the thermal conductivity in the soil layer was taken as a constant, and in (III) it was calculated as a linear combination of conductivities of soil, water and ice fractions as applied in Engelmark (1984).

Turbulent fluxes of sensible and latent heat are given by

$$H = \left(\frac{\rho_a c_p}{r_{s^*}} + E_{H0}\right)\left(T_a - T_0\right) \tag{5}$$

and

$$\lambda E = \left[\frac{0.622\lambda_s}{r_{s^*} R_d \left(T_a + 273.15\right)} + E_{E0}\right]\left(e_a - e_s\right), \tag{6}$$

where H is the sensible heat flux, λE is the latent heat flux, ρ_a is the air density, c_p is the specific heat of air, E_{H0} is the windless convection coefficient for the sensible heat flux, T_a is the air temperature, T_0 is the snow surface temperature, r_{s^*} is the aerodynamic resistance, R_d is the dry gas constant, E_{E0} is the windless convection coefficient for the latent heat flux, e_a is the air vapour pressure, e_s is the saturation vapour pressure at the snow surface, and λ_s is the latent heat of sublimation of ice. When the snow surface

temperature is 0 °C, the latent heat of vaporisation of water, λ_v, is used in Eq. (6).

Aerodynamic resistance is corrected for atmospheric stability on the basis of the estimated value of the Richardson number. The stability correction in (II) is adopted from UEB and derives from Price and Dunne (1976), but the correction procedure in (III) follows the method of Choudhury and Monteith (1988). Aerodynamic resistance for neutral atmospheric stability is computed by assuming a logarithmic wind profile above snow surface (see II for details). The influence of forest canopy on aerodynamic resistance is described in Section 3.3.2.

Jordan et al. (1999) suggested that the correction for stable atmospheric conditions might lead to cessation of turbulent heat exchange and excessive cooling of the snow surface during cold periods with low wind speeds. In the present snow model an attempt is made to alleviate these problems by limiting value of the Richardson number and by allowing windless exchange of the sensible heat. The windless convection coefficient E_{H0} in Eq. (5) enables sensible heat transfer to occur even when wind speed is zero and thereby prevents surface temperature from falling to unrealistically low values in response to radiative losses. Jordan et al. (1999) suggested that the windless convection coefficient for latent heat, E_{E0}, had no similar effect and therefore it was set equal to zero.

Net radiation flux R_{ns} into the snowpack is given by

$$R_{ns} = R_s(1-\alpha_s) + R_{ld} - R_{ls}\,, \tag{7}$$

where R_s is the incoming short-wave radiation, α_s is the albedo of the surface (snow or ground), R_{ld} is the incoming atmospheric long-wave radiation, and R_{ls} is the upward long-wave radiation. The influence of forest canopy on the net radiation flux is formulated in Section 3.3.3.

Snow albedo is not simulated in (II) where downward and reflected short-wave radiation components are used as input data. In (III) separate functions for snow accumulation and melt periods are applied to describe the decrease in snow albedo as a function of time since the last snowfall.

The advective heat flux Q_P from precipitation is calculated as the energy needed to convert precipitation to ice phase at 0 °C.

The heat content of the soil layer, U_g, is given by (e.g. Karvonen, 1988)

$$U_g = (1-\phi)D_g\rho_g c_g T_g + wD_g\rho_w c_w T_g + ID_g\rho_i c_i T_g - ID_g\rho_i\lambda_f\,, \tag{8}$$

where ϕ is the porosity of the soil, D_g is the depth of the soil layer, ρ_g is the density of soil grains, c_g is the specific heat of soil, T_g is the average soil temperature, w is the liquid water content, ρ_w is the density of water, c_w is the specific heat of water, I is the ice content, ρ_i is the density of ice, c_i is the specific heat of ice, and λ_f is the latent heat of fusion. The total water content of the soil was assumed constant. In the soil layer the relationship between

the temperature and the liquid (unfrozen) water content is determined according to a freezing depression curve, which is given as

$$w = (w + I)e^{-(T_f - T_g)/d_g},\ T_g < T_f \tag{9}$$

where T_f is the freezing point temperature, and d_g is a parameter. Equations (8) and (9) define the relationship between the soil heat content and the liquid water content. The heat conduction from the bottom snow layer into the soil layer is calculated from Eq. (4).

The heat content of a snow layer is related to the average temperature and the liquid water content of the layer (Tarboton et al., 1995), and it is computed from

$$U_j = \begin{cases} T_j c_i W_j \rho_w & T_j < 0, L_j = 0 \\ L_j \lambda_f W_j \rho_w & T_j = 0, L_j \geq 0 \end{cases}, \tag{10}$$

where T_j is the average snow temperature in layer *j*, W_j is the water equivalent of snow (liquid water and snow), and L_j is the mass fraction of liquid water. When the heat content becomes positive, the average snow temperature is 0 °C.

3.2.3 Two-layer snow model – mass balance computation (II)

In the developed snow scheme, the mass balance for a layer of snow is given by

$$\frac{dW_j}{dt} = F_{j-1} - F_j, \qquad j = 1, 2, \tag{11}$$

where F_j is the water outflow from layer *j* to *j+1*. In the present model, meltwater discharged from the bottom snow layer, F_2, does not have any effect on the total water content of the soil layer, but is discharged out of the system at the snow-soil interface. The boundary condition at the snow surface is formulated as

$$F_0 = P_r + P_s - E, \tag{12}$$

where P_r is the rainfall, P_s is the snowfall, and E is the evaporation/ sublimation. Melt water outflow is (Tarboton et al., 1995):

$$F_j = K_{sat} S_j^3, \quad j = 1, 2 \tag{13}$$

and

$$S_j = \frac{L_j/(1 - L_j) - l_r}{\rho_w/\rho_s - \rho_w/\rho_i - l_r}, \tag{14}$$

where K_{sat} is the saturated hydraulic conductivity, S_j is the relative saturation in excess of water retained by capillary forces, l_r is the liquid water retention capacity, and ρ_s is the density of snow.

3.3 Canopy processes

3.3.1 Computation of daily evaporation and interception (IV)

The structure of the canopy model depends on the measurement frequency of the meteorological data. When only daily data are available, the daily potential evapotranspiration is estimated directly from the global radiation by multiplication with a constant factor. When the air temperature is below 10 °C, but above 0 °C, the estimate is scaled down as a linear function of the temperature. The potential evapotranspiration is assumed to be equal to zero below 0 °C. The interception is simply taken as a constant fraction of the daily precipitation. The maximum interception capacity is set to a prescribed value, which is greater for snowfall than for rainfall. These schemes are adopted in the case study (IV).

In the method described above the amount of intercepted water does not depend on the interception values at previous time steps. But when records of hourly meteorological data exist, it is preferable to model the interception with the aid of an interception storage whose state is updated at each computation time step. Hourly computation of interception largely follows the method given in Wigmosta et al. (1994), but in this thesis, the computation of overstory interception and aerodynamic resistances has been modified and interception in the understory vegetation has been ignored. The following subsections present the hourly computation of canopy processes.

3.3.2 Interception (III, V)

The form of precipitation is determined on the basis of the air temperature. Below temperature T_l precipitation falls as snow and above temperature T_h as rain. Between T_l and T_h the proportion of snowfall (and rain) is a linear function of the air temperature. The canopy temperature is assumed to be equal to the air temperature. The share of precipitation falling between the trees is computed as a product of the total precipitation P and the sky-view fraction f_s. The remaining precipitation, i.e. $(1 - f_s)P$, can be intercepted in the canopy and it forms the input to the interception procedure.

Starting from an interception model proposed by Aston (1979), the following equation can be derived to determine the depth of intercepted water during a time-step, W_I (see III for details):

$$W_I = (C_I - I_0) - (C_I - I_0)e^{-k_I(1-f_s)P/C_I}, \quad (15)$$

where I_0 is the canopy storage in the beginning of the computation time-step, C_I is the interception capacity, and k_I is a model parameter. The capacity C_I is higher for interception of snow (C_{IS}) than for interception of rain (C_{IW}). Now the change in the canopy storage during a computation time-step, ΔI, can be written as

$$\Delta I = W_I - E_I, \quad (16)$$

where E_I (see Eq. 18) is the depth of interception evaporation (sublimation) during a time-step.

When the air temperature increases above the freezing point and the canopy storage is greater than C_{IW}, unloading of the intercepted snow (in excess of C_{IW}) occurs. Occurrence of snow unloading is checked in the beginning of the computation time step before the depth of intercepted water W_I is determined according to Eq. (15). Now throughfall P_T during a computation time-step can be written as

$$P_T = [(1-f_s)P - W_I] + f_s P + U_S, \quad (17)$$

where U_S is the snow unloading during a computation time-step.

Evaporation out of the interception storage, E_I, is calculated using a combination equation of the Penman-Monteith type (Monteith, 1965)

$$E_I = \frac{\Delta R_{nc} + \rho_a c_p (e_s - e_a)/r_{ao}}{\lambda_v(\Delta + \gamma)}, \quad (18)$$

where Δ is the gradient of the saturated vapor pressure – temperature curve, R_{nc} is the net radiation in the canopy, ρ_a is the air density, c_p is the specific heat of air, e_s is the saturation vapor pressure, e_a is the vapor pressure of air, r_{ao} is the aerodynamic resistance of vapor transport, λ_v is the latent heat of vaporization, and γ is the psychrometric constant. Sublimation of snow in the temperatures below 0 °C is calculated by substituting λ_v with the latent heat of sublimation λ_s and adjusting the psychrometric constant by λ_v/λ_s in Eq. (18). Condensation into the canopy is not allowed.

The aerodynamic resistance is calculated according to the eddy diffusion theory assuming equal resistances to transfer of heat, vapour and momentum. Although this assumption is known not to be strictly valid (e.g. Brutsaert, 1982; Male and Granger, 1981), it is commonly used in a hydrological context (Calder, 1990; Lundberg et al., 1998; Lundberg and Halldin, 1994; Wigmosta et al., 1994). The wind speed is logarithmic above the canopy and decreases exponentially within the canopy as assumed in earlier studies of the canopy evapotranspiration (Choudhury and Monteith, 1988; Dolman, 1993). Above the snowpack the exponential wind profile merges with a logarithmic wind profile at the height z_{rs} (= 2 m).

In the presence of forest canopy, the resistance for the turbulent heat exchange above the snowpack, r_s, is calculated from

$$r_s = r_{ao} + r_{co} + r_{ss} = \int_{d_0+z_{0o}}^{z_r} \frac{1}{K(z)} dz + \int_{z_{rs}}^{d_0+z_{0o}} \frac{1}{K(z)} dz + \int_{z_{0s}}^{z_{rs}} \frac{1}{K(z)} dz \,, \qquad (19)$$

where r_{ao}, r_{co}, and r_{ss} are aerodynamic resistances above, within, and beneath the canopy, respectively, d_o is the zero-plane displacement height, z_{0o} is the roughness length of the canopy, z_r is the reference height above the canopy, and $K(z)$ is the eddy diffusion coefficient. Computation of aerodynamic resistances is described in detail in (III). When no canopy is present, aerodynamic resistance r_s has only one term r_{ss}.

Calder (1990) and Lundberg and Halldin (1994) note that aerodynamic resistance r_{ao} for the sublimation of snow is an order of magnitude greater because of the smooth surface of the intercepted snow. To account for these effects r_{ao} is multiplied by a factor f_r = 10 (Lundberg et al., 1998) at temperatures less than 0 °C.

3.3.3 Radiation (III, V)

The net radiation absorbed by the canopy is calculated ignoring multiple reflections between canopy and snow surface, and it is given by

$$R_{nc} = R_s(1-f_s)[1-\alpha_c - \tau_c(1-\alpha_s)] + (1-f_s)(R_{ld} + R_{ls} - 2R_{lc}) \,, \qquad (20)$$

where R_s is the incoming short-wave radiation, α_c is the albedo of the canopy, τ_c is the transmittance through the canopy, α_s is the albedo of the surface beneath the canopy (snow or ground), R_{ld} is the incoming atmospheric long-wave radiation, R_{ls} is the upward long-wave radiation from the surface below the canopy, and R_{lc} is the long-wave radiation emitted by the canopy (upward and downward). The long-wave radiation terms R_{ls} and R_{lc} are calculated as a function of the snow/ground surface temperature or canopy temperature, respectively, using the Stefan-Boltzmann law. The snow energy balance model simulates the snow surface temperature, and the canopy temperature is assumed to be equal to the measured air temperature.

The net radiation flux into the snowpack beneath the canopy, R_{ns}, is given by

$$R_{ns} = R_s[\tau_c(1-f_s) + f_s](1-\alpha_s) + R_{lc}(1-f_s) + R_{ld}f_s - R_{ls} \,. \qquad (21)$$

The albedo of canopy and ground surfaces was taken equal to 0.18. Note that the net radiation flux into snow is computed according to Eq. (7) when no canopy is present.

3.3.4 Potential transpiration (IV, V)

Potential transpiration is given as an input to the runoff generation scheme. In case study (IV) potential transpiration is set equal to an estimate of potential evapotranspiration (see beginning of Section 3.3.1) from which interception evaporation has first been subtracted. In (V) the potential transpiration is derived from a reference crop potential evapotranspiration that is computed according to a modified combination equation given in Shuttleworth (1992). In all studies, the estimate of potential transpiration is multiplied with a constant scaling factor (f_{EP}), which is a calibration parameter.

3.4 Soil and ground water interactions

3.4.1 Outline

Two different discretisation schemes are tested to simulate runoff generation processes in the forested study catchment. The first approach is presented in (IV) where spatial distributions of soil moisture and ground water levels are simulated over a finite grid using a quasi-three-dimensional model. The second approach is demonstrated in paper (V), where runoff generation is simulated on a single hillslope section. In this case the three-dimensional catchment domain is simplified into a two-dimensional domain.

3.4.2 Vertical soil moisture distribution (IV, V)

In both discretisation schemes lateral water flow is assumed to occur only in the saturated part of the soil domain. Vertical unsaturated soil moisture distribution in each cell of a finite grid (IV) or in each column of a hillslope (V) is computed by approximating the Richards equation (Richards, 1931) with successive steady-state solutions of the pressure head distribution. Skaggs (1980) introduced this idea in the DRAINMOD model, which is a tool for agricultural water management in areas with a shallow water table. DRAINMOD has been applied in drained forest areas by McCarthy et al. (1992) and Amatya et al. (1997a; b), where the model was modified to account for interception and forest evaporation, and was coupled with ditch drainage and channel routing procedures.

Total air volume V_n in a soil column n is given by

$$\frac{dV_n}{dt} = E_n - i_n + \frac{\Delta Q^{old}}{A_n} \qquad (22)$$

where E_n is the actual transpiration, i_n is the infiltration into the soil column, ΔQ^{old} is the net lateral ground water flow into the soil column at the previous

time-step, and A_n is the horizontal area of the column. Transpiration is extracted from the root zone. The soil moisture state D_n in the root zone is given by

$$\begin{cases} \dfrac{dD_n}{dt} = i_n - E_n - p_n & D_n \geq 0 \\ \dfrac{dD_n}{dt} = i_n - E_n + c_n & D_n < 0 \end{cases} \tag{23}$$

where p_n is percolation of water from the root zone that is in excess of the steady state moisture distribution, and c_n is the capillary upflux into the root zone. When D_n is equal to zero, there is a steady-state soil moisture distribution above the ground water level. When D_n is positive there is water in excess of the steady-state moisture content in the root zone (Figure 3) and its percolation to the saturated part of the soil domain is controlled by the vertical hydraulic conductivity in the root zone (see IV for details). When D_n has a negative value, there is less water in the root zone than according to the steady-state moisture distribution. Root zone processes are explained more detailed in (IV) and (V).

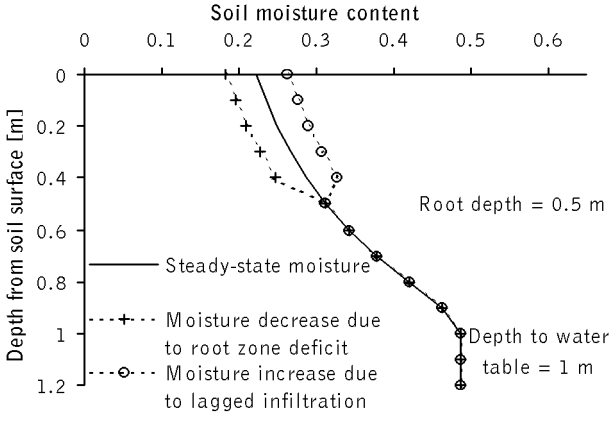

Figure 3. An example of a moisture distribution in a soil column.

When both V_n and D_n are known, the elevation of the ground water table can be determined according to the following relationships:

$$V_n^{ss} = V_n + D_n \tag{24}$$

$$V_n^{ss} = \int_{z_{gw}}^{z_s} (\theta_s - \theta) dz \tag{25}$$

where V_n^{ss} is the air volume corresponding to a steady-state moisture distribution, θ is the volumetric soil water content, θ_s is the saturated soil

water content, z_{gw} is the water table elevation, and z_s is the soil surface elevation. The relation in Eq. (25) is also prescribed in a look-up table. Use of pre-calculated look-up tables enables faster and more stable model execution than a numerical solution to the transient Richards equation.

Water retention characteristics required for computing steady-state moisture distributions, and unsaturated hydraulic conductivity required for calculating vertical movement of water (p_n, c_n), were parameterised according to Van Genuchten's model (van Genuchten, 1980). The effects of soil frost on water characteristic curves and infiltration capacity were disregarded. According to Nyberg et al. (2001) and Stähli et al. (2001) soil frost can be expected to have a minor effect on runoff dynamics in a boreal-forested catchment similar to the current study basin.

3.4.3 Quasi-three dimensional approach (IV)

In the case study (IV) the soil moisture computation scheme based on Skaggs (1980) is coupled with a simple overland flow redistribution procedure and a two-dimensional ground water model, which simulates lateral flow in the saturated part of catchment soils. The catchment was discretized horizontally using a finite two-dimensional grid, and a soil column of a prescribed depth was attached to each grid cell. The saturated soil domain was treated as an unconfined aquifer and ground water flow was computed using a numerical solution to the continuity equation:

$$s\frac{\partial h}{\partial t} = \frac{\partial}{\partial x}\left(T_x \frac{\partial h}{\partial x}\right) + \frac{\partial}{\partial y}\left(T_y \frac{\partial h}{\partial y}\right) \tag{26}$$

where h is the hydraulic head, T is the transmissivity, s is the storage coefficient, x and y are the horizontal coordinates, and t is time. The transmissivity for each grid cell was calculated using an exponential function similar to the one used in TOPMODEL (Beven and Kirkby, 1979):

$$T = \int_{z_{bot}}^{z_{gw}} K^{ls} e^{-fz} dz \tag{27}$$

where K^{ls} is the saturated hydraulic conductivity at the soil surface, z_{bot} is the elevation of impermeable bottom, and f is the shape parameter. The transmissivity between two grid cells was calculated as a harmonic average and the transmissivity at the watershed boundary was set to zero to represent a water divide. The storage coefficient s was calculated as:

$$s = -\frac{\Delta V_n^{ss}}{\Delta h_n} \tag{28}$$

where h_n is the hydraulic head. The storage coefficient is calculated inside the iteration loop to provide accurate estimates.

The combined model is quasi-three-dimensional in the sense that the water balance over a catchment during a time step is computed in two stages. Vertical water flow and the resulting change in the water table elevation in each grid cell are calculated in the first stage. After computation of vertical flow, water table elevation in each node defines the initial hydraulic head for the ground water flow computations. The horizontal ground water movement in the saturated soil and the resulting change in the water table elevation over the grid are calculated in the second stage. The coupling of the models is illustrated in Figure 4.

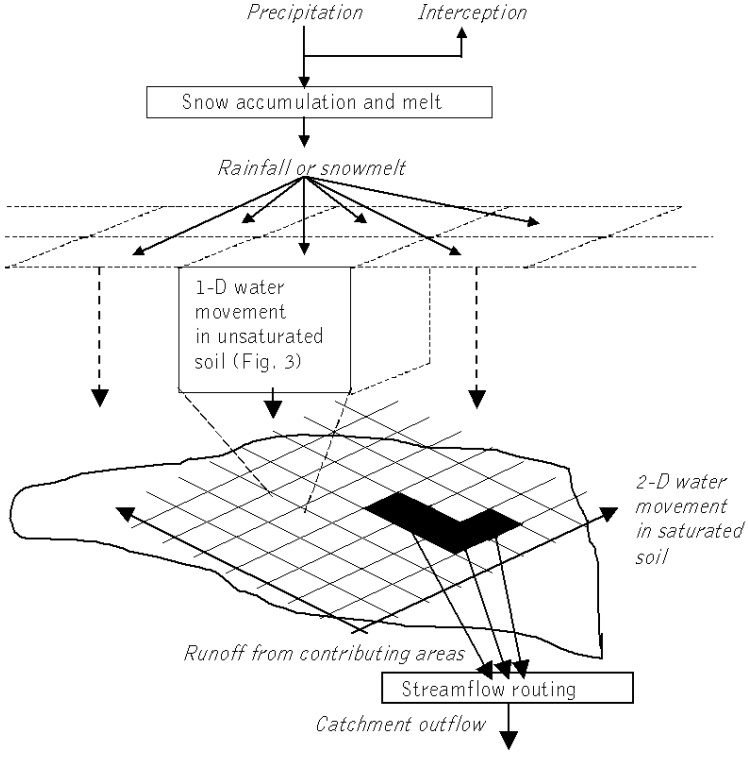

Figure 4. Representation of the quasi-three-dimensional rainfall-runoff model.

Runoff generated from vertical water movement (throughfall/snowmelt) and from lateral flow (ground water) is calculated separately. In the first stage, throughfall or snowmelt forms an input to soil surface water storage in each cell. The storage is depleted by infiltration, which is restricted only by the total air volume of the soil column from the previous time-step. Water in excess of a prescribed maximum value of the surface storage produces saturation excess overland flow, which is called direct runoff (d_n) in this work.

Direct runoff is not routed over the catchment, but runoff generated on cells classified as exposed bedrock is distributed uniformly over the cells classified as forest soil. The sum of d_n generated in the forest cells is part of the input to a streamflow routing model. According to the model d_n is generated directly from throughfall or snowmelt, and it has never infiltrated. In the results section direct runoff is compared with the isotopically traced event-water contribution.

In the second stage runoff generation via exfiltration of ground water flow is computed. Numerical solution of the ground water model allows rise of the water level above the soil surface in saturated columns. When the calculated water table level exceeds the soil surface elevation, a corresponding amount of exfiltration is added to the soil surface water storage. Water in excess of a prescribed maximum value of the surface storage produces return flow, which is called runoff from the soil domain (d_s) in this work. The sum of d_s from forest grid cells forms an input of soil water flow to a streamflow routing model. The two runoff components, d_n and d_s, are not allowed to mix in this computation scheme, which enables calculation of the runoff fraction that has never infiltrated into the soil.

3.4.4 Characteristic profile model (V)

Runoff generation processes in paper (V) are simulated on a single hillslope, which is assumed to characterise a typical longitudinal section from a water divide to a stream. This typical hillslope is called *a characteristic profile* (Figure 5), and a vertical two-dimensional water balance scheme is applied along the profile. The water balance scheme is called a characteristic profile model (CPM), which describes runoff generation within a catchment. The runoff computed in the CPM is discharged into a routing procedure, which produces modelled streamflow at the outlet of the catchment. This modelling approach will be later referred to as the semi-distributed model.

The CPM is quasi-two-dimensional in the sense that vertical and lateral water fluxes are computed separately. Lateral flow is assumed to take place only in the saturated zone. The characteristic profile is divided into soil columns, and for each column, vertical water fluxes are computed using the Skaggs (1980) method. After the vertical fluxes and the resulting ground water levels have been resolved, lateral ground water flow (per unit width) q_n between vertical soil columns is computed from Darcy's law

$$q_n = -K_n^{ls} B_n \frac{dh}{dL} \tag{29}$$

where K_n^{ls} is the saturated lateral hydraulic conductivity, B_n is the thickness of the saturated zone, and *dh/dL* is the water table gradient between the columns. Lateral ground water flow is assigned with a no-flow boundary condition at the upslope end of the characteristic profile, which lies at a

water divide. At the downslope end of the profile a fixed head type boundary condition, which determines water level in the ditch, is used (Figure 5). Ground water flow into the ditch determines the base flow and is one part of runoff discharged from the soil domain. The other part of runoff from the soil domain is produced by exfiltration of net ground water flow in saturated soil columns. Net ground water flow ΔQ (see Eq. 22) is computed as:

$$\Delta Q = \frac{1}{A_n}\left(\frac{q_n - q_{n-1}}{L_n}\right) \tag{30}$$

where A_n is the horizontal area of the column, L_n is the horizontal distance between columns n and n+1, and q_n is the lateral flow between columns n and n+1. The sum of the two runoff components that have been in contact with the soil domain, i.e. runoff generated via base flow and exfiltration, is compared with the isotopically traced pre-event water contribution.

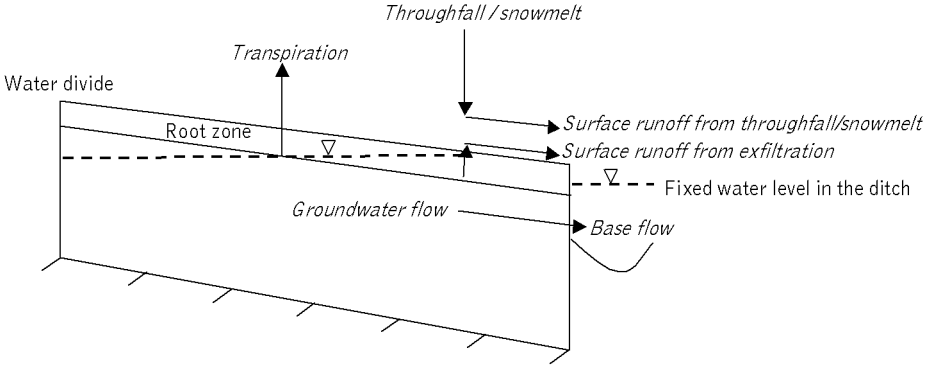

Figure 5. Schematic representation of a characteristic profile.

The following equations are used for calculating infiltration i_n and direct runoff d_n in each column n

$$\begin{cases} i_n = r_n + d_{n-1} \\ d_n = 0 \end{cases} \qquad r_n + d_{n-1} < V_n^{old} \tag{31}$$

$$\begin{cases} i_n = V_n^{old} \\ d_n = r_n + d_{n-1} - V_n^{old} \end{cases} \qquad r_n + d_{n-1} \geq V_n^{old} \tag{32}$$

where r_n is the throughfall/snowmelt, and V_n^{old} is the total air volume in the column at the previous time-step. The index n increases downslope towards the ditch. Infiltration is not restricted by the hydraulic conductivity of the soil surface, but is solely controlled by the available air volume in the soil column. Both direct runoff and exfiltration runoff are transported downslope

without any delay and they either reach the ditch, or infiltrate if the air volume further down along the hillslope allows it. These two components of surface runoff are not allowed to mix in this computation scheme, which enables separation of the runoff component d_n that has never infiltrated into the soil. In the results section direct runoff from the column next to the ditch is compared with the isotopically traced event-water contribution.

3.5 Channel routing

Computation schemes for soil and ground water interactions yield runoff components that are summed together and taken as an input to a flow routing procedure. Flow routing accounts for the water storage within the channel network and merely delays streamflow. According to Kirkby (1993), the delay from rainfall/snowmelt to basin outflow in small catchments is mainly caused by hillslope flow processes, but in catchments larger than 50-100 km^2 travel times through the channel network become increasingly important and ultimately dominate the shape of the hydrograph. Therefore, simple streamflow routing procedures, such as a single linear storage, may be applicable in small catchments. Unlike in the models described above, no physical analogy to real processes is sought after in the structure of the routing procedure.

In case study (IV) runoff produced from saturated areas forms an input to a nonlinear storage. The output of the storage is compared with the measured catchment outflow. In hillslope modelling (V) the total runoff from the CPM is the input to a linear storage. Output from the linear storage corresponds to the measured streamflow.

4 RESULTS AND DISCUSSION

4.1 Snow processes in Sodankylä (I, II)

4.1.1 Outline

The objective of the snow studies was to identify a snow model structure which can function as a subroutine in a physics-based hydrological model, and which successfully simulates snow mass and heat balance. Performance of two existing snow energy balance models, UEB and SNTHERM, was tested first in case study (I) against the snow measurements from Sodankylä. In the subsequent study (II) a new snow energy balance model was developed and compared with the results of UEB and SNTHERM. The following subsections summarise the main results of these applications.

4.1.2 Input data and model parameters

For the purposes of the comparison, the input data of the snow models ought to be meteorological variables measured at a reference height of 2 m above ground. However, meteorological variables in Sodankylä were measured at different heights leaving some measurements affected and some unaffected by the surrounding sparse forest canopy. Downward short-wave radiation and wind speed were measured above the canopy, whereas other meteorological variables were measured at the height of 2 m above ground. Prior to the model application, the influence of forest canopy on wind speed and solar radiation was quantified, and estimates at the height of 2 m were computed to provide all meteorological input variables at the same level above ground (see II for details). Interception in the sparse forest canopy, and effect of the canopy on downward long-wave radiation and turbulent transfer coefficients were ignored.

SNTHERM and UEB included dissimilar procedures for estimation of snow albedo and atmospheric long-wave radiation. These procedures yielded considerably different radiation components, which precluded further comparison of modelled snow heat balance. In order to accomplish a meaningful comparison of snow variables, UEB and SNTHERM were driven by an identical set of radiation input data, which included measured series of downward and reflected short-wave radiation, and the SNTHERM-estimate of downward long-wave radiation. The rest of the input variables were air temperature, relative humidity, wind speed and precipitation.

Parameters of UEB and SNTHERM were mostly set to values suggested in the model documentation (see II for details). In the calculation of the bulk transfer coefficients, UEB was implemented with no correction to atmospheric stability, whereas the two-layer scheme was made similar to SNTHERM by implementing a correction for the weak transfer of sensible heat. The correction in SNTHERM was according to the suggestion in the model documentation. The snow parameters of the two-layer model were adopted from the UEB documentation and the soil parameters followed ranges given in the literature.

4.1.3 Turbulent heat fluxes

Comparison of modelled turbulent heat exchange indicated the largest systematic differences between sensible heat fluxes (Figure 6). Both UEB and the two-layer model yielded a greater contribution of sensible heat compared with the cumulative flux by SNTHERM. However, the difference between the model results has only a minor effect on the snow mass balance as shown in Section 4.1.5. The computed sensible heat flux was sensitive to the roughness length and to the inclusion of the correction scheme for atmospheric stability. The greater contribution of sensible heat by UEB results from the computation procedure that ignores correction for atmospheric stability. The absolute magnitude of the latent heat flux over the snow surface was small and similar for all models.

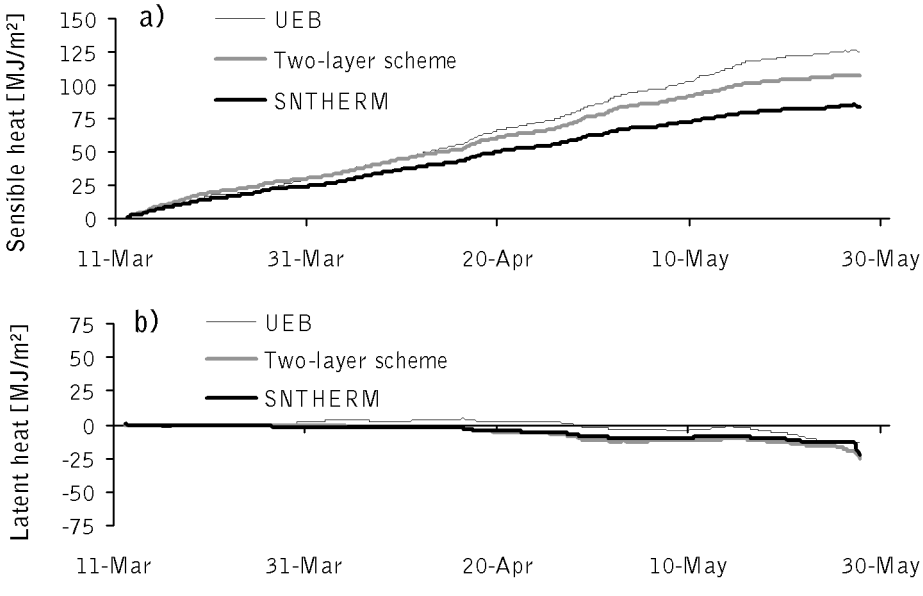

Figure 6. Calculated cumulative fluxes of sensible heat (a) and latent heat (b) during spring 1997 in Sodankylä.

Figure 7 presents a comparison of computed turbulent heat fluxes against eddy-correlation measurements for a two-week period in March. The absolute magnitude of measured and modelled sensible heat fluxes was small, and the fluxes varied mostly in range from –50 to 150 kJ m^{-2} h^{-1}. The models yielded values within the measured range of variation, but the observed dynamics was not replicated by any of the models. Correlation coefficients between computed and measured values were 0.28, 0.29, and 0.39 for SNTHERM, UEB, and the two-layer snow model, respectively. The largest discrepancies between the modelled and measured fluxes were found during the midday hours when the measurements showed negative peaks (upward heat flux). These discrepancies can be explained by the effect of surrounding tree canopy on the energy balance. Solar radiation during the daytime may contribute to heating of the canopy with increasing upward fluxes of sensible heat from the forest canopy.

The latent heat fluxes calculated by the models showed similar dynamics, but had slightly lower absolute magnitudes compared to the measurements. This deviation was not significant because the latent heat flux varied only in a range from about –100 to 50 kJ m^{-2} h^{-1}.

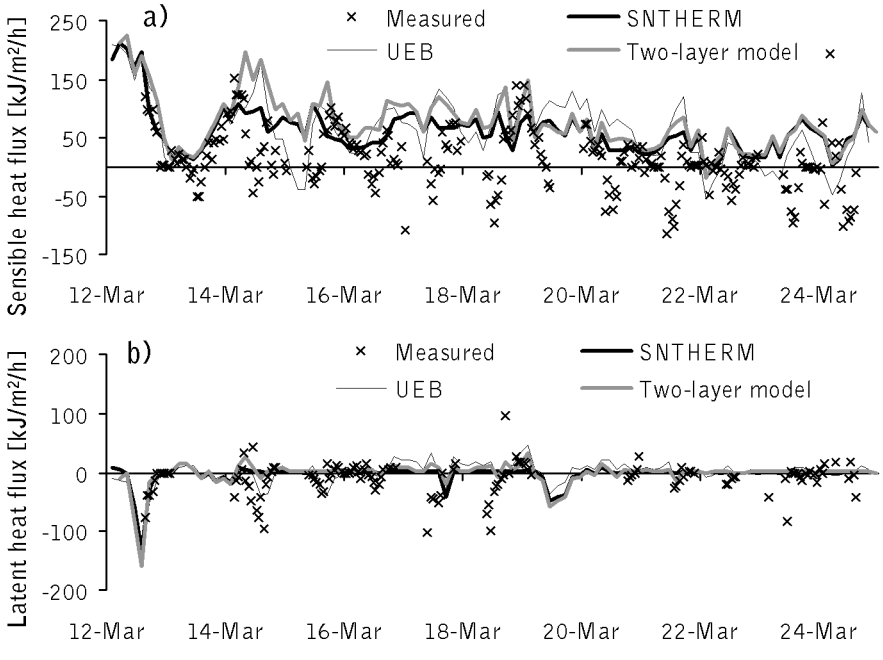

Figure 7. Measured and modelled sensible heat (a) and latent heat (b) fluxes during March 12-24, 1997.

4.1.4 Snow and soil heat balance

Snow surface temperature simulations indicated that SNTHERM and the two-layer snow scheme fit measured values equally well whereas UEB produced a systematic overprediction of nighttime temperatures and underprediction of daytime temperatures. The mean absolute error of the temperature simulation and its standard deviation during 17 Mar – 20 May 1997 were 1.2 °C and 1.3 °C, respectively, using SNTHERM, 1.2 °C and 1.2 °C using the two-layer scheme, and 1.8 °C and 1.5 °C using UEB. In contrast to the model results, when the snow surface temperature is assumed equal to the measured air temperature at a height of 2 m above the ground, the mean absolute error and standard deviation would be 3.3 °C and 2.7 °C. The nocturnal surface temperature of the snow was sensitive to the inclusion of the windless exchange of sensible heat flux and to the estimated heat conduction into the snow. The use of the windless convection coefficient in both SNTHERM and the two-layer scheme improved the simulation of nighttime low surface temperatures during periods of strong radiative cooling. Also, the results of the two-layer model improved after the heat conduction into the snow was modelled by approximating the temperature gradient between the snow surface and a thin upper layer of snow.

Measured and modelled snow and soil temperatures plotted in Figure 8a and 8b are averaged vertically over snowpack and a layer of soil, respectively. The exception is the temperature by UEB in Figure 8a, which is a bulk temperature of snow and soil layer. During most of the time SNTHERM yielded a slightly lower average snow temperature compared to the measurements. The results of the two-layer scheme showed lower snow temperature than SNTHERM, which was caused by differences in the simulated heat conduction within snow. Measurements indicate that snowpack is isothermal at 0 °C by 2 May. SNTHERM and UEB yielded isothermal snowpack conditions on 5 May, and the two-layer snow model on 30 April.

The temperature of the top 0.4 m of soil (Figure 8b) varied little during the calculation period and compared well with the SNTHERM results and moderately well with the two-layer snow scheme. The dampening of the temperature fluctuation in soil is primarily a result from the energy exchange associated with soil water freezing and thawing. Because soil water freezing and thawing was disregarded in UEB, the computed bulk soil/snow layer temperature (Figure 8a) showed wide-ranging dynamics that followed air temperature fluctuation. Separation of snow and soil in the snow energy balance model seems to be necessary for a realistic simulation of average snowpack temperature.

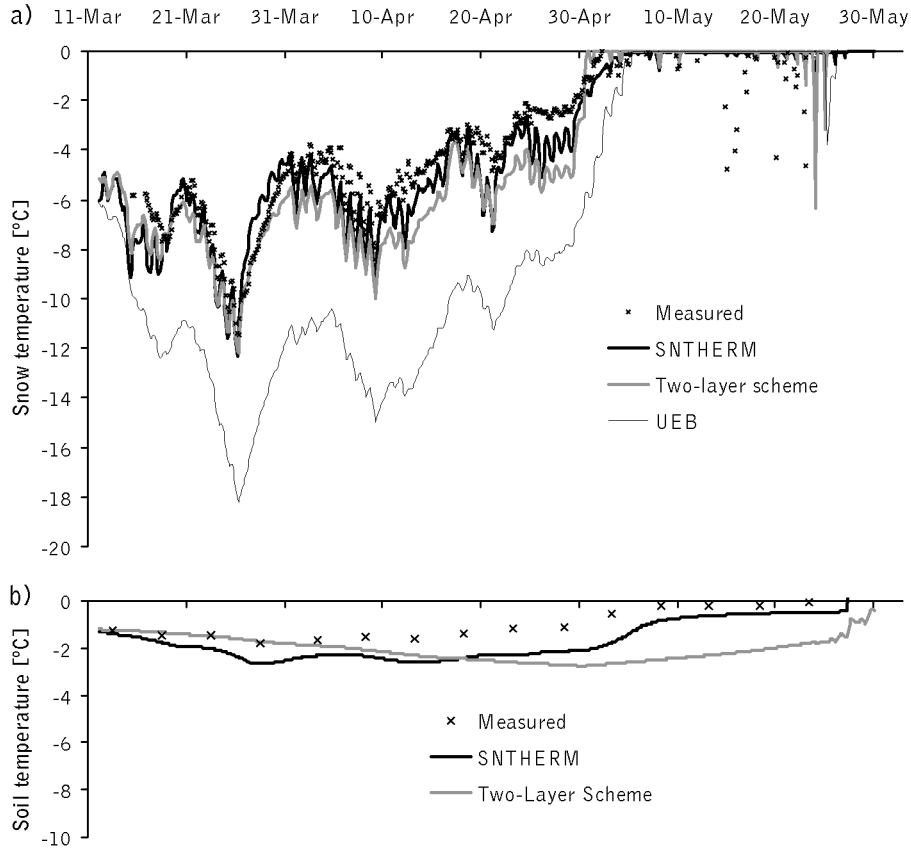

Figure 8. Measured and calculated average temperatures of snow (a) and soil (b) during spring 1997. The measured snow temperature was the average of temperature sensors located within the snowpack. The result of SNTHERM and the two-layer scheme were snow-depth averaged temperatures. The result of UEB was a temperature index of the snow and soil layer.

Comparison of SNTHERM results and temperature measurements taken inside the snowpack reveals a mean absolute error and standard deviation of 1.2 °C and 1.8 °C, respectively. The largest simulation errors were found at measurement points close to the snow surface, and occurred simultaneously with 5 - 10 cm errors in calculated snow depth. Examples of temperature profiles prior to and at the start of snowmelt are shown in Figure 9. The two-layer model approximates well the large difference between daytime and nighttime temperatures close to the snow surface.

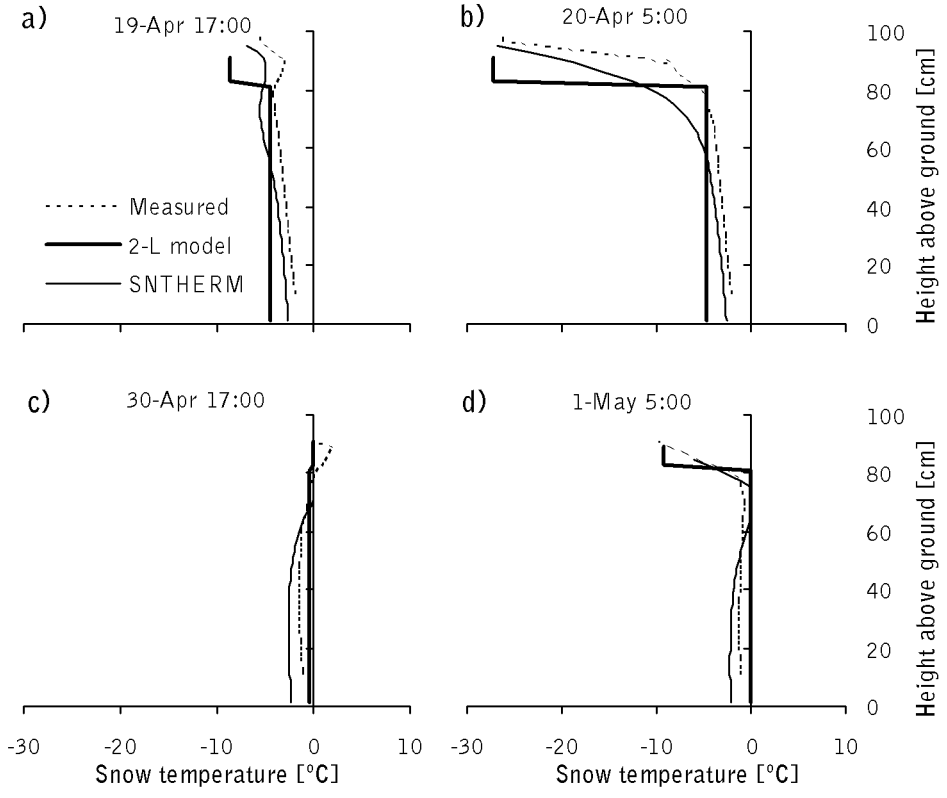

Figure 9. Calculated and measured temperature profiles prior to (a, b) and at the start (c, d) of snowmelt. Both nighttime and daytime profiles are plotted.

4.1.5 Snow mass balance

The calculated snow water equivalent is presented together with the measured range of snow mass in Figure 10. The two-layer snow scheme predicted a slightly faster snowmelt (i.e. loss of snow water equivalent) than SNTHERM, especially during the first half of the melting period. SNTHERM yielded a mean absolute error and standard deviation of 16 mm and 15 mm, respectively. The two-layer model produced corresponding values of 15 mm and 10 mm, and UEB 16 mm and 13 mm. Overall, the modifications made to the UEB approach in the two-layer snow scheme had minor effects on the calculated snow water equivalent.

The calculated depth of liquid water retained in the snow is shown in Figure 11. The results of the two-layer scheme are close to those of SNTHERM, except during 8-14 May when it predicts a faster melt than SNTHERM. The UEB model yields liquid water in snow only after the combined layer of snow and soil reach an average temperature of 0 °C (see Figure 8a).

Figure 12 presents profiles of measured and calculated snow density from the end of March until the middle of May. In late March both measurements and model results showed less dense layers of snow near the snow surface and denser layers in the middle and at the bottom of the snowpack (Figure 12a). Later the measurements indicated that the bottom of the snowpack was less dense than the middle layers, which was not predicted by the models (Figure 12b-d). Another discrepancy was the measured densification of snow near the snow surface during snowmelt, which was in contrast to the modelled densification of the bottom of the snowpack during the percolation of liquid water (Figure 12d). The measurements suggested that some snow layers near the surface were thick and dense enough to prevent percolation of melt water. The existence of such dense layers may also explain the persistently low density at the bottom of the snowpack.

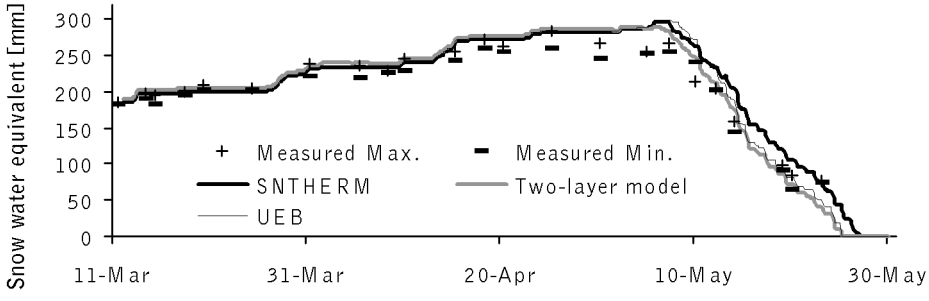

Figure 10. Measured and calculated snow depth (a) and snow water equivalent (b) during spring 1997. Measured values are plotted as a range between maximum and minimum values.

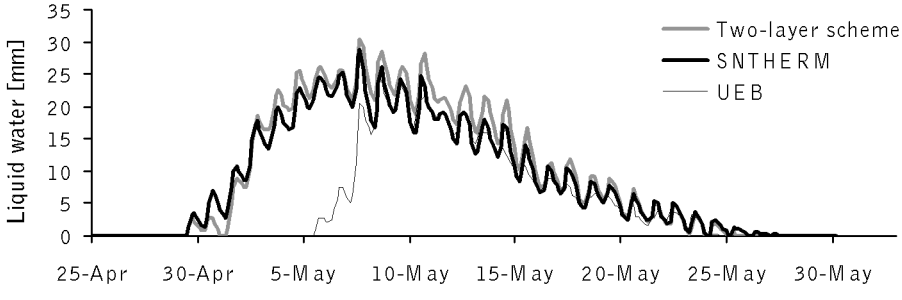

Figure 11. Liquid water mass calculated by SNTHERM, the two-layer scheme, and UEB during the spring melt of 1997.

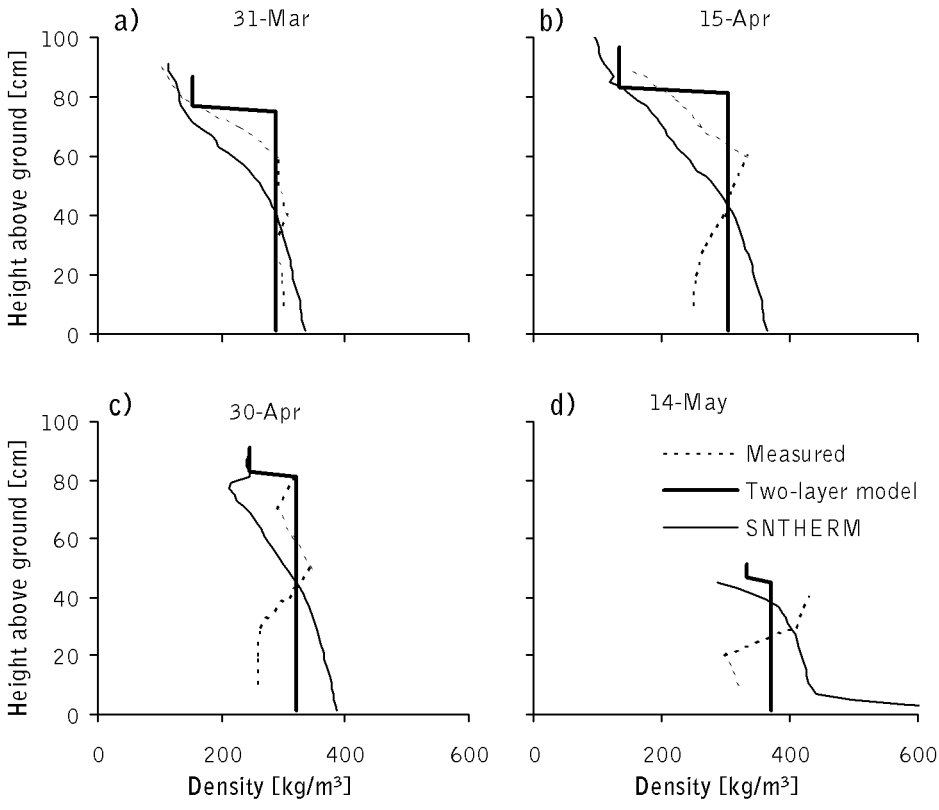

Figure 12. Measured and calculated snow density profiles prior to (a, b) and during snowmelt (c, d).

4.1.6 Discussion

Comparison of snow energy balance models indicated that model performance is dependent on both representation of snow/soil internal processes and computation procedures of surface boundary fluxes. The results of UEB, SNTHERM and the two-layer scheme showed the largest differences in the calculated sensible heat flux, snow surface temperature, average snowpack temperature and liquid water content of snow. There were only small differences in calculated snow water equivalent, i.e. the sum of ice and water masses of the snowpack.

The snow models were driven by measured or estimated meteorological input at the height of 2 m above ground. The fact that the study site was surrounded by sparse forest was assumed not to necessitate modifications to snow model parameterisations, which were developed for unforested conditions. Davis et al. (1997) and Hardy et al. (1997) successfully applied SNTHERM in a forested site in Saskatchewan, Canada, using estimated input data beneath the canopy in a similar way as in this study. The effects of

canopy on solar radiation and wind speed were taken into account using a radiative-transfer model and linear regression, respectively.

In all models, computation of turbulent heat fluxes was based on flux-gradient relationships, but in each model different correction scheme for atmospheric stability was implemented. Raupach and Legg (1984), Male and Granger (1981), and Lee (1978) question the validity of turbulent transfer theory within forest canopy and suggest that turbulent fluxes beneath dense canopy could be ignored because of reduced wind speed. The comparison between measured and modelled fluxes of sensible and latent heat during a two-week period in Sodankylä did neither validate nor falsify the model parameterisations. Uncertainties in computing turbulent heat fluxes were less important than errors in estimating radiation inputs. Hardy et al. (1998), Pomeroy and Dion (1996) and Price and Dunne (1976) report that short-wave and long-wave radiation dominate over turbulent heat fluxes, and are primary sources of energy for spring snowmelt in forests.

The comparison of snow models indicated that similar results were achieved in terms of snow mass balance with different snowpack discretisation schemes. Blöschl and Kirnbauer (1991) compared simulations of snow internal processes against measured data for both one-layer and multilayer snow models without calibration. Although the models were driven by similar surface energy input, the simpler model produced less accurate simulations of water equivalent, liquid water content, and heat content of snow compared with the detailed model. Blöschl and Kirnbauer (1991) concluded that a one-layer snow scheme was unsuitable for simulating dynamics of snow heat and liquid water contents, which were unevenly distributed through the snowpack. Discretisation of the snowpack was required to produce reasonable results of snow internal variables. Gustafsson et al. (2001) compared snowpack parameterisations implemented in SNTHERM and in one-layer model of Stähli and Jansson (1998). Processes in shallow snow cover were simulated in central Sweden, where the models were driven using identical boundary conditions at the snow and soil surfaces. The results indicated that simulated surface heat exchange was in most situations similar using different parameterisations of internal snow processes. Heat exchange depended more on the formulation of snow surface boundary condition than representation of snow internal processes.

The results of the present study are in line with the findings of Blöschl and Kirnbauer (1991). The results suggest that separation of snow and soil thermal processes is a minimum requirement to achieve meaningful snow temperature prediction. In addition, accounting for snow heat content separately in a thin surface layer improves surface temperature prediction and yields a more realistic simulation of heat conduction into snow. The importance of surface boundary condition, as noted in Gustafsson et al.

(2001), was revealed by the need to use identical radiation forcing in the model comparisons.

4.2 Influence of canopy on snow processes in Siuntio (III)

4.2.1 Outline

This section summarises canopy process and snow modelling results from (III). The snow model used is the two-layer scheme presented in Sections 3.2.2-3.2.3, and it is combined with the canopy routines described in Sections 3.3.2-3.3.3. The study attempts to quantify the effect of forest canopy on snow processes on the ground. For the purposes of this thesis, the application shows an example of how the effects of a land use change, such as forest clear-cutting in this case, can be accounted for in the current hydrological modelling system.

The model simulation in the clearing, i.e. open area without canopy, is driven by hourly data of precipitation, air temperature, relative humidity, wind speed, downward short-wave radiation, and downward long-wave radiation measured at a height of 2 m above ground. Input variables for the canopy model ought to be measured above the forest, but in this study the meteorological data measured in the open were assumed to be representative of the conditions at a height of 2 m above the canopy. The study period is from December 1996 until April 2000. Parameterisation of the model is presented in detail in (II) and (III).

4.2.2 Snow in clearing

In Figure 13 the modelled snow water equivalent is compared against measured mean snow water equivalent. Assessment of the model performance is made against the rate of change in snow water equivalent between weekly observations ($SWE_{new} - SWE_{old}$). Based on this criterion, the mean absolute error for the entire study period, i.e. for all four winters, becomes 1.29 mm d^{-1}. A large difference in model performance is seen when snow accumulation and melt periods are considered separately: Mean absolute errors for accumulation periods and melt periods are 0.88 and 2.38 mm d^{-1}, respectively, and biases are –0.11 and –1.78 mm d^{-1}. These results suggest that the model reproduces more accurately snow accumulation than snowmelt. The calculated biases indicate that the precipitation measurement has only a small systematic error, whereas snowmelt is overpredicted throughout the study period. The weather station was placed on a small ridge in the middle of the clearing in order to minimise the effects of shading and turbulence caused by the surrounding forest. However, with regard to

snowmelt, this exposed location is not representative of the snowmelt conditions in the sheltered areas on the ridge sides, where many of the snow cover observations were made. Figure 13 also shows the measured water equivalent at an observation point located next to the meteorological station. Assessment of model results against these values yields mean absolute errors of 0.99 and 1.73 mm d^{-1}, and biases of –0.16 and –0.29 mm d^{-1} for accumulation and melt periods, respectively. The small absolute value of bias for melt periods indicates that now there is less systematic error in snowmelt predictions than when comparing against the mean snow water equivalent.

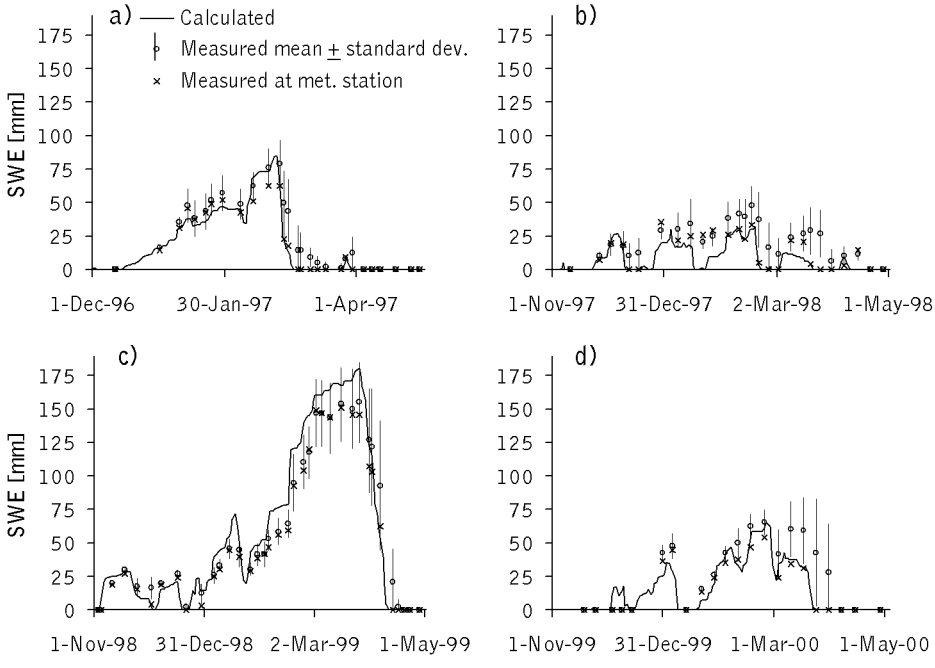

Figure 13. Calculated snow water equivalent (SWE), and measured SWE (mean ± standard deviation) in the open during four winters (a, b, c, d) from 1996 to 2000. Measured SWE at an observation site located next to the meteorological station is also shown.

The readings of temperature sensors residing within the snow cover were used to derive the average snowpack temperature, which was compared with the modelled snow temperature. The mean absolute error for the entire study period is 1.26 °C and bias is –0.61 °C. Large errors occurred when a temperature sensor actually measured the air temperature even though according to the interpolated snow depth it has resided within the snowpack.

4.2.3 Canopy and snow processes in forest

The canopy model was calibrated against meteorological data measured beneath the canopy. Sky-view fraction f_s, canopy transmittance τ_c, and the extinction coefficient n were calibrated against measured downward long-wave radiation, short-wave radiation, and wind speed, respectively. The parameter values and details of the calibration are given in (III). Figure 14 shows the measured and calculated cumulative throughfall, and measured cumulative precipitation in the open separately for winter (November - April) and summer (May - October) seasons. The interception parameters (C_{IS}, C_{IW}, k_I) in Eq. (15) were calibrated and validated against measured throughfall. Mean absolute errors were 0.31 and 0.16 mm d^{-1} and biases were 0.02 and 0.01 mm d^{-1} for the calibration period (December 1996 - April 1999) and the validation period (May 1999 - 28 April 2000), respectively. There is little difference between interception losses in summer and winter seasons. The average interception loss for summer seasons is 29 % and for winter seasons 26 %. Interception evaporation during the winter, when the zenith angle of the sun is wide and net radiation is of low intensity, is mainly explained by advection of energy caused by turbulence within and above the forest canopy.

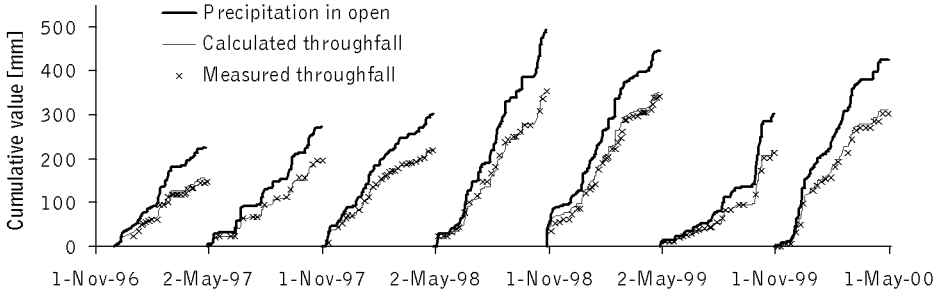

Figure 14. Measured and calculated cumulative throughfall, and measured cumulative precipitation in the open for winter and summer seasons from 1996 to 2000.

The snow water equivalent on the ground beneath the canopy is plotted in Figure 15 for the entire study period. Similarly to the clearing, the spatial variability in the measured water equivalent is high, as indicated by the large standard deviation. In the forest, this variability is mostly a result of spatial differences in throughfall and snowmelt. Snow drift has little impact, because wind speeds beneath the canopy are low. Performance of the snow model is again assessed against the rate of change in snow water equivalent between observations. The mean absolute error for the entire study period is 1.12 mm d^{-1}. Mean absolute errors for accumulation periods and melt

periods are 1.03 and 1.26 mm d^{-1}, respectively, and biases are –0.29 and –0.03 mm d^{-1}. In terms of the performance criteria, the snow model beneath the canopy yields similar results compared with those obtained in the clearing.

Comparison between the measured and calculated daily average snow temperature for a three-month period (January - March 1997) indicated similar model performance in the forest as in the open. The mean absolute error was 0.82 and the bias –0.12 °C.

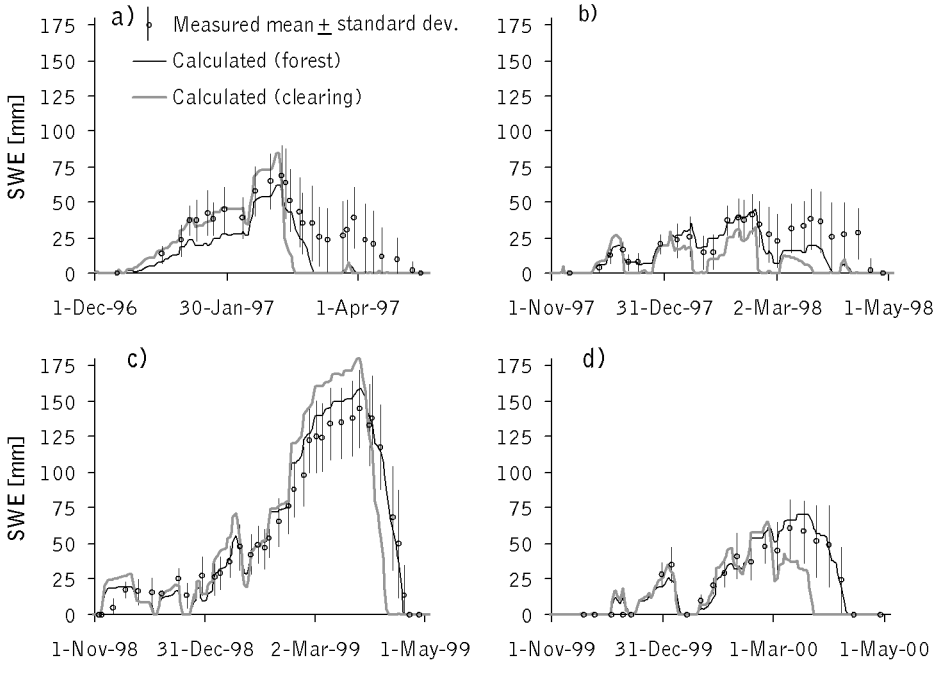

Figure 15. Calculated snow water equivalent (SWE), and measured SWE (mean ± standard deviation) in the forest during four winters (a, b, c, d) from 1996 to 2000. Simulation results from the clearing are also shown.

4.2.4 Comparison between open and forest

Differences in snow processes with and without forest canopy were studied in terms of modelled snow water equivalent, cumulative snowmelt and energy fluxes above the snow surface in the open (clearing) and beneath the canopy. The same set of meteorological input data was used for the snow model in the open, and the coupled canopy and snow model in the forest. The objective was to isolate the effect of canopy on snow processes from other factors, such as snow drift and spatial differences in snowmelt. Hence, the modelled values of snow water equivalent were used in the comparison instead of the measured averages, which are affected by the spatial

differences in snowmelt, especially in the clearing (see Section 4.2.2). Furthermore, there are no measured data on all energy flux components of interest.

The modelled snow water equivalent both in the open and in the forest is shown for the study period in Figure 15. Throughout the winter, depending on meteorological conditions, snow water equivalent may be greater either in the open or beneath the canopy. Because of greater net precipitation in the open, snowfall events, such as those in February 1999, cause the water equivalent to increase more rapidly in the open than in the forest. On the other hand, the greater intensity of snowmelt in the open causes the water equivalent to decrease faster than in the forest. During a sequence of warm spells snow mass in the open falls below that in the forest (see e.g. December 1997 to January 1998). The maximum value of the snow water equivalent is in each winter nearly equal in the forest and in the open. Even though the open receives more precipitation than the forest, the more intense snowmelt in the open is capable of compensating for this difference.

Figure 16 shows cumulative energy fluxes above the snow surface in the open and in the forest. Note that the fluxes are accumulated only when there is snow on the ground. Positive flux is directed towards the snow. The most prominent differences can be seen in net radiation and sensible heat fluxes. Net all-wave radiation in the open (Figure 16a) is dominated by an upward net flux of long-wave radiation until spring. In the spring the intensity of solar radiation increases, and reverses the direction of net radiation flux to point downwards. In mid-winter net radiation is much less negative in the forest where the canopy contributes significantly to downward long-wave radiation. In spring net radiation intensity is lower in the forest because of a canopy shading effect. The loss of radiative energy in the open results in an efficient cooling of the snow surface in mid-winter, which together with greater wind speeds gives rise to a much greater flux of sensible heat compared to that in the forest (Figure 16b). The latent heat fluxes contribute only a little to the total energy balance of snow (Figure 16c).

The advective heat flux from precipitation as defined in Section 3.2.2, includes energy associated with phase change (freezing) in the case of rain, and temperature changes to bring the precipitation to the reference temperature (0 °C). The phase change energy is the largest component of the advective heat flux. During rain on snow events the energy associated with phase change does not actually go to generating melt. Rain on a cold snowpack freezes, releasing energy to the snow and raising its temperature until the snowpack is isothermal (0 °C). After this occurs, rain does not freeze, so the only energy that goes to melt snow is from temperature changes. In order to explore the importance of advective heat flux in generating snowmelt, Figure 16d shows only the advective heat component

associated with temperature changes. From Figure 16 it is clear that the advective heat flux contributes very little to snowmelt.

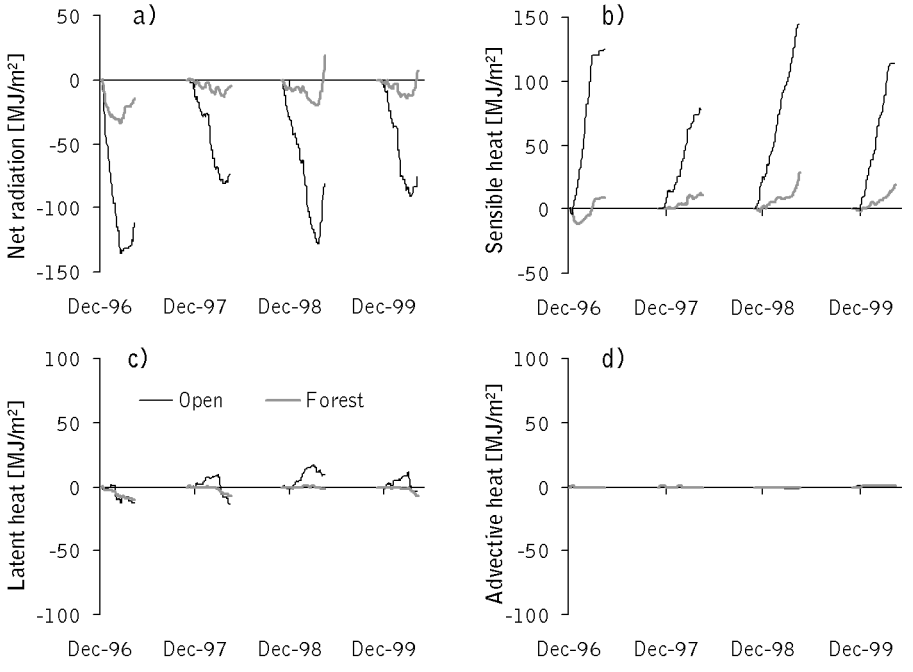

Figure 16. Modelled cumulative fluxes of net radiation (a), sensible heat (b), latent heat (c), and advective heat associated with temperature change (d) above snow surface in the open and beneath the canopy from 1996 to 2000. Positive flux is directed towards the snow.

In Figure 17 daily total net radiation, sensible heat, and latent heat are plotted for winter 1998-1999. In the open, snowmelt events in mid-winter occur when the weather is warm and cloudy. In such conditions snowmelt is driven mainly by sensible heat, with latent heat flux occasionally having a significant contribution. Also, net radiation flux is only slightly negative, or sometimes even positive. In late spring the increase in solar radiation intensity causes net radiation to become the most significant source of energy contributing to snowmelt. Unlike in the open, net radiation in the forest contributes significantly to snowmelt throughout the winter. In mid-winter, peak values of net radiation arise from long-wave radiation emitted by the canopy, and in spring from both short- and long-wave radiation. During melt events in mid-winter sensible heat flux is of the same magnitude as net radiation flux. Latent heat flux in the forest is insignificant throughout the winter.

It is noteworthy that wind speed below the canopy is low and the contribution of the sensible heat flux to snowmelt is largely dependent on

the selection of the windless convection coefficient (E_{H0} in Eq. 5). The value of this coefficient was adopted from Jordan (1992). Unlike the radiation components, the computed turbulent heat fluxes have not been validated against measurements. Particularly in the forest the modelled partitioning of the turbulent energy into sensible and latent heat fluxes is sensitive to assigning E_{H0} a nonzero value and setting E_{E0} to zero. As documented and cited above (see Section 3.2.2), this parameterisation was based on previous snow modelling studies.

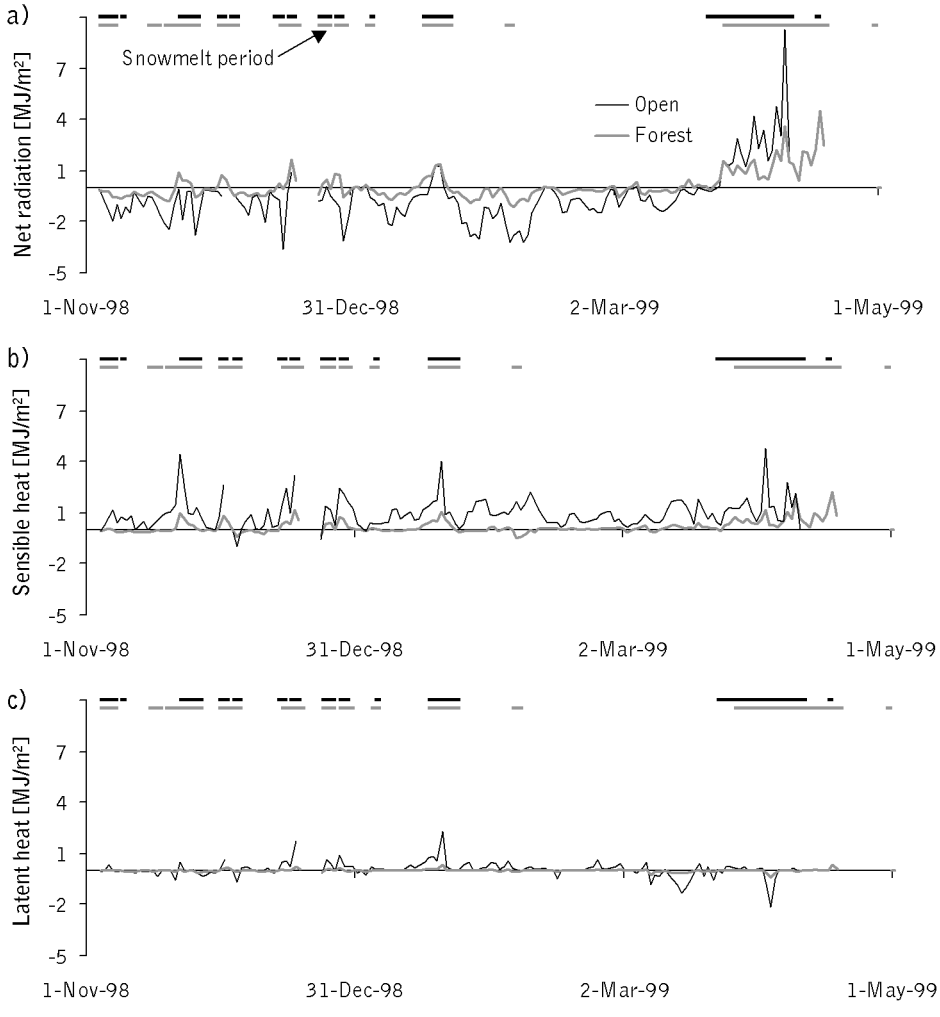

Figure 17. Computed daily total net radiation (a), sensible heat (b), and latent heat (c) in the open and beneath the canopy for winter 1998-1999. Fluxes are shown only when there is snow on the ground. Horizontal lines on top of the fluxes indicate periods when snowmelt occurred.

4.2.5 Discussion

In this study precipitation measurements taken in the open and beneath the canopy suggested that 29 % of precipitation was lost through interception in the summer and 26 % was lost in the winter. Considerable wintertime interception has also been reported in Japan by Nakai et al. (1999), in Canada by Pomeroy et al. (1998), in northern Sweden by Lundberg and Halldin (1994), and in Scotland by Calder (1990). While these studies attribute interception losses primarily to evaporation/sublimation, Troendle (1983) reminds that it is difficult to isolate the roles of depositional differences between forest and clearing during snowfall events, redistribution of snow following the event, and interception evaporation. Storck (2000) reported that in a coniferous forest in Oregon, where the annual precipitation was up to 2000 mm, the dominant removal mechanism of intercepted snow (60 % of snowfall) was meltwater drip and snow unloading. Although removal of intercepted snow via sublimation was of secondary importance, it totalled 100 mm per winter season on average.

In the current study the average interception loss for the winter season was 92 mm. Lundberg et al. (1998) noted that determination of interception on the basis of the difference between precipitation in open and forest is uncertain, because snowfall measurements in particular are prone to gauging errors. In the present study precipitation measurement in the open was corrected to account for gauge catch deficiencies, and precipitation and throughfall estimates in open and in forest were validated by comparing modelled and measured snow water equivalent. Snow simulation results gave no reason to assume that the magnitude of precipitation in the open was incorrect. In the forest, there was a bias of –0.29 mm d^{-1} between measured and computed snow accumulation, which indicated that the increase of snow mass was slightly underpredicted. This bias was found to be approximately 10 % of measured precipitation during the accumulation periods. As shown in a sensitivity analysis in (III), simulated snow water equivalent is sensitive to both the magnitude and form of throughfall. Therefore, the bias in simulated snow accumulation may be an indication of a systematic error, either in the magnitude or form of estimated throughfall. According to model interception loss was explained to result from evaporation/sublimation. However, it should be noted that no direct measurement of interception loss through evaporation or through other mechanisms, such as wind-driven redistribution effects, was available.

Measured throughfall in this study did not include stemflow, which was assumed to be negligible. Based on measurements in central Finland, Päivänen (1966) found negligible stemflow in spruce forest, and stemflow amounted only up to 1.9 % of gross precipitation in pine forest during the growing season. Rutter et al. (1975) report greater values of stemflow (7.7 %) for a Douglas fir. During snowmelt in winter and spring the role of stemflow

can be expected to be greater than in summer, which may result in overestimation of interception loss when it is based on the difference between precipitation gauge measurements.

Comparison of snow simulation results in open and forest indicated that snow accumulation was greater and snowmelt was more intensive in the open relative to the forest. These results are qualitatively similar to the findings of Hardy et al. (1997), Troendle and King (1987), Kuusisto (1984), Troendle (1983), Gary (1974), and Seppänen (1961). Hardy et al. (1997) compared snowmelt simulations in open and beneath a boreal jack pine forest in Canada. They used SNTHERM driven by input meteorological variables measured or estimated at a reference height close to snow surface. Their results indicated that small openings in the forest accumulated considerably more snow than large openings. Large open areas were influenced by wind redistribution and more pronounced energy fluxes. Snow depth beneath the canopy was substantially lower than in small openings, and melt occurred four days later, and was less intense beneath the canopy than in the openings.

For conditions similar to the current study site the impact of forest clear-cutting would be most clearly seen as an increase of net precipitation on the ground and, hence, an increase of water volume potentially contributing to streamflow over the winter season. However, because the maximum values of snow water equivalent were similar in the open and in the forest, the volume of spring runoff resulting from the final melt may not change. It should be noted that these considerations disregard the effect of soil water storage differences on runoff generation in clearcut and forested areas. Heikurainen and Päivänen (1970) measured the effect of forest clear-cutting and thinning on snow depth and runoff in central Finland. Their findings suggested that snow accumulation increased with increased thinning, and melting of the snow cover occurred earlier in the thinned and cut areas than in the untouched areas. In the case of partial forest removal, the spring runoff peaks may be decreased, because average snowmelt from plots of different treatments occurs during a longer time span than snowmelt from the untouched forest preceding the treatment.

The dominant role of net radiation as a source of energy for spring snowmelt is consistent with earlier results from boreal forests (Link and Marks, 1999; Hardy et al., 1997; Pomeroy and Dion, 1996; Price and Dunne, 1976). These studies do not address mid-winter snowmelt, since it rarely occurs in the climatic conditions exhibited by their study sites. The mid-winter melt events occurring in the current study site are associated with warm, cloudy weather when both long-wave radiation and sensible heat flux contribute to snowmelt. As mentioned earlier, solar radiation intensity in the middle of the winter is insignificant. Sources of energy contributing to snowmelt in mid-winter, both in the open and in the forest, are strongly

dependent on air temperature. Sensible heat flux is directly proportional to the temperature gradient above the snow surface, and net radiation is dominated by the long-wave components, which are functions of radiation source temperatures. As winters in coastal areas of southern Finland comprise several melt periods, and melt intensity is sensitive to the air temperature, a change in the local climate would have a prominent effect on the extent and depth of the snow cover.

The canopy model results were more sensitive to parameters of turbulent flux computation schemes than to parameters influencing computation of net radiation intensity within the canopy. This is in line with the finding of Lundberg and Halldin (1994), who reported the estimation of interception evaporation to be very sensitive to the aerodynamic resistance. Calder (1990) noted that evaporation tends to be driven by energy available from radiation when surface resistance is large, but energy stemming from turbulence becomes important when surface resistance is small, which is the case for tall vegetation such as forest.

Computed snowmelt during mid-winter conditions was sensitive to the parameters of the turbulent energy fluxes, particularly to the windless exchange coefficient of sensible and latent heat. Because the turbulent energy fluxes were not measured beneath the canopy, the parameterisation of the turbulent heat fluxes cannot be validated in this study. However, the total contribution of turbulent heat fluxes to snowmelt in mid-winter is likely to be accurate, because the other major energy fluxes, short-wave and long-wave radiation, were calibrated and validated against data measured beneath the canopy.

4.3 Runoff generation processes in Siuntio (IV, V)

4.3.1 Outline

This section presents results from studies (IV) and (V), which deal with modelling of precipitation-streamflow relationship. The objective is to calibrate and validate three- and two-dimensional runoff models, which couple vertical soil water movement and lateral ground water flow. Snow and canopy process schemes presented in the preceding sections produce the input to one of the studied runoff models. Assessment of the Skaggs routine (Skaggs, 1980) is presented first, followed by simulation results from two case studies.

4.3.2 Computation of vertical soil-water flow

Computation of vertical pressure head distribution was either based on the steady-state approach of Skaggs (1980), or on a finite difference solution to the Richards equation (e.g. Karvonen, 1988). Performance of the two methods is compared in terms of computed soil moisture in the unsaturated zone and depth to water table (Figure 18). Model set-up is explained in detail in (IV).

Results of comparison in Figure 18 indicate that the two methods simulate nearly identical soil moisture and ground water table dynamics during a study period in 1996. For another period in 1995 simulated soil moisture close to the soil surface shows a discrepancy at the time of infiltration that occurs after a rainless period of one month. Overall, the closer the water table is to the soil surface, the better is the agreement between the Skaggs approximation and the numerical solution of the Richards equation. The Skaggs steady-state routine replicates Richards solution during the time periods, when most of the runoff is generated and the depth to the water table is less than about 1 m from the soil surface. The steady-state routine becomes less appropriate during dry periods.

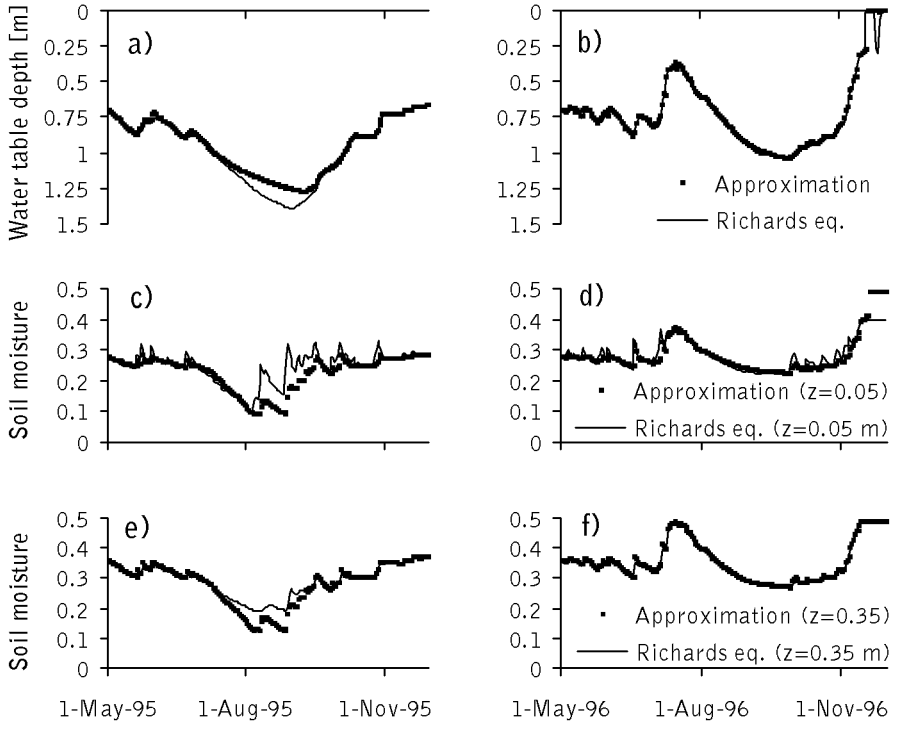

Figure 18. Calculated water table depth (a, b), and soil moisture time series (c-f) at the depths of 0.05 and 0.35 m during May-November 1995 and 1996. Results using the numerical solution to the one-dimensional Richards equation and the Skaggs approximation are presented.

4.3.3 Quasi-three-dimensional model

In case study (IV) soil and ground water interactions are described in three dimensions to simulate soil moisture distribution and dynamics of saturated areas within the study catchment. The model is driven by daily air temperature and precipitation from January 1991 to December 1996. A degree-day snowmelt model is used to simulate snow accumulation and melt, and the quasi-three-dimensional scheme (Section 3.4.3) describes runoff generation. Potential evapotranspiration and interception are according to daily schemes described in the beginning of Section 3.3.1.

Description of model parameterisation is given in (IV). Only the main results are presented here. The model was calibrated against daily streamflow data from January 1991 until December 1993, and validated against data from January 1994 until December 1996 (Figure 19). The coefficient of efficiency, R_{eff}, (Nash and Sutcliffe, 1970) was 0.72 for the calibration period and 0.68 for the validation period. Table 2 shows the calculated annual water balance and the coefficients of efficiency. Low values for the coefficients in 1993 and 1995 are the result of large errors in predicting the annual maximum flows. For example, the greatest daily flow in 1993 occurred at the end of December, and it was underpredicted by nearly 80 %. In 1995, the greatest streamflow peaks in the middle of winter were underestimated, but the later spring melt was overestimated. Annual cumulative streamflow was in accordance with measurements during years other than 1991 and 1995. Autumn base flow was overpredicted during 1991, and spring snowmelt was greater than measured during 1995. Small measured and simulated streamflow volumes during summers of 1992-1996, and successful timing of first streamflow events after the summers, suggest that the estimate of evapotranspiration was realistic. Coefficients of efficiency in different seasons imply that the model performance is better in summer (June-August, R_{eff} = 0.75) and autumn (September – November, R_{eff} = 0.71) than in winter (December - February R_{eff} = 0.66) and spring (March - May R_{eff} = 0.69). Winter and springtime results are affected by uncertainties in snowmelt simulation.

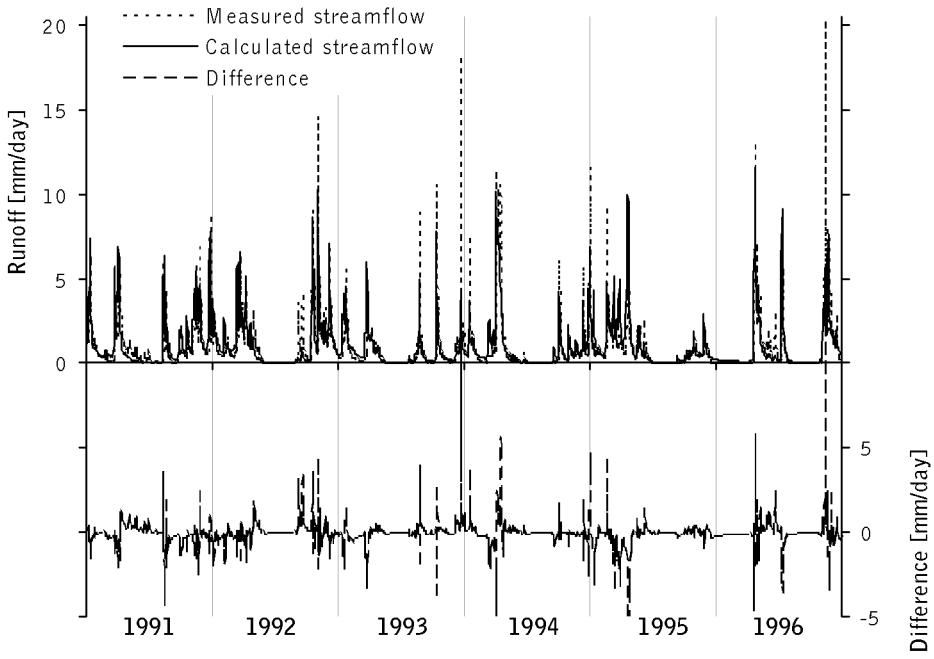

Figure 19. Measured and calculated catchment runoff and their difference during 1991-96. The period of 1991-93 was used for model calibration and 1994-96 for validation.

Table 3 shows the average monthly fractions of modelled direct runoff (that has never infiltrated) and fractions of event water according to Lepistö (1994). Based on measured oxygen isotope concentrations in precipitation, stream water and ground water, Lepistö (1994) traced event water to direct rainfall or snowmelt generating saturated overland flow and some shallow ground water flow with a very short transit time. The total fraction of computed direct runoff was 65 and 63 % for 1991 and 1992, respectively, and was significantly greater than the fraction from tracer analysis. According to the model, nearly all runoff in summertime is generated directly from throughfall.

Table 2. Efficiency coefficients between measured and calculated runoff, annual runoff components, and annual precipitation during 1991-96. All hydrological variables are in mm/a.

	1991	1992	1993	1994	1995	1996	Total
Efficiency	0.73	0.82	0.59	0.81	0.34	0.67	0.69
Measured runoff	377	415	273	339	291	321	2016
Calculated runoff	441	420	261	347	386	326	2181
Calc. direct runoff	288	262	160	241	230	239	1420
Meas. precipitation	864	830	677	735	798	705	4609

Table 3. Calculated fractions of direct rainfall/snowmelt from total runoff. Measured fractions of event water are taken from Lepistö (1994).

	Calculated fraction of direct runoff [%]		Measured fraction of event water from tracer analysis [%]	
	1991	1992	1991	1992
January	60	41	13	13
February	23	42	3	14
March	70	65	33	9
April	58	61	3	4
May	44	25	3	1
June	66	28	1	0
July	92	0	10	0
August	91	98	66	12
September	72	92	26	13
October	52	86	27	8
November	67	65	24	15
December	59	58	14	14
Total	65	63	21	10

4.3.4 Characteristic profile model

In case study (V) all submodels included in the precipitation-streamflow model were calibrated and validated separately against a relevant set of hydrometric data. This approach was selected in an attempt to keep track of time delays and water losses associated with hydrological subprocesses. Meteorological data measured in the clearing adjacent to the study catchment (see Figure 1) during 1998-2000 were taken as an input for the canopy model, which in turn yielded input variables for computation of snow processes beneath the canopy. This part of the application is identical to results presented in Section 4.2.3 (III). Throughfall and snowmelt given by the canopy and snow models were used to drive the CPM. Potential transpiration is estimated as explained in Section 3.3.4. The estimate of potential transpiration is multiplied by a constant scaling factor (f_{EP}), which is one the calibration parameters.

In the study catchment, ground water levels were monitored at three points (see Figure 1) along a hillslope, which was assumed to represent a typical water travel path from a water divide to a ditch. Geometry of the CPM was fixed according to the surface and bedrock topographies of this hillslope (Figure 20). Parameterisation of the CPM is explained more detailed in (V).

Calibration of the CPM was carried out for a period from January to December, 1999, examining winter and summer time data separately. Different dominant processes control the hillslope response during these periods, which provides guidance for restricting the number of calibration parameters in each period. The rest of the data from February to December 1998, and from January to April 2000, were used for validation. Calibration

was based on ground water levels, which were carefully examined in an attempt to explain mechanisms behind the observed dynamics.

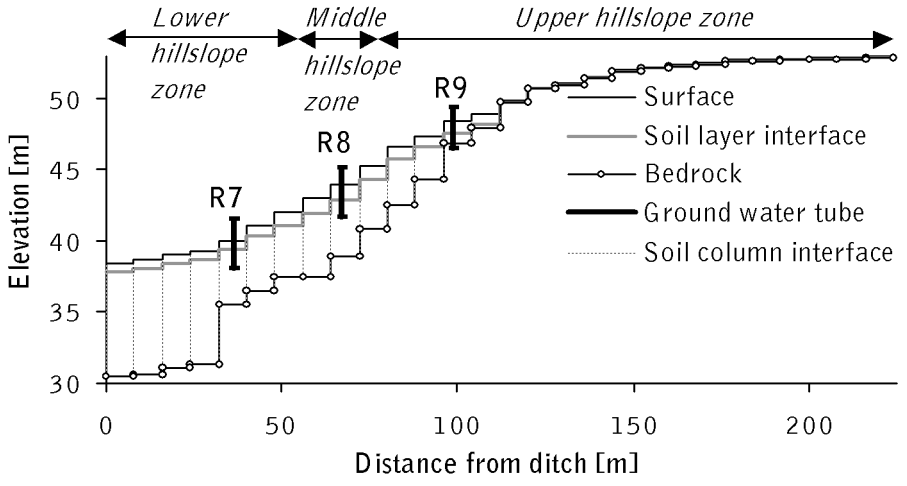

Figure 20. Geometry of the CPM for the study catchment, locations of ground water measurement tubes (R7, R8 and R9), and location of the interface between top and bottom soil layers.

Wintertime data from January to April 1999, were used to calibrate the lateral hydraulic conductivities, and to identify the depth of the interface between the two soil layers. As observed in Figure 21, ground water levels in winter show a fairly quick decline to a depth of 70 to 110 cm, depending on the ground water tube. Thereafter, decline of the water levels ceases almost completely. As the transpiration during the winter is insignificantly small, dynamics of the ground water levels are attributable only to lateral flow within the soil profile. Based on these findings, lateral hydraulic conductivity of the top soil layer was given a high value of 10 to 30 cm h^{-1}, and the bottom soil layer a low value of 0.15 to 0.35 cm h^{-1}. Also, location of the interface between the soil layers around each tube was set to a depth, where decline of the water level stopped.

Calibration was continued using measured ground water levels from summer 1999. The most prominent feature in seasonal ground water dynamics was that in the summer water levels dropped substantially lower than during the winter. Water level decline that continues far below the conductive top soil layer is explained by transpiration. The scaling factor, i.e. the constant with which the reference crop potential transpiration is multiplied, was adjusted in an attempt to replicate the rapid rise of water levels caused by autumn storms. Water level drop resulting from transpiration was calibrated by adjusting the root zone depth (z_r), the vertical

hydraulic conductivity, and the water retention parameters of the bottom soil layer. These two steps were repeated until no further improvement in the model fit against the measured ground water levels was achieved. Despite intensive calibration, the calculated water levels at the lower part of the hillslope (R7, R8) compare only moderately with measurements throughout the summer 1999 (Figure 21). Validation results indicated a good match to measured ground water levels during winter seasons, but the model failed to replicate some of the observed peaks in tubes R8 and R9 in summer 1998.

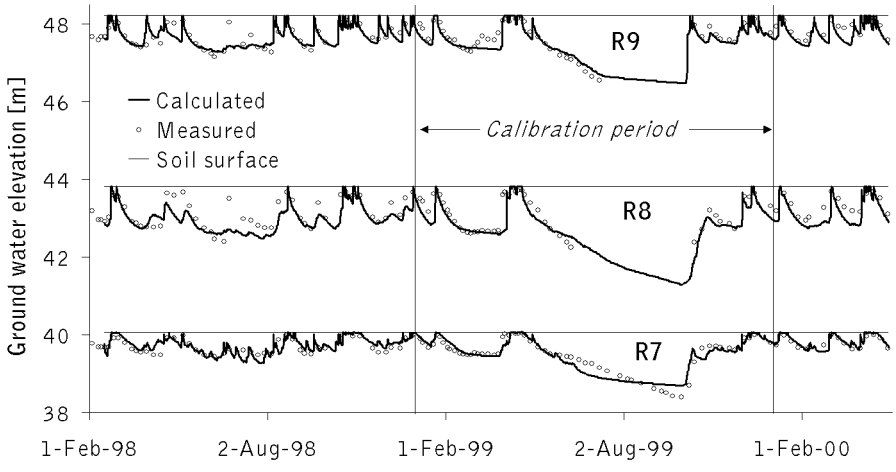

Figure 21. Measured and calculated ground water elevations along the study hillslope (tubes R7, R8, R9). Data from 1999 were used for calibration and the remaining data for validation.

After calibration of the CPM parameters, the computed runoff components were used as input to the linear storage streamflow model. The retention coefficient of the linear storage was calibrated and validated against measured streamflow for the same periods as the CPM (Figure 22). The efficiencies (Nash and Sutcliffe, 1970) were 0.85 and 0.72 for calibration and validation periods, respectively. The volume of total streamflow was overestimated by 1.3 % for the calibration period, and by 16 % for the validation period. Most of the volume error during the validation period accumulated in spring 1998, when instrumentation problems at the weir posed uncertainty on the streamflow measurements.

The validated CPM was applied to a period from 1991 to 1992 in order to compare modelled runoff against tracer study results of Lepistö (1994). Application of the CPM required hourly input data, which were simulated from available daily meteorological measurements. Description of this input data simulation is presented in (V). The simulated hourly data were used to drive the canopy and snow procedures, whose output - throughfall and

snowmelt - were given as input to the CPM calibrated above. Streamflow simulation results from 1991 to 1992 yielded a Nash and Sutcliffe efficiency of 0.66 and a total volume error of –0.4%. By comparison, the quasi-three-dimensional precipitation-streamflow model showed an efficiency of 0.78 (Section 4.3.3), and the total streamflow was overpredicted by 9 % for the study period under examination. It is not surprising that a model calibrated to streamflow measured in that particular period yields a better fit than a model that was calibrated against data measured in another time period. In fact, validation (1994-96) of the quasi-three-dimensional model yielded an efficiency of 0.68, which is of the same magnitude as the efficiency reported here.

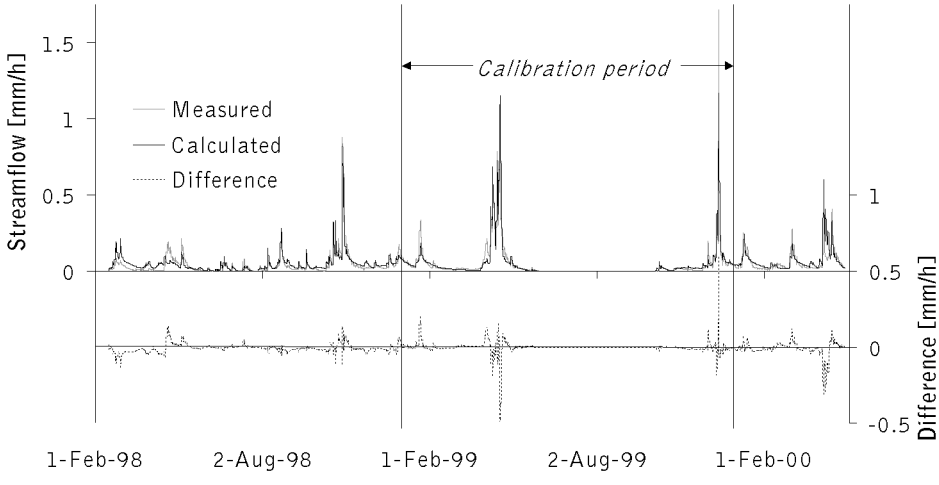

Figure 22. Modelled and measured hourly streamflow and their difference. Data from 1999 were used for calibration and the remaining data for validation.

Direct runoff, i.e. water that never infiltrated into the soil, was compared with the isotopically traced event water. In the following, both direct runoff and event water are called new water. Runoff generated via baseflow and exfiltration, i.e. water that has been in contact with the soil domain, is assumed to be comparable with the pre-event water. In the model all water that enters the soil domain becomes instantly pre-event water, while in reality some of the water that infiltrates may appear in the stream as event water. A sounder way of separating event and pre-event waters would be to track migration of water particles through the modelling domain and then calculate residence times for each particle. All particles having a shorter residence time than the span of the event would be considered to form the event water fraction.

Figure 23 shows monthly totals of measured and calculated runoff, and fractions of direct runoff and isotopically traced event water. Isotope tracer results were adopted from Lepistö (1994). Fractions for months when the model computed less than 5 mm total runoff were omitted. The fractions of calculated and measured values are approximately at the same level, except for the last quarter of 1992. Also, both model and isotope results show high contributions of new water in August 1991, which had a large monthly rainfall of 191 mm, and included the greatest value of daily rainfall (77 mm) recorded over the study period. Lepistö et al. (1994) studied the relationships between event water fraction and event rainfall in Siuntio and found that new water fraction becomes dominant only in response to intense storms.

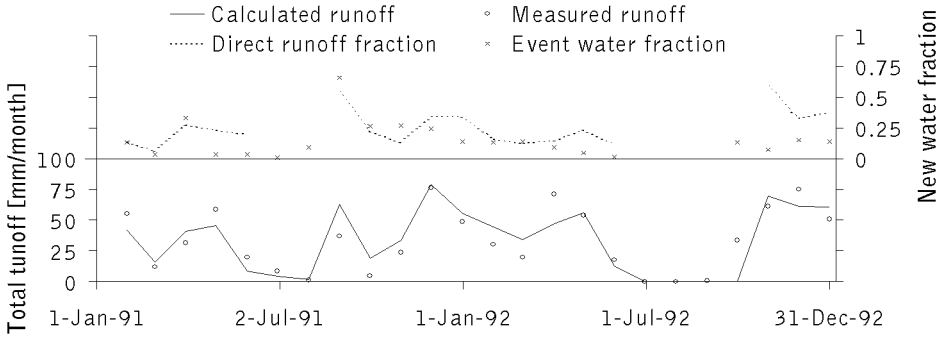

Figure 23. Monthly totals of measured and calculated runoff, and fractions of direct runoff and isotopically traced event water.

When August 1991 is omitted, the monthly variation of event water fraction shows no similarities to the variation of the direct runoff fraction. Rather, the modelled fraction of direct runoff shown in Figure 23 depends on the amount of monthly streamflow (correlation coefficient = 0.72). The event water fraction shows no relation to streamflow (correlation coefficient = 0.04). It appears that the volume of monthly streamflow alone does not explain how much event water is produced, but it is rather more dependent on the temporal distribution, and hence intensity, of throughfall/snowmelt. The fact that the fraction of direct runoff shows interdependence with streamflow suggests that the modelled runoff generation mechanism may not be plausible for low intensity streamflow events. In the model, water input on near-stream saturated areas always produces direct runoff, regardless of the event intensity.

The fraction of new water for the entire period from 1991 to 1992 was 0.64 according to results of the quasi-three-dimensional model, 0.30 as computed in the CPM, and 0.15 based on tracer analysis. The results of the hillslope model are significantly closer to the tracer results than those

obtained by the quasi-three-dimensional model. Here the CPM was calibrated against ground water levels, whereas in Section 4.3.3 both soil water and channel routing routines were calibrated against streamflow records. It is believed that examination of ground water level dynamics in winter and summer seasons, when control of different processes on the water levels can be isolated, leads to a more realistic separation of runoff components.

4.3.5 Discussion

Applicability of the presented approaches for simulating rainfall-runoff processes cannot be ranked without a note of caution. With respect to reproduction of streamflow alone there is no reason to believe that the presented approaches provide more (or less) accurate predictions than any other type of model calibrated against streamflow data. Similar simulation results in terms of streamflow predictions have been achieved with models of different structure (Ye et al., 1997; Lindström et al., 1997). Seibert (1999), Refsgaard (1997) and Grayson et al. (1992) point out that a hydrological model having an excess of parameters and including separate routines for hydrological subprocesses should be calibrated and validated against measured internal fluxes and state variables. Calibration and validation of the present modelling system (CPM) aimed at following this direction.

Comparison between two different discretisation schemes indicated that: 1) the available data on internal hydrological measures did not support calibration of a large set of spatial parameters in a distributed model; and 2) comparison between field measurements and model results was most straightforward with the simpler discretisation scheme and more restricted modelling domain. Similar results were found in other applications of (semi) distributed models (Kite and Kouwen, 1992; Wigmosta et al., 1994; Zhang et al., 1999). Calibration of a hydrological model with spatially variable parameter input must be restricted to a minimum number of parameters by fixing as many parameters *a priori* as possible. Parameters of physics-based models have a physical meaning, which should enable determination of their values on the basis of field measurements or experiments. Detailed measurements are often made in an extent that is directly comparable to the modelling domain inherent in hillslope hydrological models (Bronstert, 1999).

Hydrological processes were explored in a small catchment covering an area of only 0.18 km^2. The case studies cannot prove the applicability of the modelling system to basins much larger than the study catchment. The main obstruction for the transferability of the present system is the overly simplified flow routing procedure. Several authors (Orlandini and Rosso, 1998; Kirkby, 1993; Blöschl and Sivapalan, 1995) point out that in small catchments (< 50-100 km^2) the delay from rainfall to streamflow is mainly

controlled by hillslope flow processes, but in large catchments (>100 km^2) channel processes become increasingly important. The application of the present modelling system to large basins requires first of all use of more advanced routing techniques. The modelling component producing the share of precipitation that becomes runoff could be identical to the CPM, which is shown to work in the study catchment exhibiting homogeneous land-use. In larger catchments, which comprise areas with various land-use practises, a set of CPMs can be formed on the basis of both topography and land-use distribution. Then, the model framework provides some tools to quantify the effects human activities may have on the hydrological response of a catchment. For example, Karvonen et al. (1999) applied a model similar to the semi-distributed approach presented in Section 4.3.4 to a river basin having an area of 1 285 km^2. A set of CPMs was used to separate runoff contributions from predefined areas exhibiting hydrological similarity in terms of land-use, vegetation, and mean slope. Total runoff formed an input to a geomorphologic instantaneous unit hydrograph (GIUH) used as a flow routing scheme (Rodríguez-Iturbe, 1993). Ideally, CPM parameters should be related to landscape and terrain properties, and GIUH parameters to stream network characteristics (Gupta et al., 1980), but Karvonen et al. (1999) ended up calibrating the GIUH parameters against measured streamflow.

In addition to flow routing, the modelling concentrates less on derivation of actual transpiration, which is simply a function of estimated potential transpiration and soil moisture content. Kellomäki and Wang (1999), Liu et al., (1998), and Nijssen et al., (1997) showed how actual transpiration can be controlled by relationships between stomatal resistance and vapor pressure deficit, soil temperature, photosynthetically active radiation, and soil moisture content. The hillslope case study in Section 4.3.4 showed the largest prediction errors against summertime water table dynamics. These errors are likely to be affected by transpiration estimates. Vakkilainen (1982) compared potential evapotranspiration estimates against measured transpiration in grass-covered lysimeters in southern Finland and noted that estimates may fail during spring and early summer when net radiation may not be fully available for transpiration but is partly used to heat the soil. A more consistent coupling of snow and runoff models would necessitate account for feedback between soil thermal state and transpiration (Metcalfe and Buttle, 1999; Levine and Knox, 1997).

Streamflow simulations utilising Siuntio 1991-94 data can be compared with TOPMODEL predictions in Lepistö and Kivinen (1997). Their results were realistic in terms of reproduction of annual streamflow volumes. However, similar problems were encountered in replicating the peak flows as were reported in the present study. Lepistö and Kivinen (1997) had more difficulties with summer flows, which were overpredicted compared to the

measured negligible flows. The annual streamflow dynamics were replicated better using the present models, but the annual water balances were similar to the results of Lepistö and Kivinen (1997). They compared the calculated average depth to the water table with the point measurements. Present studies allowed a more detailed comparison at the measurement locations. For example, the water table calculated by the quasi-three-dimensional model was closer to the soil surface and compared better with the measurements than the average water table depth computed by TOPMODEL.

The data quality of the measured streamflow in Siuntio caused some concern because water freezing during the winter and spring snowmelt may have had an effect on the operation of the measurement weir. The largest errors in the annual water balance computed by the quasi-three-dimensional model occurred in 1995, when calculated streamflow was 33 % greater than measured. The streamflow records in 1995 may be affected by measurement errors, because the annual flow was inconsistent with streamflow measured at a weir located 1.5 km downstream and draining an area of 1.42 km^2. In 1995, the total streamflow at the downstream weir was 42 % greater compared with the study catchment, but during 1991-94 and 1996 the annual flow in the downstream weir was on the average 17 % greater than the flow from the study catchment. Precipitation during 1996, and air temperature during 1991-96 were measured 30 km north of the site on the other side of the Salpausselkä ridge. The meteorological observations in Vihti may not represent the study site well enough to support accurate snowmelt and evaporation calculations.

5 CONCLUSIONS

The main inferences of the snow energy balance studies (I, II) can be summarised as the following points:

1) Comparison of a one layer snow model (UEB) and a multi-layer model (SNTHERM) revealed major differences in simulated energy flux components at the snow surface. Even after the models were driven by identical radiation input, the models produced dissimilar surface temperatures, average snowpack temperatures, and liquid water content in snow. These differences were affected most by the disregard of soil water freezing and thawing in UEB, which treated snowpack and soil down to a prescribed depth as one lumped layer. In spite of differing snow heat balance simulations, the models showed only minor differences in computed water equivalent of snow.

2) Assessment of the model results against measured snow water equivalent, snowpack temperature, and snow surface temperature indicated that SNTHERM replicated well both snow mass and heat balance, and its results could be used as a reference in modifying and improving simple energy balance models.

3) A new snow energy balance scheme was developed on the premise that separation of snow and soil in the model parameterisation is necessary for a realistic simulation of average snowpack temperature. In addition to separate treatment of snow and soil heat processes, the surface temperature prediction was improved after: 1) a procedure was implemented to account for windless exchange of sensible heat flux; and 2) the heat conduction into the snow was described by approximating the temperature gradient between the snow surface and a thin upper layer of snow.

In the subsequent case study (III) snow processes in the open and forest were studied by coupling the developed snow model with a canopy process scheme. The main conclusions were:

4) The difference between measured precipitation in open and throughfall in forest suggested that a significant proportion of the precipitation was captured in the canopy both during summer and winter. The average interception loss was 26 % of precipitation for winter seasons, and 29 % for summer seasons. There is little difference in cumulative interception losses in winter and summer, although radiation intensity in the winter is drastically lower. According to model interception evaporation during the winter was mainly explained by advection of energy caused by turbulence within and above the forest canopy.

5) The effect of the canopy on snow mass balance on the ground can be seen as greater snow accumulation and more intense snowmelt in the open. Because winters in the study site typically comprise several accumulation-melt cycles, the snow water equivalent may be greater at any time either in the open or beneath the canopy. Also, there is little difference in the maximum values of the average snow water equivalent in each winter. When a warm spell is short enough to leave snow on the ground both in the open and in the forest, the cumulative snowmelt during one event is always greater in the open. Because the maximum snow water equivalent prior to the spring melt is nearly equal in both sites, there is not much difference in the cumulative spring snowmelt. Melt is more rapid in the open, leaving the ground free of snow when there is still snow melting in the forest.

6) The comparison of modelled energy fluxes above the snow surface revealed major differences in net radiation and sensible heat fluxes in the open and beneath the canopy. In mid-winter the contribution of canopy to downward long-wave radiation was clearly seen as smaller radiation losses in the forest. In spring the net radiation is of lower intensity in the forest because of the canopy shading effect on short-wave radiation. Sensible heat flux in the open is much greater than beneath the canopy. In mid-winter the main source of energy for snowmelt is sensible heat in the open, whereas both sensible heat and net radiation contribute to snowmelt in the forest. Solar radiation intensity increases towards the spring, which causes net radiation to become dominant in both sites.

Findings from the precipitation-streamflow modelling studies (IV, V) are:

7) Use of a DRAINMOD-type approximation (Skaggs, 1980) for simulating the pressure head distribution in the unsaturated zone is a promising option for simplifying the coupling of vertical soil water and lateral ground water models in both two and three-dimensional settings. The approximation yields results comparable to a numerically solved Richards equation, and enables effective estimation of storage coefficients as a function of water table depth.

8) The hydrological models based on quasi-three dimensional and quasi-two dimensional discretisation schemes produced similar results in terms of fit against measured daily streamflow. With respect to streamflow reproduction alone there is no reason to believe that the presented physics-based approaches provide more (or less) accurate predictions than any other type of model calibrated against streamflow data. The strength of the current models lies in spatially distributed predictions of state variables and fluxes from all hydrological subprocesses.

9) Even though the results of the quasi-three-dimensional model were acceptable in terms of fit against streamflow data, the modelled volume of

direct runoff from throughfall/snowmelt, i.e. runoff that has never infiltrated into the soil domain, was overly large compared with the volume of event-water estimated from isotopic tracer analysis. As shown in the subsequent hillslope study, separate calibration of the hydrological submodels aids in obtaining a more realistic separation of runoff components. In the hillslope model, where the soil water routine is calibrated against ground water levels, the fraction of event-water in streamflow is more realistically estimated than in the quasi-three-dimensional model, where only streamflow data were used for calibration.

In the end, the suitability of the presented modelling system for studying the impacts of land use changes on hydrological processes was assessed. The following arguments can be pointed out:

10) In the current hydrological model, processes and areas affected and unaffected by changing conditions can be considered independently. The case study of snow processes in clear-cut and forested sites shows an example of how influence of changing conditions on hydrological subprocesses is identified. Separating the affected and unaffected areas can be accomplished by assigning a CPM to each area.

11) A CPM outlined in this thesis can be used to simulate runoff generation in a non-contiguous area that is similar in terms of its land-use. A system where a set of CPMs is combined together can be used to quantify runoff contributions from pre-classified areas of different land-use and constitutes a tool for studying hydrological impacts of land use changes. The complete modelling system is likely to be unreasonably complex for calibration against merely streamflow measurements in catchments having mixed landscape and terrain properties. Calibration and validation of individual CPMs should be conducted against combined hydrometric and tracer/chemical data from basins that are homogeneous with respect to properties important for hydrological response. The present work shows one example how CPM can be calibrated and validated against data from a catchment exhibiting homogeneous land-use.

5.1 Future directions

In the current work an attempt was made to formulate a hydrological model that provides linkages to atmospheric models through implementation of surface energy balance and to water quality models through quantification of runoff components. Advancement of these linkages is one of the future challenges in hydrological modelling.

In long-term simulations climate predictions are sensitive to the accuracy of estimated land surface hydrology and surface energy balance (Gustafsson,

2002). Improvements in computation schemes of land surface processes, such as evapotranspiration, interception, snow accumulation, snowmelt, and areal soil moisture distribution can aid in obtaining more realistic boundary conditions for climate models.

Tracer and other new techniques for measuring runoff source areas and water flow pathways through soils provide clues for improving runoff generation schemes (Uhlenbrook and Leibundgut, 2002). Beven (2001) notes that model developments are most likely to happen when one is forced to reject all the available models because of inconsistency with data. Validation of a hydrological model against tracer and chemical data increases its credibility for simulating solute transport and nutrient leaching.

Many hydrological models including the CPM presented in this thesis cannot fully exploit spatial data of input variables and catchment physical properties. For example, it is not resolved how spatial data on land use, topography, and soils are used objectively to determine geometry and parameters of typical hillslopes (CPMs). Effective use of spatial data resources becomes an issue when process-models tested at point-scale or in small catchments are transferred to large heterogeneous catchments.

6 REFERENCES

Abbott, M.B., Bathurst, J.C., Cunge, J.A., O'Connell P.E., Rasmussen, J. 1986. An introduction to the European Hydrological System - Système Hydrologique Européen, "SHE", 1: History and philosophy of a physically-based, distributed modelling system. Journal of Hydrology, 87, 45-59.

Amatya, D.M., Skaggs R.W., Gregory J.D. 1997a. Evaluation of a watershed scale forest hydrologic model. Agricultural Water Management, 32, 239-258.

Amatya, D.M., Skaggs, R.W., Gregory, J.D., Herrmann, R.B. 1997b. Hydrology of a drained forested pocosin watershed. Journal of the American Water Resources Association, 33, 535-546.

Anderson, E.A. 1968. Development and testing of snow pack energy balance equations. Water Resources Research, 4, 19-37.

Anderson, E.A. 1976. A point energy and mass balance model of a snow cover. NOAA Technical Report NWS 19, 150 pp.

Aston, A.R., 1979. Rainfall interception by eight small trees. Journal of Hydrology, 42, 383-396.

Bathurst, J.C. 1986. Physically-based distributed modelling of an upland catcment using the Système Hydrologique Européen. Journal of Hydrology, 87, 79-102.

Becker, A. 1992. Criteria for a hydrologically sound structuring of large scale land surface process models. In: O'Kane, J.O.P. (ed) Advances in Theoretical Hydrology. Elsevier, Amsterdam, 97-111.

Becker, A., Braun, P. 1999. Disaggregation, aggregation and spatial scaling in hydrological modelling. Journal of Hydrology, 217, 239-252.

Becker, A., Güntner, A., Katzenmaier, D. 1999. Required integrated approach to understand runoff generation and flow-path dynamics in catchments. In: Leibundgut, Ch., McDonnell, J., Schultz, G. (eds) Integrated Methods in Catchment Hydrology - Tracer, Remote Sensing and New Hydrometric Techniques, IUGG Symposium, Birmingham, July 1999. IAHS Publication 258, 3-9.

Bergström, S. 1976. Development and application of a conceptual runoff model for Scandinavian catchments. Department of Water Resources Engineering, Lund Institute of Technology, Bulletin Series A No 52, 134 pp.

Bergström, S., Forsman, A. 1973. Development of a conceptual deterministic rainfall-runoff model. Nordic Hydrology, 4, 147-170.

Bergström, S., Graham, L.P. 1998. On the scale problem in hydrological modelling. Journal of Hydrology, 211, 253-265.

Beven, K.J. 1989. Changing ideas in hydrology: the case of physically-based models. Journal of Hydrology, 105, 157-172.

Beven, K. 2001. How far can we go in distributed hydrological modelling? Hydrology and Earth System Sciences, 5, 1-12.

Beven, K.J., Kirkby, M.J. 1979. A physically based, variable contributing area model of basin hydrology. Hydrological Sciences Bulletin, 24, 43-69.

Blöschl, G., Kirnbauer, R. 1991. Point snowmelt models with different degrees of complexity - internal processes. Journal of Hydrology, 129, 127-147.

Blöschl, G., Sivapalan, M. 1995. Scale issue in hydrological modeling: a review. Hydrological Processes 9, 251-290.

Blöschl, G., Kirnbauer, R., Gutknecht D. 1991. Distributed snowmelt simulations in an alpine catchment, 1. model evaluation on the basis of snow cover patterns. Water Resources Research, 27, 3171-3179.

Bonell, M. 1993. Progress in the understanding of runoff generation dynamics in forests. Journal of Hydrology, 150, 217-275.

Box, G.E.P., Jenkins, G.M. 1976. Time Series Analysis, Forecasting and Control. 2nd Edition, Holden-Day.

Bronstert, A. 1999. Capabilities and limitations of detailed hillslope hydrological modelling. Hydrological Processes, 13, 21-48.

Brown, V.A., McDonnell, J.J., Burns, D.A., Kendall, C. 1999. The role of event water, a rapid shallow flow component, and catchment size in summer stormflow. Journal of Hydrology, 217, 171-190.

Brun, E., Martin, E., Simon, V., Gendre, C., Coleou, C. 1989. An energy and mass model of snow cover suitable for operational avalanche forecasting. Journal of Glaciology, 35, 333-342.

Brun, E., David, P., Sudul, M., Brunot, G. 1992. A numerical model to simulate snow-cover stratigraphy for operational avalanche forecasting, Journal of Glaciology, 38, 13-22.

Brutsaert, W. 1982. Evaporation Into the Atmosphere - Theory, History, and Applications. D. Reidel Publishing Company, Dordrecht, 299 pp.

Burnash, R.J.C., Ferral, R.L., McGuire, R.A. 1973. A generalized streamflow simulation system, Conceptual modeling for digital computers. Joint Federal-State River Forecasting Center, US Department of Commerce, National Weather Service, State of California, Department of Water Resources, 204 pp.

Calder, I.R. 1990. Evaporation in the uplands. John Wiley & Sons, Chichester.

Calver, A. 1988. Calibration, sensitivity and validation of a physically-based rainfall-runoff model. Journal of Hydrology, 103, 103-115.

Cazorzi, F., Fontana, G.D. 1996. Snowmelt modelling by combining air temperature and a distributed radiation index. Journal of Hydrology, 181, 169-187.

Choudhury, B.J., Monteith, J.L. 1988. A four-layer model for the heat budget of homogeneous land surfaces. Quarterly Journal of the Royal Meteorological Society, 114, 373-398.

Crawford, N.H., Linsley, R.K. 1966. Digital simulation in hydrology: Stanford Watershed Model IV, Department of Civil Engineering, Technical Report 39, Stanford University, California, 210 pp.

Davis, R.E., Hardy, J.P., Ni, W., Woodcock, C., McKenzie, J.C., Jordan, R., Li, X. 1997. Variation of snow cover ablation in the boreal forest - a sensitivity study on the effects of conifer canopy. Journal of Geophysical Research-Atmospheres, 102, 29389-29395.

Dolman, A.J. 1993. A multiple-source land surface energy balance model for use in General Circulation Models. Agricultural & Forest Meteorology, 65, 21-45.

Dooge, J.C.I. 1957. The rational method for estimating flood peaks. Engineering, September 1957, 311-313.

Dunne, T., Black, R.D. 1970. Partial area contributions to storm runoff in a small New England watershed. Water Resources Research, 6, 1296-1311.

Dunne, T. 1983. Relation of field studies and modeling in the prediction of storm runoff. Journal of Hydrology, 65, 25-48.

Engelmark, H. 1984. Infiltration in unsaturated frozen soil. Nordic Hydrology, 15, 243-252.

Ewen, J., Parkin, G. 1996. Validation of catchment models for predicting land-use and climate change impacts. Journal of Hydrology, 175, 583-594.

Flügel, W-A. 1995. Delineating hydrological response units by geographical information system analyses for regional hydrological modelling using PRMS/MMS in the drainage basin of the River Bröl, Germany. Hydrological Processes, 9, 423-436.

Franchini, M., Pacciani, M. 1991. Comparative analysis of several conceptual rainfall-runoff models. Journal of Hydrology, 122, 161-219.

Freeze, R.A., Harlan, R.L. 1969. Blueprint for a physically-based, digitally-simulated hydrologic response model. Journal of Hydrology, 9, 237-258.

Førland, E.J., Allerup, P., Dahlström, B., Elomaa, E., Jónsson, T., Madsen, H., Perälä, J., Rissanen, P., Vedin, H., Vejen, F. 1996. Manual for operational correction of Nordic precipitation data. Report 24, Norwegian Meteorological Institute, 66 pp.

Gary, H.L. 1974. Snow accumulation and snowmelt as influenced by a small clearing in a Lodgepole pine forest. Water Resources Research, 10, 348-353.

Giesbrecht, M.A., Woo, M. 2000. Simulation of snowmelt in a subarctic spruce woodland: 2. Open woodland model. Water Resources Research, 36, 2287-2295.

Gray, D.M., Prowse, T.D. 1992. Snow and Floating Ice, Chapter 7. In: Maidment, D.R. (ed) Handbook of Hydrology, McGraw-Hill Inc., New York, 7.1-7.58.

Grayson, R.B., Moore, I.D., McMahon, T.A. 1992. Physically based hydrologic modeling, 2, is the concept realistic? Water Resources Research. 28, 2659-2666.

Green, W.H., Ampt, G. 1911. Studies of soil physics, Part I - The flow of air and water through soils. Journal of Agricultural Science, 4, 1-24.

Gupta, V.K., Waymire, E., Wang, C.T. 1980. A representation of an instantaneous unit hydrograph from geomorphology. Water Resources Research, 16, 855-862.

Gustafsson, D. 2002. Boreal land surface water and heat balance – Modelling soil-snow-vegetation-atmosphere behaviour. Kungl Tekniska Högskolan, Department of Land and Water Resources Engineering, TRITA-LWR PHD 1002, 35 pp.

Gustafsson, D., Stähli, M., Jansson, P.-E. 2001. The surface energy balance of a snow cover: comparing measurements to two different simulation models. Theoretical and Applied Climatology, 70, 81-96.

Gürer, I. 1975. Hydrometeorological and water balance studies in Finland, Helsinki University of Technology, Research Papers 49, 164 pp.

Halldin, S., Gottschalk, L., van de Griend, A.A., Gryning, S.-E., Heikinheimo, M., Högström, U., Jochum, A., Lundin, L.-C. 1998. NOPEX – a northern hemisphere climate processes land surface experiment. Journal of Hydrology, 212-213, 172-187.

Halldin, S., Gryning, S.-E., Gottschalk, L., Jochum, A., Lundin, L.-C., van de Griend, A.A. 1999. Energy, water and carbon exchange in a boreal forest landscape - NOPEX experiences, Agricultural and Forest Meteorology, 98-99, 5-29.

Harding, R.J., Pomeroy, J.W. 1996. Energy balance of the winter boreal landscape. Journal of Climate, 9, 2778-2787.

Harding, R.J., Gryning, S.-E., Halldin, S., Lloyd, C.R. 2001. Progress in understanding of land surface/atmosphere exchanges at high latitudes. Theoretical and Applied Climatology, 70, 5-18.

Hardy, J.P., Davis, R.E., Jordan, R., Ni, W., Woodcock, C.E. 1998. Snow ablation modelling in a mature aspen stand of the boreal forest. Hydrological Processes, 12, 1763-1778.

Hardy, J.P., Davis, R.E., Jordan, R., Li, X., Woodcock, C., Ni, W., McKenzie, J.C. 1997. Snow ablation modeling at the stand scale in a boreal jack pine forest. Journal of Geophysical Research-Atmospheres, 102, 29397-29405.

Heikinheimo, M., Halldin, S. 1996. WINTEX - The planned third NOPEX Concentrated Field Effort on winter-time land-surface-atmosphere interactions. In: HIRLAM Workshop on Physical Parameterizations. Finnish Meteorological Institute 14-16 October 1996, Helsinki. Finnish Meteorological Institute, 51-53.

Heikurainen, L., Päivänen, J. 1970. The effect of thinning, clear cutting, and fertilization on the hydrology of peatland drained for forestry. Acta Forestalia Fennica, 104, 23 pp.

Hewlett, J.D., Hibbert, A.R. 1967. Factors affecting the response of small watersheds to precipitation in humid areas. In: Sopper, W.E, Lull, H.W. Forest Hydrology. Pergamon Press, Oxford, 275-290.

Hiitiö, M. 1982. In Finnish: Lumen sulannasta ja sen aiheuttaman valunnan arvioinnista, with English summary. Department of Civil Engineering, Helsinki University of Technology, 96 pp.

Horton, R.E. 1933. The role of infiltration in the hydrologic cycle. Transactions, American Geophysical Union, 14, 446-460.

Horton, R.E. 1940. An approach toward a physical interpretation of infiltration-capacity. Soil Science Society of America Proceedings, 5, 399-417.

Illangasekare, T.H., Walter Jr., R.J., Meier, M.F., Pfeffer, W.T. 1990. Modeling of meltwater infiltration in subfreezing snow. Water Resources Research, 26, 1001-1012.

Jansson, P.-E. 1998. Simulation model for soil water and heat conditions. Description of the SOIL model. Swedish University of Agricultural Science, Department of Soil Science, Uppsala, Sweden, 81 pp.

Jauhiainen, M., Nissinen, A. 1994. Calibration of the SOIL model with autumn and summer data of forest soil water tension. In: Kettunen, J., Granlund, K., Paasonen-Kivekäs, M., Sirviö, H. (eds) Spatial and Temporal Variability and Interdependencies Among Hydrological Processes. Proceedings of a Nordic seminar, Report No 36, NHP, Kirkkonummi, Finland, 17-30.

Jordan, R. 1991. A one-dimensional temperature model for a snow cover: Technical documentation for SNTHERM.89. Special Report 91-16, U. S. Army Cold Regions Research and Engineering Laboratory, Hanover, 49 pp.

Jordan, R. 1992. Estimating turbulent transfer functions for use in energy balance modeling. Internal Report 1107, U. S. Army Cold Regions Research and Engineering Laboratory, Hanover, 13 pp.

Jordan, R.E., Andreas, E.L., Makshtas, A.P. 1999. Heat budget of snow-covered sea ice at North Pole 4. Journal of Geophysical Research (C4), 104, 7785-7806.

Kaila, M. 1977. In Finnish: Hydrologiset ennusteet Saimaan säännöstelyä varten, with English summary. Department of Civil Engineering, Helsinki University of Technology, 191 pp.

Kaitera, P. 1939. In Finnish: Lumen kevätsulamisesta ja sen vaikutuksesta vesiväylien purkautumissuhteisiin Suomessa, Maataloushallituksen Kulttuuriteknillisiä Tutkimuksia N:o 2, Helsinki, 255 pp.

Karvonen, T. 1988. A model for predicting the effect of drainage on soil moisture, soil temperature and crop yield. Helsinki University of Technology, Publications of the Laboratory of Hydrology and Water Resources Engineering, 1, 215 pp.

Karvonen, T., Skaggs, R.W. 1993. Comparison of different methods for computing drainage water quality and quantity. In: Lorre, E. (ed) Subsurface Drainage Simulation Models. Transactions of Workshop, 15th Congress ICID, The Hague, 201-216.

Karvonen. T., Koivusalo, H., Jauhiainen, M., Palko, J., Weppling, K. 1999. A hydrological model for predicting runoff from different land use areas. Journal of Hydrology, 217, 253-265.

Kellomäki, S., Wang, K.-Y. 1999. Short-term environmental controls of heat and water vapour fluxes above a boreal coniferous forest: model computations compared with measurements by eddy correlation. Ecological Modelling, 124, 145-173.

Kelly, R.J., Morland, L.W., Morris, E.M. 1986. A three phase mixture model for melting snow. In: Morris, E.M. (ed) Modelling Snowmelt-Induced Processes. IAHS Publication No. 155, 17-26.

Kendall, C., Sklash, M.G., Bullen, T.D. 1995. Isotope tracers of water and solute sources in catchments, Chapter 10. In: Trudgill, S.T. (ed) Solute Modelling in Catchment Systems. John Wiley & Sons, London, 261-303.

Kirkby, M.J. 1985. Hillslope hydrology, In: Anderson, M.G., Burt, T.P. (eds) Hydrological Forecasting. John Wiley & Sons, Chichester, UK, 37-75.

Kirkby, M. 1988. Hillslope runoff processes and models. Journal of Hydrology, 100, 315-339.

Kirkby, M.J. 1993. Network Hydrology and Geomorphology. In: Beven K., Kirkby, M.J. (eds) Channel Network Hydrology. John Wiley & Sons, Chichester, 1-12.

Kite, G.W., Kouwen, N. 1992. Watershed modeling using land classifications. Water Resources Research, 28, 3193-3200.

Korhonen, W.W. 1915. In German: Die Ausdehnung und Höhe der Schneedecke. Untersuchungen über die Schnee- und Eisverhältnisse in Finnland. Mitteilungen der Meteorologischen Zentralanstalt des finnischen Staates, Helsinki, 184 pp.

Korhonen, W.W. 1923. In German: Beobachtungen über die Dichte der Schneedecke in verschieden-artigem Gelände und in verschiedenen Tiefen. Untersuchungen über die Schnee- und Eisverhältnisse in Finnland. Mitteilungen der Meteorologischen Zentralanstalt des finnischen Staates, Helsinki, 58 pp.

Kuusisto, E. 1980. On the values and variability of degree-day melting factor in Finland. Nordic Hydrology, 11, 235-242.

Kuusisto, E. 1984. Snow accumulation and snowmelt in Finland. Publications of the Water Research Institute 55, National Board of Waters, Helsinki, Finland, 149 pp.

Lee, R. 1978. Forest Microclimatology. Columbia University Press. New York.

Lepistö, A. 1994. Areas contributing to generation of runoff and nitrate leaching as estimated by empirical isotope methods and TOPMODEL. Aqua Fennica, 24, 103-120.

Lepistö, A. 1996. Hydrological processes contributing to nitrogen leaching from forested catchments in Nordic conditions. Monographs of the Boreal Environment Research No. 1, 72 pp.

Lepistö, A., Kivinen, Y. 1997. Effects of climatic change on hydrological patterns of a forested catchment: a physically based modeling approach. Boreal Environment Research, 2, 19-31.

Lepistö, A., Seuna, P., Bengtsson, L. 1994. The environmental tracer approach in storm runoff studies in forested catchments. In: Seuna, P., Gustard, A., Arnell, N.W., Cole, G.A. (eds) FRIEND: Flow Regimes from Experimental and Network Data. Braunschweig conference, IAHS Publication No. 221, 369-379.

Levine, E.R., Knox, R.G. 1997. Modeling soil temperature and snow dynamics in northern forests. Journal of Geophysical Research, 102(D24), 29407-29416.

Liang, X.D., Lettenmaier, D.P., Wood, E.F., Burges, S.J. 1994. A simple hydrologically based model of land surface water and energy fluxes for GCMs. Journal of Geophysical Research, 99(D7), 14415-14428.

Lindström, G., Johansson, B., Persson, M., Gardelin, M., Bergström, S. 1997. Development and test of the distributed HBV-96 hydrological model. Journal of Hydrology, 201, 272-288.

Link, T., Marks, D. 1999. Distributed simulation of snowcover mass- and energy-balance in the boreal forest. Hydrological Processes, 13, 2439-2452.

Linsley, R.K., Crawford, N.H., 1960. Computation of a synthetic streamflow record on a digital computer. Publication 51, International Association of Scientific Hydrology, 526-538.

Liu, S., Riekerk, H., Gholz, H.L. 1998. Simulation of evapotranspiration from florida pine flatwoods. Ecological Modelling, 114, 19-34.

Lundberg, A. 1993. Evaporation of intercepted snow - review of existing and new measurement methods. Journal of Hydrology, 151, 267-290.

Lundberg, A. 1996. Interception evaporation, processes and measurement techniques. 196 D, Luleå University of Technology, 24 pp.

Lundberg, A., Calder, I., Harding, R. 1998. Evaporation of intercepted snow - measurement and modelling. Journal of Hydrology, 206, 151-163.

Lundberg, A., Halldin, S. 1994. Evaporation of intercepted snow - analysis of governing factors. Water Resources Research, 30, 2587-2598.

Male, D.H., Granger, R.J. 1981. Snow surface energy exchange. Water Resources Research, 17, 609-627.

Marks, D. 1988. Climate, energy exchange, and snowmelt in Emerald Lake Watershed, Sierra Nevada. University of California, Santa Barbara, 149 pp.

Marshall, S., Oglesby, R.J., Maasch, K.A., Bates, G.T. 1999. Improving climate model representations of snow hydrology. Environmental Modelling & Software, 14, 327-334.

McCarthy, E.J., Flewelling, J.W., Skaggs, R.W. 1992. Hydrologic model for drained forest watershed. Journal of Irrigation and Drainage Engineering, 118, 242-255.

Metcalfe, R.A., Buttle, J.M. 1999. Semi-distributed water balance dynamics in a small boreal forest basin. Journal of Hydrology, 226, 66-87.

Monteith, J.L. 1965. Evaporation and environment. In: Fogg, G.E. (ed) The State and Movement of Water in Living Organisms. 19th Symposia of the Society for Experimental Biology. Cambridge Univ. Press, 205-234.

Morris, E.M. 1983. Modelling the flow of mass and energy within a snow pack for hydrological forecasting. Annals of Glaciology, 4, 198-203.

Mustonen, S.E. 1965. In Finnish: Meteorologisten ja aluetekijöiden vaikutuksesta valuntaan, with English abstract: Effects of meteorologic and basin characteristics on runoff. Soil and Hydrotechnical Investigations, Helsinki, 109 p.

Nakai, Y., Sakamoto, T., Terajima, T., Kitamura, K., Shirai, T. 1999. Energy balance above a boreal coniferous forest: a difference in turbulent fluxes between snow-covered and snow-free canopies. Hydrological Processes, 13, 515-529.

Nash, J.E. 1957. The form of the instantaneous unit hydrograph. IASH Publication No. 45, Vol. 3-4, 114-121.

Nash J.E. 1959. Systematic determination of unit hydrograph parameters. Journal of Geophysical Research, 64, 111-115.

Nash, J.E., Sutcliffe, J.V. 1970. River flow forecasting through conceptual models, Part I - A discussion of principles. Journal of Hydrology, 10, 282-290.

Nijssen, B., Haddeland, I., Lettenmaier, D.P. 1997. Point evaluation of a surface hydrology model for BOREAS. Journal of Geophysical Research, 102(D24), 29367-29378.

Nyberg, L., Stähli, M., Mellander, P.-E., Bishop, K.H. 2001. Soil frost effects on soil water and runoff dynamics along a boreal forest transect: 1. Field investigations. Hydrological Processes, 15, 909-926.

Ohta, T. 1994. A distributed snowmelt prediction model in mountain areas based on an energy balance method. Annals of Glaciology, 19, 107-113.

Orlandini, S., Rosso, R. 1998. Parameterization of stream channel geometry in the distributed modeling of catchment dynamics. Water Resources Research, 34, 1971-1985.

Pearce, A.J., Stewart, M.K., Sklash, M.G. 1986. Storm runoff generation in humid headwater catchments, 1. Where does the water come from? Water Resources Research, 22, 1263-1272.

Pomeroy, J.W., Dion, K. 1996. Winter radiation extinction and reflection in a boreal pine canopy - measurements and modelling. Hydrological Processes, 10, 1591-1608.

Pomeroy, J.W., Parviainen, J., Hedstrom, N., Gray, D.M. 1998. Coupled modelling of forest snow interception and sublimation. Hydrological Processes, 12, 2317-2337.

Price, A.G., Dunne, T. 1976. Energy balance computations of snowmelt in a subarctic area. Water Resources Research, 12, 686-694.

Päivänen, J. 1966. In Finnish: Sateen jakautuminen erilaisissa metsiköissä, with English summary: The distribution of rainfall in different types of forest stand. Reprint from Silva Fennica 119, Helsinki, 37 pp.

Rango, A., Martinec, J. 1995. Revisiting the degree-day method for snowmelt computations. Water Resources Bulletin, 31, 657-669.

Raupach, M.R., Legg, B.J. 1984. The uses and limitations of flux-gradient relationships in micrometeorology. Agricultural Water Management, 8, 119-131.

Refsgaard, J.C. 1997. Parameterisation, calibration and validation of distributed hydrological models. Journal of Hydrology, 198, 69-97.

Renqvist, H., Cautón, A.J., Gylling, R., Kaitera, P. 1939. In Finnish: Tulvakomitean mietintö. Komiteanmietintö N:o 14-1939, Valtioneuvoston kirjapaino, Helsinki, 306 s.

Rice, K.C., Hornberger, G.M. 1998. Comparison of hydrochemical tracers to estimate source contributions to peak flow in a small, forested, headwater catchment. Water Resources Research, 34, 1755-1766.

Richards, L.A. 1931. Capillary conduction of liquids through porous mediums, Physics, 1, 318-333.

Rodhe, A. 1987. The origin of streamwater traced by oxygen-18, Uppsala University, Department of Physical Geography, Division of Hydrology, Rep. A 41, 260 pp.

Rodríguez-Iturbe, I. 1993. The geomorphological unit hydrograph. In: Beven, K., Kirkby, M.J. (eds) Channel Network Hydrology. John Wiley & Sons, Chichester, 42-68.

Rutter, A.J., Morton, A.J., Robins, P.C. 1975. A predictive model of rainfall interception in forests. II. Generalization of the model and comparison with observations in some coniferous and hardwood stands. Journal of Applied Ecology, 12, 367-380.

Schultz, G.A. 1993. Hydrological modeling based on remote sensing information. Advances in Space Research, 13, (5)149-(5)166.

Seibert, J. 1999. Conceptual runoff models – Fiction or representation of reality. Comprehensive Summaries of Uppsala Dissertations from the Faculty of Science and Technology, 436, Acta Universitatis Upsaliensis, Uppsala, Sweden, 52 pp.

Seppänen, M. 1961. On the accumulation and the decreasing of snow in pine dominated forest in Finland. Hydrologisen Toimiston Tiedonantoja, Fennia 86, 1, 51 pp.

Sherman, L.K. 1932. Streamflow from rainfall by the unit-hydrograph method. Engineering News Record, 108, 501-505.

Shuttleworth, W.J. 1992. Evaporation, Chapter 4. In: Maidment, D.R. (ed) Handbook of Hydrology. McGraw-Hill, New York, 4.1.-4.53.

Sivapalan, M., Beven, K., Wood, E.F. 1987. On hydrologic similarity. 2. A scaled model of storm runoff production. Water Resources Research, 23, 2266-2278.

Skaggs, R.W. 1980. A water management model for artificially drained soils. North Carolina Agricultural Research Service, Raleigh, NC, 54 pp.

Sklash, M.G., Farvolden, R.N. 1979. The role of groundwater in storm runoff. Journal of Hydrology, 43, 45-65.

Smith, R.E., Goodrich, D.C., Quinton, J.N. 1995. Dynamic, distributed simulation of watershed erosion: The KINEROS2 and EUROSEM models. Journal of Soil and Water Conservation 50, 517-520.

Sueker, J.K., Ryan, J.N., Kendall, C., Jarrett, R.D. 2000. Determination of hydrologic pathways during snowmelt for alpine/subalpine basins, Rocky Mountain National Park, Colorado. Water Resources Research, 36, 63-75.

Storck, P. 2000. Trees, snow and flooding: an investigation of forest canopy effects on snow accumulation and melt at the plot and watershed scales in the Pacific North West. Water Resources Series, Technical Report No. 161, University of Washington, Seattle, 176 pp.

Stähli, M., Jansson. P.-E. 1998. Test of two SVAT snow submodels during different winter conditions. Agricultural and Forest Meteorology, 92, 31-43.

Stähli, M., Nyberg, L., Mellander, P.-E., Jansson, P.-E., Bishop, K.H. 2001. Soil frost effects on soil water and runoff dynamics along a boreal transect: 2. Simulations. Hydrological Processes, 15, 927-941.

Tarboton, D.G., Chowdhury, T.G., Jackson, T.H. 1995. A spatially distributed energy balance snowmelt model. In: Tonnessen, K.A., Williams, M.W., Tranter, M. (eds) Biogeochemistry of Seasonally Snow-Covered Catchments. IUGG Symposium, Boulder, July 1995. IAHS Publications 228, 141-155.

Tao, T., Kouwen, N. 1989. Remote sensing and fully distributed modeling for flood forecasting. Journal of Water Resources Planning and Management, 115, 809-823.

Todini, E. 1996. The ARNO rainfall-runoff model. Journal of Hydrology, 175, 339-382.

Troendle, C.A. 1983. The potential for water yield augmentation from forest management in the Rocky Mountain region. Water Resources Bulletin, 19, 359-373.

Troendle, C.A., King, R.M. 1987. The effect of partial and clearcutting on streamflow at Deadhorse Creek, Colorado. Journal of Hydrology, 90, 145-157.

Tuteja, N.K., Cunnane, C. 1997. Modelling coupled transport of mass and energy into the snowpack - model development, validation and sensitivity analysis. Journal of Hydrology, 195, 232-255.

Uhlenbrook, S., Leibundgut, Ch. 1999. Integration of tracer information into the development of a rainfall-runoff model. In: Leibundgut, Ch., McDonnell, J., Schultz, G. (eds) Integrated Methods in Catchment Hydrology - Tracer, Remote Sensing and New Hydrometric Techniques. IUGG Symposium, Birmingham, July 1999. IAHS Publication 258, 93-100.

Uhlenbrook, S., Leibundgut, Ch. 2002. Process-oriented catchment modelling and multiple-response validation. Hydrological Processes, 16, 423-440.

U. S. Army Corps of Engineers. 1956. Snow Hydrology, Summary Report of the Snow Investigations, North Pacific Division, Portland Oregon, 437 pp.

Vakkilainen, P. 1982. In Finnish: Maa-alueelta tapahtuvan haihdunnan arvioinnista, with English abstract: On the estimation of evapotranspiration. Department of Hydraulic Engineering, University of Oulu, Acta Univiversitatis Ouluensis, C 20, Artes Constructionum, 6, 146 pp.

Vakkilainen, P., Karvonen, T. 1982. Adaptive Rainfall-Runoff Model, SATT-I. Civil Engineering and Building Construction Series No 81, Acta Polytechnica Scandinavica, Helsinki, 54 pp.

van Genuchten, M.T. 1980. A closed-form equation for predicting the hydraulic conductivity of unsaturated soils. Soil Science Society of America Journal, 44, 892-898.

Vehviläinen, B. 1992. Snow cover models in operational watershed forecasting. Publications of Water and Environment Research Institute 11, National Board of Waters and the Environment, Finland, 112 pp.

Vertessy, R.A., Hatton, T.J., O'Shaughnessy, P.J., Jayasuriya, M.D.A. 1993. Predicting water yield from a mountain ash forest catchment using a terrain analysis based catchment model. Journal of Hydrology, 150, 665-700.

Wigmosta, M.S., Vail, L.W., Lettenmaier, D.P. 1994. A distributed hydrology-vegetation model for complex terrain. Water Resources Research, 30, 1665-1679.

WMO. 1986. Intercomparison of models of snowmelt runoff. Operational Hydrology, Report No. 23, WMO – No. 646, World Meteorological Organization, Geneva, 36 pp.

Woo, M., Giesbrecht, M.A. 2000. Simulation of snowmelt in a subarctic spruce woodland: 1. Tree model. Water Resources Research, 36, 2275-2285.

Wood, E.F., O'Connell, P.E. 1985. Real-time forecasting, In: Anderson, M.G. and Burt, T.P. (eds) Hydrological Forecasting. John Wiley & Sons, Chichester, UK, 505-558.

Wood, E.F., Lettenmaier, D.P., Zartarian, V.G. 1992. A land-surface hydrology parameterization with subgrid variability for general circulation models. Journal of Geophysical Research, 97(D3), 2717-2728.

Woolhiser, D.A. 1996. Search for physically based runoff model - a hydrologic El Dorado. Journal of Hydraulic Engineering-ASCE, 122, 122-129.

Ye, W., Bates, B.C., Viney, N.R., Sivapalan, M., Jakeman, A.J. 1997. Performance of conceptual rainfall-runoff models in low-yielding ephemeral catchments. Water Resources Research, 33, 153-166.

Zhang, L., Dawes, W.R., Hatton, T.J., Reece, P.H., Beale, G.T.H., Packer, I. 1999. Estimation of soil moisture and groundwater recharge using the TOPOG_IRM model. Water Resources Research, 35, 149-161.

Zhao, R.-J., Zuang, Y.-L., Fang, L.-R., Liu, X.-R., Zhang, Q.-S. 1980. The Xinanjiang model. Proceedings of the Symposium on the Application of Recent Developments in Hydrological Forecasting to the Operation of Water Resource, Oxford, IAHS Publication 129, 351-356.

Zoch, R.T. 1934. On the relation between rainfall and stream flow. Monthly Weather Review, 62, 315-322.

APPENDIX 1: LIST 0F SYMB0LS

A_n area of soil column n [m^2]
B_n thickness of saturated zone in soil column n [m]
c_g specific heat of soil [kJ kg^{-1} $^oC^{-1}$]
c_i specific heat of ice [kJ kg^{-1} $^oC^{-1}$]
C_I interception capacity [m]
C_{IS} snow interception capacity [m]
C_{IW} rain interception capacity [m]
c_n capillary upflux into the root zone [m h^{-1}]
c_p specific heat of air [kJ kg^{-1} $^oC^{-1}$]
c_w specific heat of water [kJ kg $^oC^{-1}$]
d_g freezing curve parameter [^oC]
D_g depth of the soil layer [m]
d_o zero-plane displacement height [m]
d_n direct runoff [m h^{-1}]
D_n root zone soil moisture state in column n [m]
d_s runoff from soil domain [m h^{-1}]
E evaporation/sublimation [m h^{-1}]
e_a air vapour pressure [Pa]
E_{E0} windless convection coefficient for the latent heat flux [kJ m^{-2} Pa^{-1} h^{-1}]
E_{H0} windless convection coefficient for the sensible heat flux [kJ m^{-2} $^oC^{-1}$ h^{-1}]
E_I interception evaporation [m h^{-1}]
E_n actual transpiration [m h^{-1}]
e_s saturation vapour pressure [Pa]
f shape parameter (of transmissivity)
F liquid water flow in snow [m h^{-1}]
f_{EP} scaling factor of potential transpiration
f_r interception parameter
f_s sky-view fraction
h pressure head [m]
H sensible heat flux [kJ m^{-2} h^{-1}]
h_r pressure head in the root zone [m]
I soil ice content
I_0 initial canopy water storage [m]
i_n infiltration into the soil column n [m h^{-1}]
$K(z)$ eddy diffusion coefficient [m^2 h^{-1}]
k_I interception model parameter
K^{ls} lateral saturated hydraulic conductivity of soil [m h^{-1}]
K_{sat} saturated hydraulic conductivity of snow [m h^{-1}]
k_T thermal conductivity [kJ $^oC^{-1}$ m^{-1} h^{-1}]

L_j fraction of liquid water in snow
L_n soil column length [m]
l_r liquid water retention capacity of snow
M energy advected with liquid water [kJ m^{-2} h^{-1}]
n extinction coefficient (of wind speed within canopy)
P precipitation [m h^{-1}]
p_n percolation from root zone moisture storage [m h^{-1}]
P_r rainfall [m h^{-1}]
P_s snowfall [m h^{-1}]
P_T throughfall [m h^{-1}]
Q heat conduction [kJ m^{-2} h^{-1}]
Q_p advective heat flux [kJ m^{-2} h^{-1}]
r_{ao} aerodynamic resistance above canopy [h m^{-1}]
r_{co} aerodynamic resistance within canopy [h m^{-1}]
R_d dry gas constant [J kg^{-1} K^{-1}]
R_{lc} long-wave radiation emitted by the canopy [kJ m^{-2} h^{-1}]
R_{ld} incoming atmospheric long-wave radiation [kJ m^{-2} h^{-1}]
R_{ls} upward long-wave radiation [kJ m^{-2} h^{-1}]
r_n throughfall/snowmelt [m h^{-1}]
R_{nc} net radiation in the canopy [kJ m^{-2} h^{-1}]
R_{ns} net radiation into snowpack [kJ m^{-2} h^{-1}]
R_s incoming short-wave radiation [kJ m^{-2} h^{-1}]
r_s total aerodynamic resistance [h m^{-1}]
r_{s*} aerodynamic resistance (corrected for atmospheric stability) [h m^{-1}]
r_{ss} aerodynamic resistance beneath canopy [h m^{-1}]
s storage coefficient
S_j relative saturation in excess of water retained by capillary forces
t time [h]
T transmissivity [m^2 h^{-1}]
T_0 surface temperature [ºC]
T_a air temperature [ºC]
T_f freezing point temperature [ºC]
T_g soil temperature [ºC]
T_h temperature limit for snowfall [ºC]
T_l temperature limit for rainfall [ºC]
T_j temperature in snow layer j [ºC]
U_g heat content of soil layer [kJ m^{-2}]
U_j heat content of snow layer j [kJ m^{-2}]
U_S snow unloading [m h^{-1}]
V_n air volume in a soil column n [$m^3 m^{-2}$]
V^{ss} air volume corresponding to steady-state moisture distribution [$m^3 m^{-2}$]
w liquid water content
W water equivalent of snow [m]
W_I depth of intercepted water [m h^{-1}]

x distance [m]
y distance [m]
z_{0o} roughness length of the canopy [m]
z_{bot} elevation of impermeable bottom
z_{gw} water table elevation [m]
z_r reference height above the canopy [m]
z_{rs} reference height above ground [m]
z_s soil surface elevation [m]
α_c canopy albedo
α_s snow/ground albedo
Δ gradient of the saturated vapor pressure – temperature curve [Pa $^oC^{-1}$]
ΔI change in the canopy storage [m h^{-1}]
ΔQ net lateral groundwater flow [m^3 h^{-1}]
Δz vertical distance [m]
ϕ porosity of the soil
γ psychrometric constant [Pa $^oC^{-1}$]
λE latent heat flux [kJ m^{-2} h^{-1}]
λ_f latent heat of fusion [kJ kg^{-1}]
λ_s latent heat of sublimation of ice [kJ kg^{-1}]
λ_v latent heat of vaporisation of water [kJ kg^{-1}]
θ soil water content
θ_s saturated soil water content
ρ_a air density [kg m^{-3}]
ρ_g density of soil grains [kg m^{-3}]
ρ_i density of ice [kg m^{-3}]
ρ_s density of snow [kg m^{-3}]
ρ_w density of water [kg m^{-3}]
τ_c transmittance through the canopy

HELSINKI UNIVERSITY OF TECHNOLOGY WATER RESOURCES PUBLICATIONS

TKK-VTR-1 Järvelä, J.
Environmental river engineering and restoration: guiding principles and hydraulic performance. (in Finnish) 1998.

TKK-VTR-2 Laininen, E.
Development of the Finnish Orienteering Federation's environmental management system. (in Finnish) 1998.

TKK-VTR-3 Silander, J.
Floating breakwater and environment. 1999.

TKK-VTR-4 Jolma, A.
Development of river basin management decision support systems: Two case studies. 1999.

TKK-VTR-5 Tamm, T.
Effects of meteorological conditions and water management on hydrological processes in agricultural fields: Parameterization and modeling of Estonian case studies. 2002.

ISBN 951-22-6214-2
ISSN 1456-2596